Distribution Category:
Magnetic Fusion Energy
(UC-20)

ANL/FPP/TM-210

ANL/FPP/TM--210

DE87 004633

ARGONNE NATIONAL LABORATORY
9700 South Cass Avenue
Argonne, Illinois 60439

Proceedings of the Regional Electromagnetic Workshop at Argonne National Laboratory 23 and 24 June 1986

Larry R. Turner
Editor

The submitted manuscript has been authored by a contractor of the U. S. Government under contract No. W-31-109-ENG-38. Accordingly, the U. S. Government retains a nonexclusive, royalty-free license to publish or reproduce the published form of this contribution, or allow others to do so, for U. S. Government purposes.

December 1986

Study Supported by

Office of Fusion Energy
U.S. Department of Energy

DISCLAIMER

This report was prepared as an account of work sponsored by an agency of the United States Government. Neither the United States Government nor any agency thereof, nor any of their employees, makes any warranty, express or implied, or assumes any legal liability or responsibility for the accuracy, completeness, or usefulness of any information, apparatus, product, or process disclosed, or represents that its use would not infringe privately owned rights. Reference herein to any specific commercial product, process, or service by trade name, trademark, manufacturer, or otherwise does not necessarily constitute or imply its endorsement, recommendation, or favoring by the United States Government or any agency thereof. The views and opinions of authors expressed herein do not necessarily state or reflect those of the United States Government or any agency thereof.

MASTER

DISTRIBUTION OF THIS DOCUMENT IS UNLIMITED

TABLE OF CONTENTS

ABSTRACT

At the Second Regional Workshop, held at Argonne National Laboratory 23-24 June 1986, fifteen participants from four countries heard ten presentations on Problems 1, 2, and 6. This technical memo includes the text of presentations, summaries of the results for Problems 1 and 2, and information about the workshop.

1. INTRODUCTION

1.1 The Workshop at ANL

The Second International Electromagnetic Workshop was held at ANL 23 and 24 June, 1986. There were fifteen participants from the U.S., Canada, U.K., and Japan. Chris Emson of the Rutherford Appleton Laboratory (RAL), U.K. described the first workshop at RAL in March and distributed proceedings of that workshop, RAL report RAL-86-049. There were four presentations on Problem 1, the FELIX Cylinder experiments; four on Problem 2, a cylinder in a sinusoidal field; and two on Probelm 6, a hollow sphere.

A change introduced after the RAL workshop was to provide a table for the presentation of results. The table makes it easier to compare results. After the oral presentations, the presenters for problems 1 and 2 met and prepared summaries of the results for the two problems. Preparing the summaries took each group two hours of intense work, largely because they wished to include the results from the RAL workshop, which were not in the tabular form. The summaries comparing results were seen as very useful, but the suggestion was made that in the future workshops, results not presented in the tabular form should not be included in the summaries.

Discussions also included the question of how to encourage more presentations on Problems 3, 4, and 5, and the suggestion that a future problem (after the Graz workshop) include the coupling of magnetic effects to mechanical and/or thermal effects.

1.2 Problem 2

At the RAL Workshop, O. Biro presented an analytic solution to Problem 2, and U. Hamm and R. J. Lari had prepared solutions using PROFI and PE2D respectively. At the ANL Workshop, C. Emson reported on those solutions. R. J. Lari described further PE2D computations. Quadrupling the number of elements and/or using quadratic elements rather than linear elements did not improve the accuracy of the solution appreciably.

T. Morisue used the boundary integral method to find the vector potential on the inner and outer conductor surfaces, then used a finite element method to find the potential and fields in the conductor.

1.3 Problem 1

L. Turner described the FELIX experiments with cylindrical test pieces on which Problem 1 is based. C. Emson described the solutions to Problem 1 which were presented at the RAL Workshop.

D. F. Ostergaard solved problems 1A and 1B with ANSYS in the 2-D approximation, using a vector potential. Solutions with 4-node and 8-node isoparametric quadrilateral elements were compared.

K. Davey solved the problem in 3-D by using the U-V method to replace the vector Helmholtz equation with two scalar Helmholtz equations. The eigenvalues of the resulting matrix were found. More than one eigenvalue were required to give good agreement with the experimental results.

1.4 Problem 6

Nathan Ida calculated the hollow sphere with the code EDDY3D, which is designed to calculate impedances for NDT. To avoid flux-normal boundary conditions, he calculated one quadrant of the sphere.

T. Morisue presented a 3-D eddy current method using the vector potential A and including the gauge condition implicitly through interface conditions on the normal component of A. He applied the method to a cylinder with constant conductivity and permeability and to a solid sphere.

ELECTROMAGNETIC WORKSHOP
held at
RUTHERFORD APPLETON LAB.
27 MAY 1986

MEETING SUMMARY

presented by

C R I EMSON

1

A one day meeting was held at Rutherford Appleton Laboratory on Thursday 27 March.

There were about 30 attending, including 3 from USA. The rest from UK and Europe.

7 presentations made, covering problems 1,2,3 and 5. + 6

SUMMARY

This will include outline of the presentations including points not in the Proceedings.

Plus report of discussions at the workshop

PROBLEM 2 – Infinite Cylinder

1) ANALYTIC SOLUTION

O Biro, Budapest

Details in proceedings. These are the analytic solutions used as comparison with numerical results in tables.

2) PE2D

R Lari, Argonne

Using PE2D, a 2–D steady state and transien code.

This shows some interesting features, eg usin slightly different meshes, different boundary condition implementations.

Results will be presented later in this workshop.

3

3) PROFI

U Hamm, Darmstadt

This is 2-D finite difference code.

PROBLEM 1 - Finite Cylinder (transient)

1) PROFI

J Gerstenberger, Darmstadt

2-D approximation.

Using backward Euler for time domain

$$\frac{\partial A}{\partial t} = \frac{A_{t+1} - A_t}{dt}$$

with constant dt=5ms.

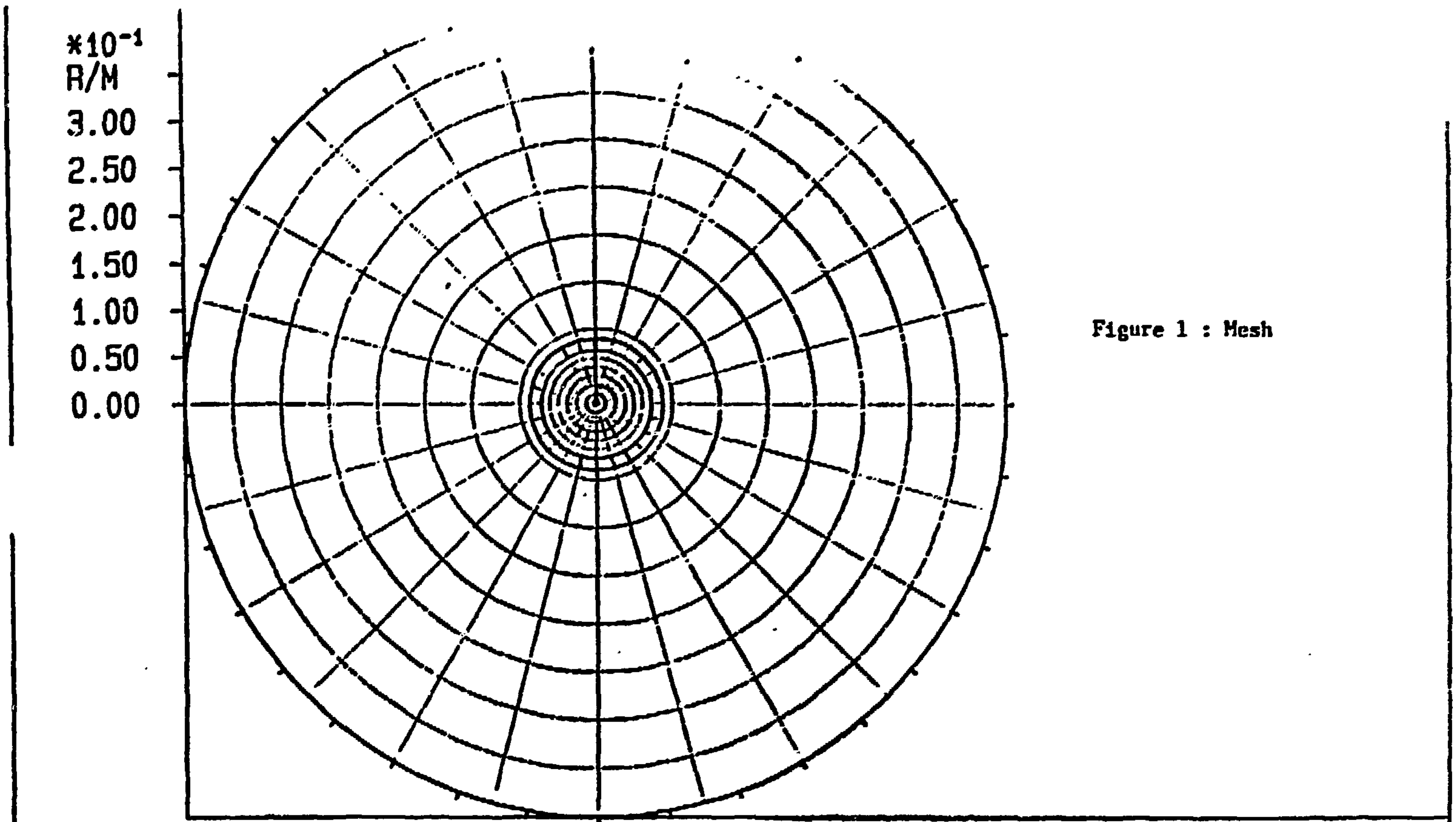

Figure 1 : Mesh

UNENDLICHER HOHLZYLINDER IM HOMOGENEN FELD

PROFI

10000

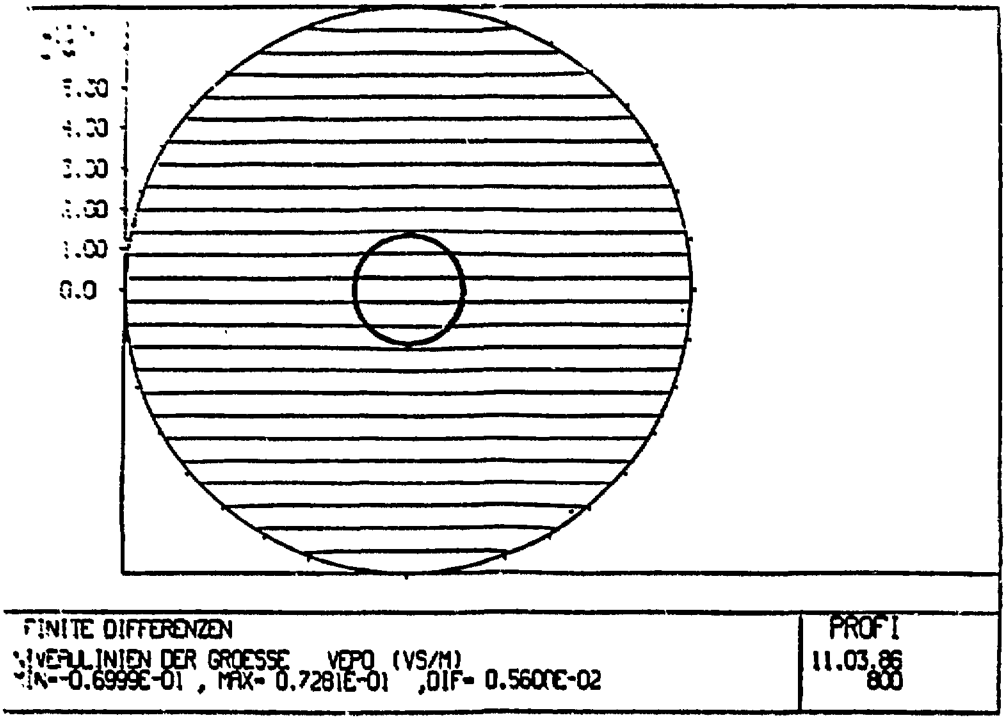

Pic. 1: stationary magnetic flux density

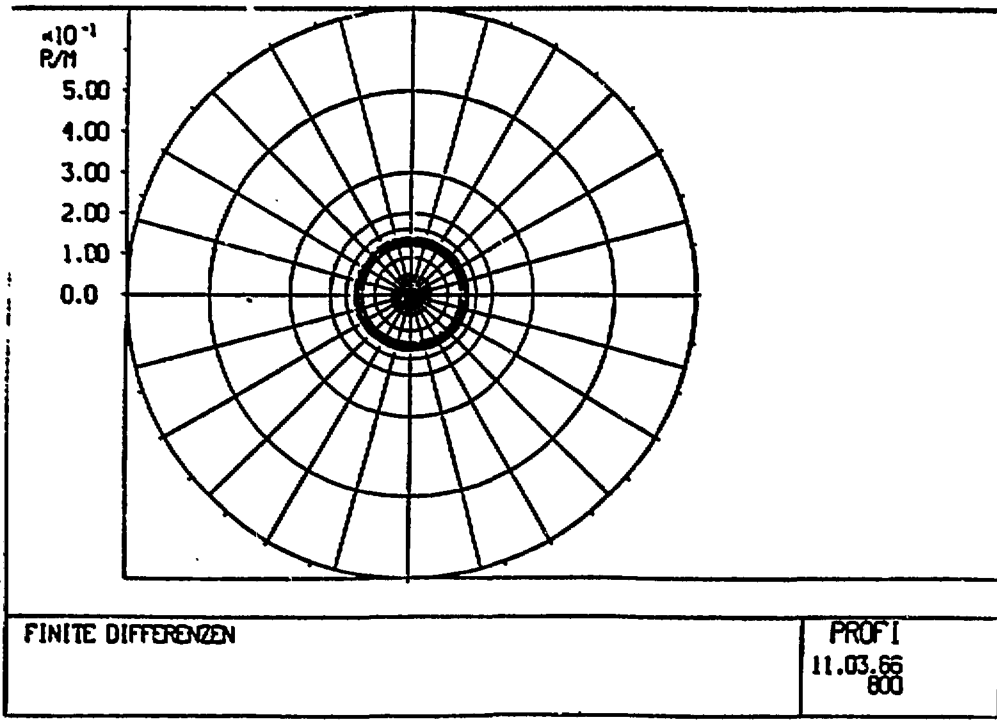

Pic. 2: grid

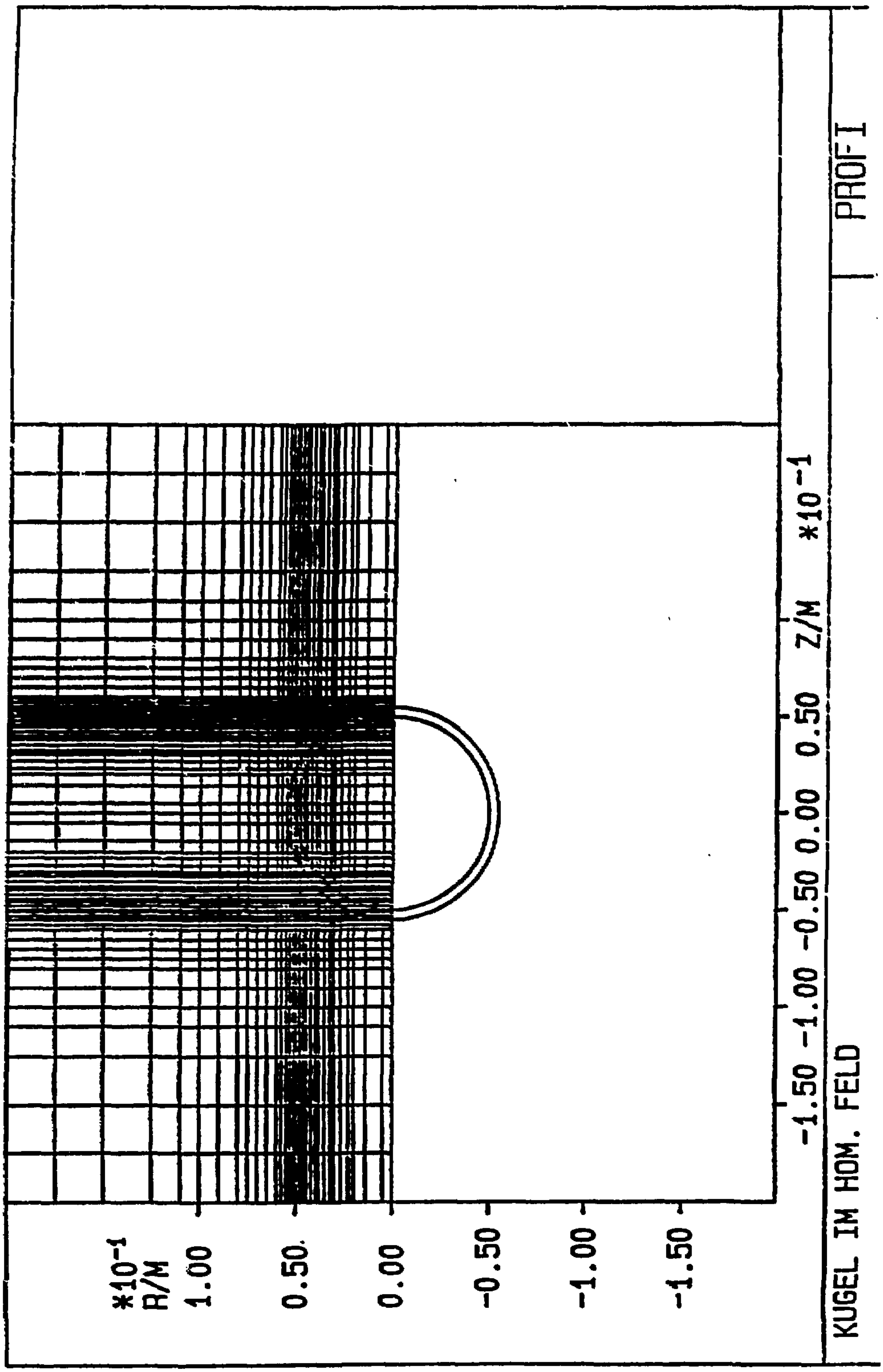
PROFI
KUGEL IM HOM. FELD
*10^{-1}
R/M
1.00
0.50
0.00
-0.50
-1.00
-1.50
-1.50 -1.00 -0.50 0.00 0.50 Z/M *10^{-1}

2) NONAME
P Leonard, Bath, UK

2-D approximation.

1ms time steps used. Solving for update to solution rather than new solution. Theta method, with theta=2/3.

Analytic solution presented due to single sheet representation.

3) UNISH
G Rubinacci, Salerno

Solve finite length arc of torus, with large major radius.

Thin sheet model of cylinder. Results for single sheet, for long cylinder.
Results for 1,2 and 3 sheet model for short cylinder.

PROBLEM 3 – Bath Plate with Holes

1) NONAME

D Rodger, Bath, UK

Experimental results as well as numerical results were presented, for a plate with 2 holes.

PROBLEM 6 – Sphere

1) PROFI

M Schaefer, Darmstadt

2–D axisymmetric solution.

Not using the specified mesh, but 2400 grid points as shown in diagram.

PROBLEM 5 — Bath Cube

1) TRIFOU

J Verite, E D France

Boundary Integral program. FE for conductors, and BI to model air outside.

Results for three cases of geometry, with varying number of degrees of freedom.

Difficulty with getting field at requested points, so tried few ways of getting round this problem.

Calculation of the field at measurement points.

We have tried 3 methods.

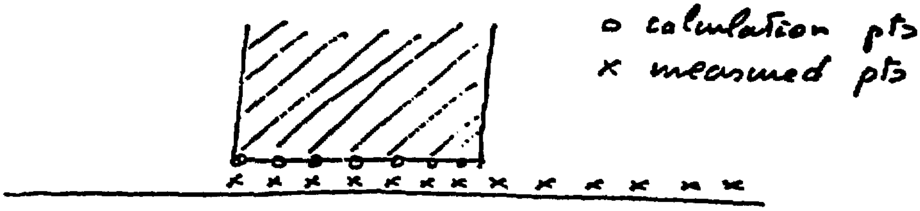

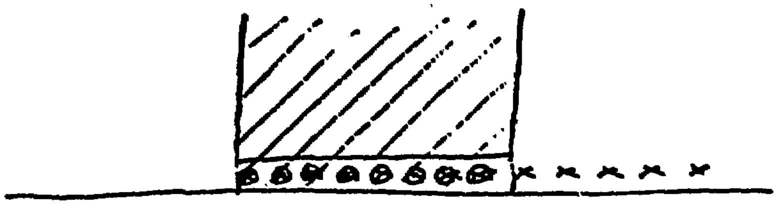

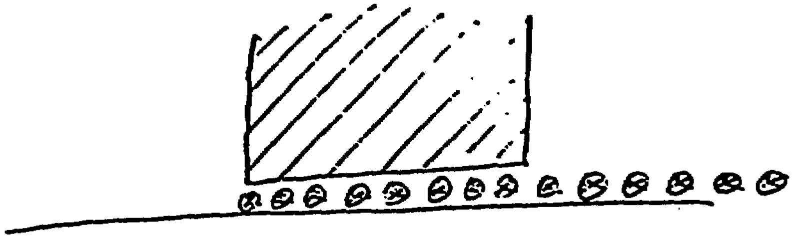

Biot and Savart's law.

- o it works
- o it does not work very well

7 DISCUSSIONS

Format of Workshop –

- tabulate results, and collate before the workshop

- use finer meshes

- ambiguity of FE / BI comparison

Additional Problems

- realistic excitation
- higher frequencies
- velocity terms
- discontinuous conductivity
- sharp corners
- non–linear materials
- conical test pieces

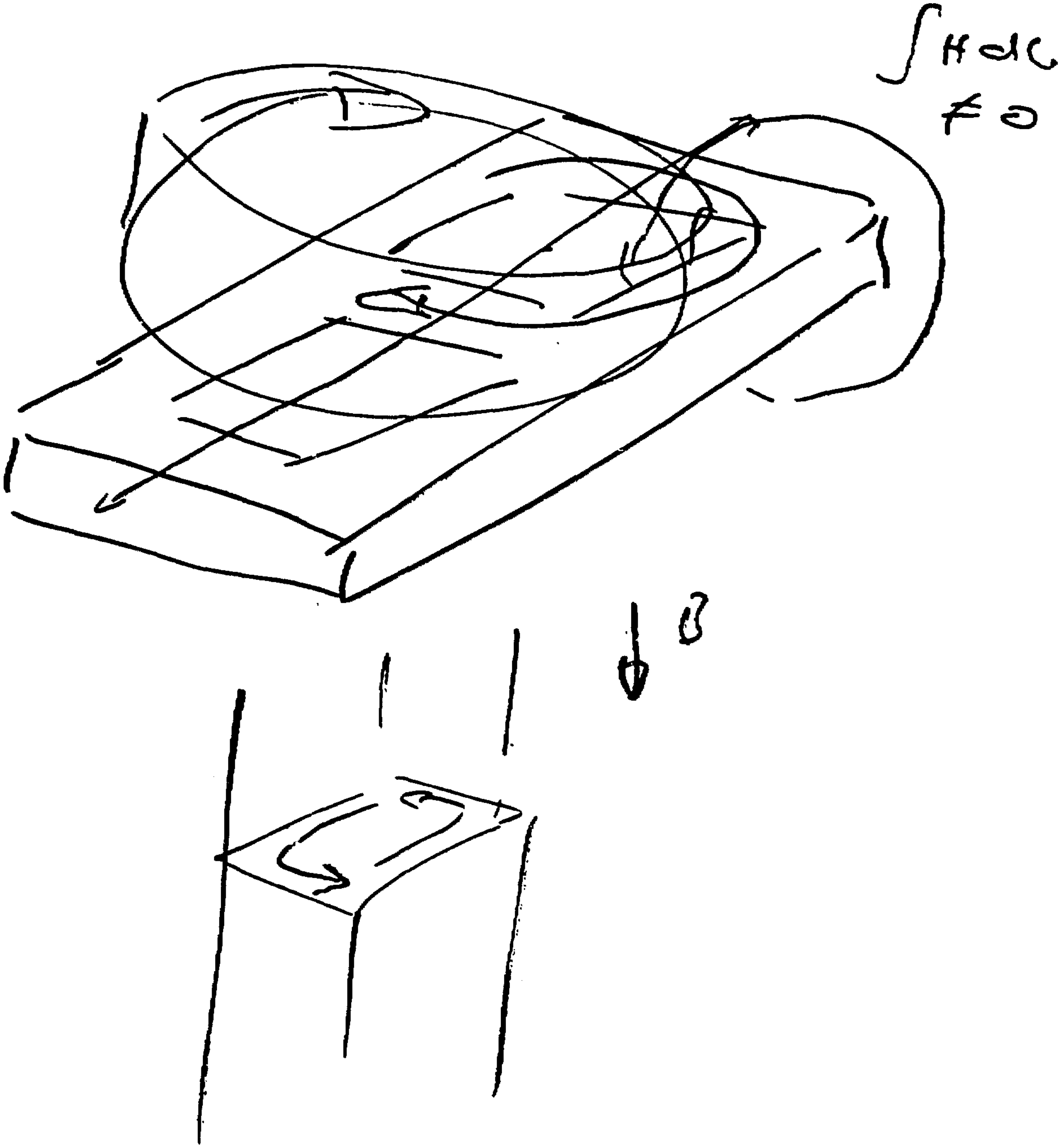
$\int H\,dl$
$\neq 0$
B

3.0 Workshop Problem 1

3.1 Summary of Results

The following tables summarize the results for Problem 1A (the FELIX long cylinder) and Problem 1B (the FELIX short cylinder). The codes refer either to the presentations that follow or to those that appear in the proceedings of the RAL workshop (RAL-86-049).

ANSYS	Dale F. Ostergaard - below, Sec. 3.3
BIE	Kent R. Davey - below, Sec. 3.2
BATH	P. Leonard - RAL p. 27
PE2D	C. Emson - , Sec. 3.4
UNISH	G. Rubinacci - RAL p. 15

Felix Long Cylinder Experiment
(Problem 1A)
Induced Field B_y (t)

Z, (m)	Time .01	Time .02	Time .04	Time	Peak Value	Code
	.0137	.0155	.0113	.0175	.0156	ANSYS (2-D)
	.0114	.0128	.0098	.021	.0128	BIE
0	.0113	.0166	.0115			BATH (2-D)
	.0132	.0148	.0107			PE2D (2-D)
	.0141	.0162	.0121	<.02	>.016	UNISH
	.0114	.0128	.0098	.0186	.0128	EXPERIMENT
				.0193	.0119	BIE
0.4	.0119	.0130	.0092	.02	.013	UNISH
				.0175	.0097	EXPERIMENT
				.0164	.00896	BIE
0.5	.00518	.00508	.00328			UNISH
				.0187	.00514	EXPERIMENT

FELIX Long Cylinder
(Problem 1A)

	Time 0.01	0.02	0.04	Peak	Peak Value	Code
Total J	2941	3442	2537	3449	.01875	ANSYS (2-D)
	2550	3450	2450	3470	.018	BATH (2-D)
	3111	3445	2467			PE2D (2-D)
Power Loss	418	573	311	575	.01875	ANSYS (2-D)
	474	548	298			PE2D (2-D)
Force F_x	241	225	102	250	.0125	ANSYS (2-D)
	244	220	100			BATH (2-D)
	253	223	97.4			PE2D (2-D)

Felix Short Cylinder Experiment
(Problem 1B)
Induced Field B_y (t)

Z, (m)	Time(s) .004	.008	.010	Time	Peak Value	Code
	.0390	.0495	.0494	.0088	.0498	ANSYS (2-D)
	.037	.048	.047	.009	.048	BIE
0						BATH (2-D)
						PE2D (2-D)
	.0328	.0387	.0371			UNISH (3-LAYER)
	.035	.042	.0375	.008	.042	EXPERIMENT
				.0077	.0432	BIE
0.05	.0263	.0298	.0282			UNISH
				.00739	.025	EXPERIMENT

3-D TRANSIENT EDDY CURRENT FIELDS USING INTEGRAL TECHNIQUES AND CHARACTERISTIC EIGENVALUES

Kent R. Davey
School of Electrical Engineering
Georgia Institute of Technology
Atlanta, Georgia 30332-0250

ABSTRACT

The three-dimensional eddy current transient field problem is formulated first using the U-V method. This method breaks the vector Helmholtz equation into two scalar Helmholtz equations. Eigenvalues are found by equating the determinant of the identification matrix (the matrix for determining the problem unknowns) to zero. When the initial forcing function is Fourier decomposed into its respective spatial harmonics, it is possible to associate with each Fourier component a unique set of eigenvalues by this technique. The technique is applied to the Felix medium and large cylinders and compared to data. Inclusion of higher order eigenvalues for each modal shape is seen to yield a substantial improvement in the field prediction correlation to data. The effect of these higher order eigenvalues/modes is of specific interest in this paper; the necessity of including the higher order eigenvalues indicates a drawback of this eigenvalue approach.

INTRODUCTION

A general theory involving the use of null field integral equations determining 3-D eigenvalues is developed. The theory is applied to the Argonne Felix cylinder experiments [1]. The general formulation preceding the null field integral technique involves the use of a second order vector potential, a method discussed by [2-3] but as far as the authors are aware of, never implemented here to date. After the null field integral technique predicts the eigenvalues associated with the problem, the total transient field solution is realized through a convolution of the impulse response with a particular external field decay generating the transient.

BASIS FUNCTIONS AND THE NULL FIELD TECHNIQUE

The vector Helmholtz equation for the magnetic vector potential is

$$\nabla^2\overline{A} - \mu\sigma \frac{\partial \overline{A}}{\partial t} = 0 \ . \tag{1}$$

Assume that $\overline{A} = \vec{A}e^{-\lambda t}$. The parameter "$\lambda$" is a key eigenvalue of the problem representing the characteristic temporal decay time of the field. It is, of course, a function of the forcing function (shape) giving rise to the transient. It is this eigenvalue λ (actually a set of them) that we seek. Defining $k^2 = \mu\sigma\lambda$, (1) is written as

$$\nabla^2\vec{A} + k^2\vec{A} = 0 \tag{2}$$

where $\vec{B} = \nabla \times \vec{A}$. It is useful to represent $\vec{A}$ in terms of a second vector potential $\vec{W}$,

$$\vec{A} = \nabla \times \vec{W} \quad (3)$$

where

$$\vec{W} = \hat{e}u + \hat{e} \times \nabla v \quad (4)$$

and $\hat{e}$ is a fixed unit vector $(\hat{a}_r, \hat{a}_z, \hat{a}_\theta, \ldots)$.

Figure 1 depicts the geometry of the problem. The cylindrical shell (inner radius "a", outer radius "b", length "ℓ") is stressed by a y directed field. At time t = 0, this external field collapses to zero with a time constant τ (5 to 40 msec). It is appropriate to think about this as a three region problem (note all three regions come in contact at $z = \pm \ell/2$). In regions 1 and 3, we let $\vec{H} = -\nabla\psi$ and solve

$$\nabla^2\psi = 0 \; . \quad (4)$$

In region 2, we solve (2) in light of (3) and (4) which gives [3,4]

$$\nabla^2 u + k^2 u = 0 \quad (5)$$

$$\nabla^2 v + k^2 v = 0 \; . \quad (6)$$

The integral solution of (4)-(6) is respectively

$$\left.\begin{array}{ll} \beta(r) & ; \; r \in V \\ \dfrac{\beta(r)}{2} & ; \; r \text{ surface} \\ 0 & ; \; r \notin V \end{array}\right\} = \oint_S \left[\frac{\partial\beta(r')}{\partial n} G(r,r') - \beta(r') \frac{\partial G(r,r')}{\partial n}\right] ds \quad (7)$$

where

if $\quad \beta = \psi \; , \; G(r,r') = \dfrac{1}{4\pi|\bar{r}-\bar{r}'|} \; ; \; V = V_{Air}$

else $\quad \beta = u \text{ or } v \; , \; G(r,r') = \exp(jk|\bar{r}-\bar{r}'|)/4\pi|\bar{r}-\bar{r}'| \; ; \; V = V_{conductor}$

We choose to solve the system equations using (7c). The approach is as follows:

1. Assign appropriate basis functions to the interfacial fields ψ, u, v, and their normal derivatives.
2. Pick arbitrary null field points outside the volumes of interest.
3. Impose the boundary conditions that tangential H and normal B be continuous across each interface.
4. Set up a matrix, the identification matrix, using the equations from (7c).
5. Determine the eigenvalues k for which the determinant of the identification matrix is zero.
6. Reconstruct the transient response in terms of these eigenvalues.

Both J_θ and J_z can be expressed as a combination of sinusoidal functions as follows:

$$J_\theta = \Sigma \, C_{\theta n} \sin \frac{n\pi}{\ell} z \cos\theta \quad (8)$$

$$J_z = \Sigma\, C_{zn} \cos \frac{n\pi}{\ell} z \sin\theta \tag{9}$$

The appropriate basis functions on u, v, and ψ follow directly from these expressions for J and are summarized in [4].

Solution proceeds by assuming a modal surface shape for the unknowns ψ, u, and v and their normal derivatives. For each modal shape, the matrix determinant defining these unknowns is set to zero giving us the eigenvalues for each mode.

TOTAL TRANSIENT RESPONSE

Which modal eigenvalue is used is dictated entirely by the initial field causing the transient. In general, one must decompose the initial field into its spatial Fourier components (to a flat stimulus at t = 0 ($H = H_o$ for all z)); we have

$$\vec{H} = \sum_{n=1,\mathrm{odd}}^{\infty} (-1)^{\frac{n-1}{2}} \frac{4H_o}{n\pi} \cos\left(\frac{n\pi}{\ell} z\right) . \tag{10}$$

Thus, the response to each component of the initial field is calculated separately (each with its own decay time) and weighted by the value "$\frac{4}{n\pi}$". Note the higher order modal surfaces decay rapidly. But since the higher order Fourier components contribute most significantly to the skirt regions of the field (near $z = \pm \ell/2$), one expects these regions to fall off more quickly due to the higher k values associated with the higher order modes.

RESULTS

A plot of the predicted induced fields for both the medium and large cylinders is shown in Figures 2 and 3. As evident in the above plots, the results agree reasonably well, but there is room for improvement, especially as regards the large cylinder field predictions. As mentioned above, the results were obtained by treating the problem as a three region problem, employing 6 null field equations to derive the identification matrix. Borrowing on some techniques from the scattering research community, we suspected that a better approach would be to use equations (7b) to yield 6 boundary equations, as well as (7c) to give an additional null field equation. Thus, we formulate 7 equations for 6 unknowns. The matrix (now 7 x 6) must be multiplied by its transpose before searching for the eigenvalues as the determinant of this modified matrix. This numerical trick greatly stabilizes the problem. In fact, with this change, the problem can indeed by solved as a two region problem without artificial interfaces.

A second surprise resulted after this modification. In addition to the base resonances found for each mode as before, additional resonances (eigenvalues) appeared. For the 2-D problem we found 2 eigenvalues (k = 51 and k = 150). The second value is quite far removed and it so happens that the weighting constant multiplying the second eigenvalue (based on the initial conditions) is nearly zero.

The 3-D eigenvalues for mode 1 $\left(\cos \frac{\pi}{\ell} z\right)$ are k = 57, 107, 128, 151, 178. We seek the eigenvectors for each eigenvalue mode by mode exactly as explained above.

$$\underline{x} = \begin{vmatrix} A \\ B \\ C \\ D \\ E \\ F \end{vmatrix} = c_{11}x_{11}e^{\lambda_{11}t} + c_{21}\underline{x}_{21}e^{-\lambda_{21}t} + \cdots c_{n1}e^{-\lambda_{n1}t}$$

(for mode 1: $\cos\left(\frac{\pi}{\ell} z\right)$ or $\sin\left(\frac{\pi}{2} z\right)$)

$$+ c_{13}\underline{x}_{13}e^{-\lambda_{13}t} + c_{23}\underline{x}_{23}e^{-\lambda_{23}t} + \cdots c_{n3}e^{-\lambda_{n3}t}$$

(for mode 2: $\cos\left(\frac{3\pi}{\ell} z\right)$ or $\sin\left(\frac{3\pi}{\ell} z\right)$)

$$+ \text{ higher order modes in } z \text{ space} \qquad (16)$$

Each eigenvector is weighted with a constant c chosen to satisfy the initial conditions. Constant "c_n" at $\theta = 0$, $z = 0$, must be equal to that part of the initial field which has a $\cos\left(\frac{n\pi}{\ell} z\right)$ dependence which happens to be $H_o \frac{4}{n\pi} (-1)^{n+1/2}$ for a uniform field - from the spatial Fourier decomposition. With 2 eigenvectors/mode, we can use these conditions to specify the weighting constants in (16).

By way of testing how important these additional eigenvalues/mode actually are, the additional eigenvalues for mode n = 1 were included (recall n = 1 has the lowest eigenvalues and strongest weighting). A dramatic improvement is evident in Fig. 4 for the large cylinder (τ = 39.6 msec) as an additional eigenvector is included. As a check, we see that when reasonable agreement exists using one eigenvalue as is the case for the medium cylinder, adding an additional eigenvalue to the problem does not disturb the agreement.

CONCLUSIONS

Areas of future work include:

1. Selection of smart basis functions for generalized problems.
2. Assessment of the effects of the higher order eigenvalues (> 150) ignored in this work.

It appears that the more complicated is the structure, the more likely each mode chosen will have significant higher order eigenvalues. For these cases an accurate, concise answer using the eigenvalue approach may be very costly.

REFERENCES

[1] L. R. Turner, et al., "Results from the Felix Experiments on Electromagnetic Effects in Hollow Cylinders," Fifth Compumag Conference, Fort Collins, Colorado, pp. 356-359, 1985.

[2] P. Hammond, "Use of Potentials in Calculation of Electromagnetic Fields," IEE Proceedings, Vol. 129, Part A, No. 2, pp. 106-112, 1982.

[3] C. R. I. Emsin, C. W. Trowbridge, and J. Simkin, "Further Developments in Three Dimensional Eddy Current Analysis," IEEE Trans. Magnetics, Vol. MAG-21, No. 6, pp. 2231-2234, November 1985.

[4] H. Han, K. Davey, and L. Turner, "3-D Transient Eddy Current Fields Using the U-V Integral Eigenvalue Formulation," accepted for publication in IEEE Trans. Magnetics, 1986-1987.

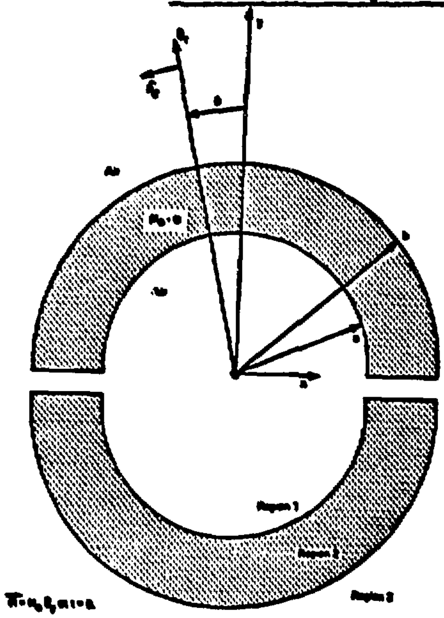

Fig. 1 Felix Cylinder Experiment. Slit cylinder is immersed in a homogeneous field $\vec{H} = H_o a_y$ at t=0; a=57.1 mm, b=69.8 mm, length = 300 mm, σ = 2.538 x 10^7 mho/m; field collapses with the constant τ = 39.68 msec.

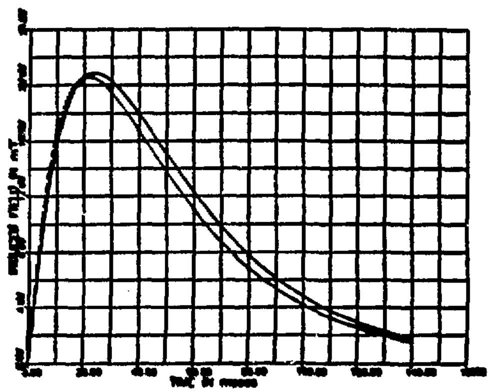

Fig. 2 Medium 60 cm Cylinder, Time Constant = 39.68 msec.

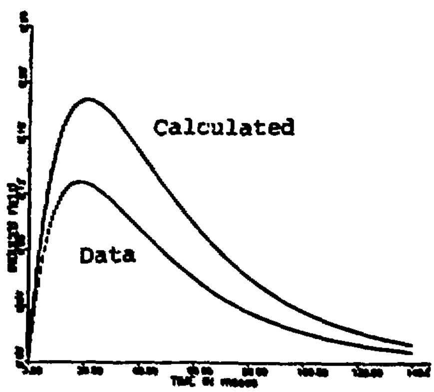

Fig. 3 Large Cylinder (1 Eigenvalue) with Normalized Input Field, Time Constant = 39.68 msec.

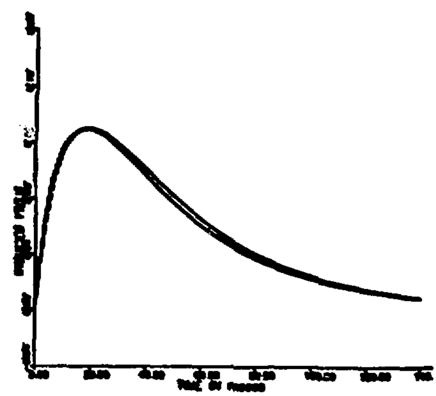

Fig. 4 Large Cylinder (2 Eigenvalues) with Normalized Input Field, Time Constant = 39.68 msec.

RESULTS FOR EDDY CURRENT WORKSHOP PROBLEMS 1A AND 1B
FELIX CYLINDER EXPERIMENTS

By

Dale F. Ostergaard
Swanson Analysis Systems, Inc.

INTRODUCTION

The commercially available finite element program ANSYS was used to model the magnetic field problems 1A and 1B of the Eddy Current Workshop problem series. The analysis uses a two-dimensional vector magnetic potential formulation. Two elements were investigated for each problem, the STIF55 4-node isoparametric quadrilateral element and the STIF77 8-node isoparametric quadrilateral element. The meshes used in the analyses were identical to those prescribed in the problem statements. The STIF77 runs included additional mid-side nodes.

FORMULATION

The transient magnetic field solution is formulated from the following two-dimensiional diffusion equation:

$$\frac{\partial}{\partial x}\left(\nu \frac{\partial A_z}{\partial x}\right) + \frac{\partial}{\partial y}\left(\nu \frac{\partial A_z}{\partial y}\right) = \sigma \frac{\partial A_z}{\partial t} - J_s \tag{1}$$

where: ν = reluctivity
A_z = magnetic vector potential
σ = material conductivity
J_s = source current density

The distribution of the vector potential, A, in each element is given by:

$$A = A(x,y) = \{N\}^T\{A_e\} \tag{2}$$

where: $\{N\}$ = vector of shape functions
$\{A_e\}$ = nodal potential vector

The equations for A for the STIF55 and STIF77 elements are shown in Figure 1 and 2 and are given in terms of s-t space. Derivation of the element matrices and load vectors can be found in references [1], [2].

The complete set of equations in matrix form can be written as

$$[C]\{\dot{A}\} + [K]\{A\} = \{Q\} \tag{3}$$

The time-integration procedure used to solve equation (3) is based on a modified Houbolt implicit time integration scheme in which a quadratic instead of a cubic order is used [2]. In addition, a variable time-step is allowed. The resulting equation solved is:

$$\left(\frac{2\Delta t_0+\Delta t_1}{\Delta t_{01}}\,\frac{1}{\Delta t_0}\,[C]+[K]\right)\{A_n\} = \{Q_n\} + [C]\left(\frac{\Delta t_{01}}{\Delta t_0 \Delta t_1}\,\{A_{n-1}\} - \frac{\Delta t_0}{\Delta t_0 \Delta t_1}\{A_{n-2}\}\right)$$

Figure 3 illustrates the parameters defined in equation 4.

Eddy current density is obtained for each conducting element from the element nodal potentials at the n^{th} and (n-1) time step through the following equation,

$$J_e^{eddy} = -\sigma\left(\frac{\partial A_z}{\partial t}\right)_e = -\sigma\left(\frac{1}{s}\,\frac{\sum_{i=1}^{s} A_n - \sum_{i=1}^{s} A_{n-1}}{\Delta t_0}\right)_e \tag{5}$$

where: s = number of nodes per element

Output parameters such as eddy current, power, and forces are based on the eddy current calculations in equation (5).

RESULTS

Results for problems 1A and 1B for each element formulation are given in Tables 1-4. Plots of desired parameters for the STIF77 results are shown in Figures 4-11. The time stepping procedure for problem 1A used 96 equal time steps while for problem 1B 100 time steps were used. Although an automatic time-stepping procedure could have been used, it was decided that accuracy of the eddy current calculations was best performed with equal time increments.

References

1. Cook, R.D., "Concepts and Applications of Finite Element Analysis", John Wiley and Sons, New York, 1981.

2. Kohnke, P.C., "ANSYS Engineering Analysis Systems Theoretical Manual", Swanson Analysis Systems, Inc., Houston, PA, 1985.

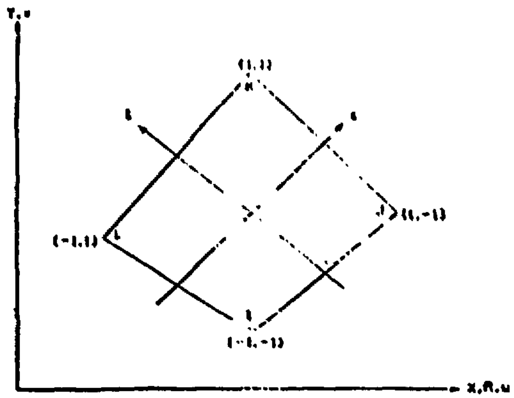

$$A = \frac{1}{4}(A_I(1-s)(1-t) + A_J(1+s)(1-t) + A_K(1+s)(1+t) + A_L(1-s)(1+t))$$

Figure 1 ANSYS STIF55 2-D Isoparametric Element

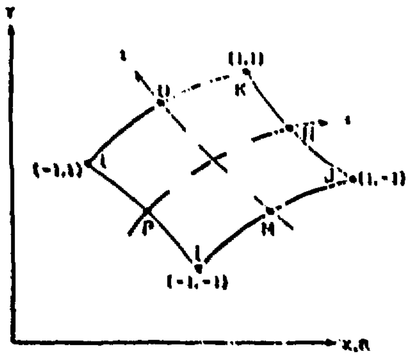

$$\begin{aligned} A = {} & \frac{1}{4}(A_I(1-s)(1-t)(-s-t-1) \\ & + A_J(1+s)(1-t)(s-t-1) \\ & + A_K(1+s)(1+t)(s+t-1) \\ & + A_L(1-s)(1+t)(-s+t-1)) \\ & + \frac{1}{2}(A_M(1-s^2)(1-t) \\ & + A_N(1+s)(1-t^2) \\ & + A_O(1-s^2)(1+t) \\ & + A_P(1-s)(1-t^2)) \end{aligned}$$

Figure 2 ANSYS STIF77 2-D Isoparametric Element

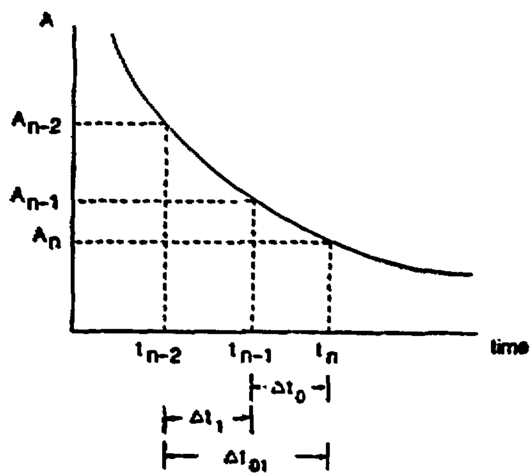

Figure 3 Implicit Time Integration Scheme Parameters

PROBLEM ~~1B~~ 1A RESULTS

Felix ~~Short~~ Long Cylinder Experiment

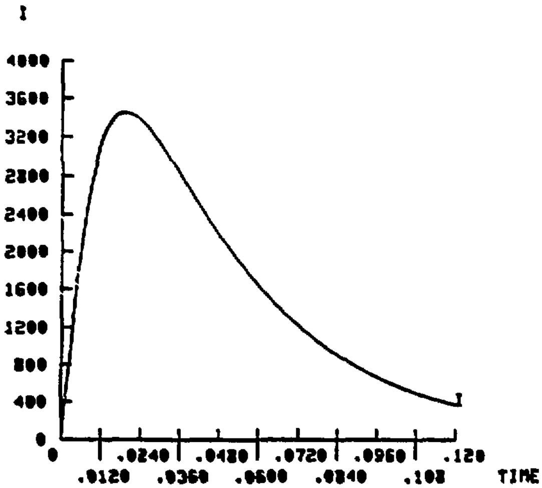

Figure 8 Total Eddy Current (Ampere)

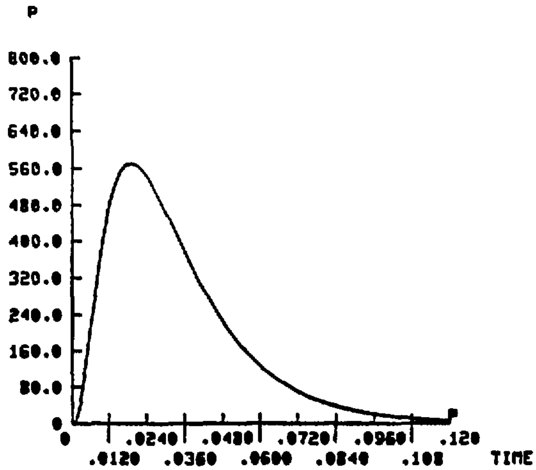

Figure 9 Power Loss (Watt)

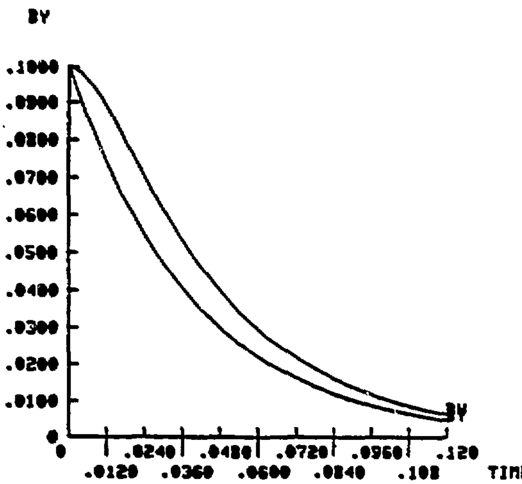

Figure 10 Total and Applied Magnetic Field - By (Testa)

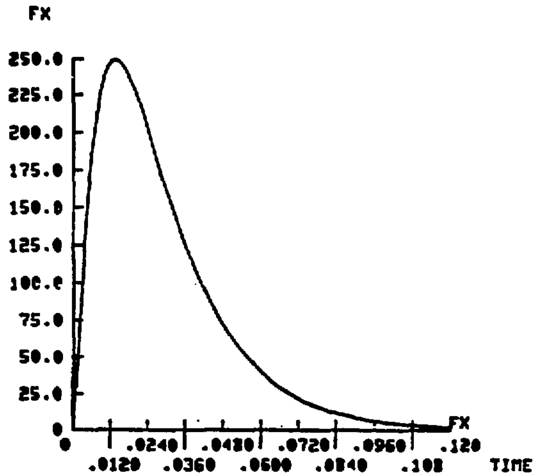

Figure 11 FX on Cylinder (Newton)

1B
PROBLEM ~~1A~~ RESULTS

Felix ~~Long~~ Short Cylinder Experiment

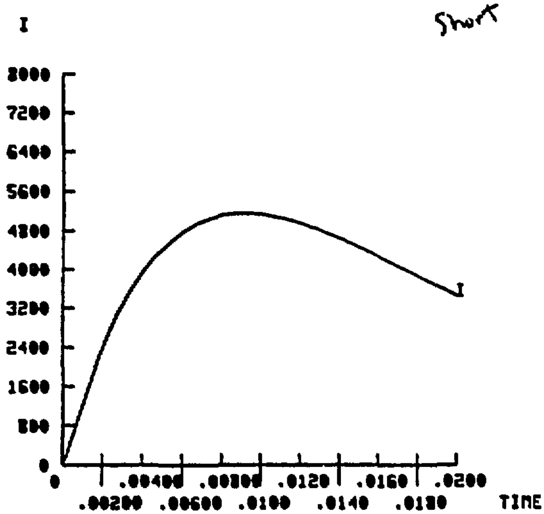

Figure 4 Total Eddy Current (Ampere)

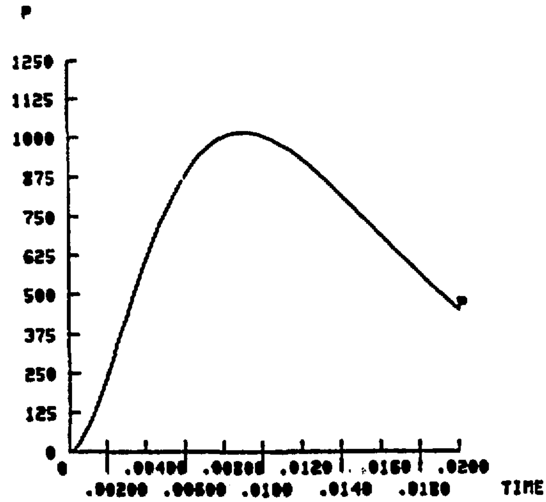

Figure 5 Power Loss (watt)

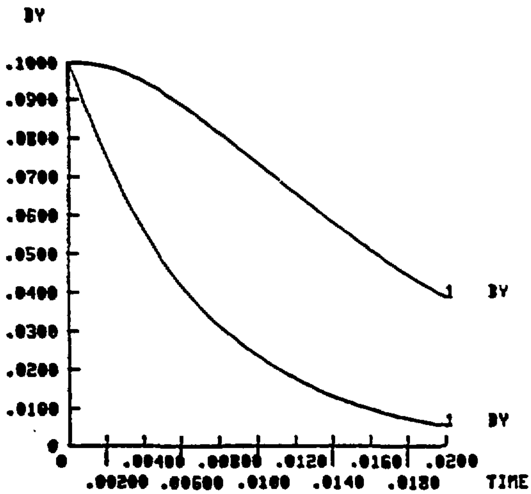

Figure 6 Total and Applied Magnetic
Field - B_y (Testa)

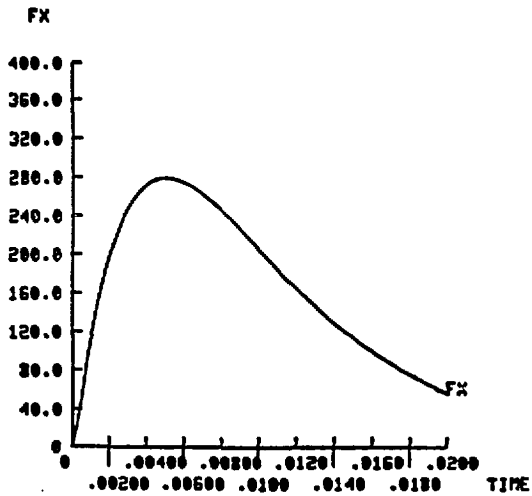

Figure 7 FX on Cylinder (Newton)

Table 1

RESULTS TABLE FOR PROBLEM 1A

ANSYS STIF55 2-D 4-NODE ISOPARAMETRIC ELEMENT

Quantity	Units	Value at Time 0.00s	0.01s	0.02s	0.04s	0.08s	0.12s	Peak Value	Time of Peak Value(s)
a) Current Crossing z = 0 m	A	0	-2941.16	-3442.15	-2537.29	-967.318	-353.797	-3449.66	.01875
b) Current Crossing z = 0.5 m	A								
c) B_y at									
z = 0 m	T	0	.013737	.015537	.011310	.00430	.0015731	.015609	.0175
z = 0.2 m	T								
z = 0.45 m	T								
z = 0.5 m	T								
z = 0.55 m	T								
z = 0.6 m	T								
z = 0.7 m	T								
z = 0.9 m	T								
d) Power	W	0	418.325	572.914	311.292	45.2445	6.05252	575.420	.01875
e) Total stored energy	J	2420.05	1464.46	886.345	324.068	43.2166	5.73278	2420.05	0
f) Stored energy from induced field	J	0	2.160	2.762	1.463	0.2116	0.02832	2.785	.01875
g) F_x	N	0	241.19	224.621	101.583	14.1887	1.89503	249.923	.0125
F_y	N	0	-13.8889	-18.3947	-9.87364	-1.4317	-.191505	-18.5121	.01875
F_z	N								

Table 2

RESULTS TABLE FOR PROBLEM 1A

ANSYS STIF77 2-D 8-NODE ISOPARAMETRIC ELEMENT

	Quantity	Units	Value at Time 0.00s	0.01s	0.02s	0.04s	0.08s	0.12s	Peak Value	Time of Peak Value(s)
a)	Current Crossing z = 0 m	A	0	-2895.44	-3451.9	-2589.98	-995.747	-364.465	-3453.29	.01875
b)	Current Crossing z = 0.5 m	A								
c)	B_y at									
	z = 0 m	T	0	.013819	.015845	.011716	.00449	.0016434	.015889	.01875
	z = 0.2 m	T								
	z = 0.45 m	T								
	z = 0.5 m	T								
	z = 0.55 m	T								
	z = 0.6 m	T								
	z = 0.7 m	T								
	z = 0.9 m	T								
d)	Power	W	0	400.888	569.616	320.633	47.392	6.34918	570.083	.01875
e)	Total stored energy	J	2420.05	1464.49	888.472	324.185	43.237	5.73278	2420.05	0
f)	Stored energy from induced field	J	0	2.190	2.889	1.580	0.232	0.02832	2.905	.01875
g)	F_x	N	0	238.458	226.870	104.708	14.7687	1.97413	249.419	.01375
	F_y	N	0	-13.6943	-18.7372	-10.399	-1.53249	-.205281	-18.7953	.01875
	F_z	N								

Table 3

RESULTS TABLE FOR PROBLEM 1B

ANSYS STIF55 2-D 4-NODE ISOPARAMETRIC ELEMENT

Quantity	Units	Value at Time 0.000 s	0.002 s	0.004 s	0.006 s	0.008 s	0.010 s	0.020 s	Peak Value	Time of Peak Value(s)
a) Current Crossing $z = 0$ m	A	0	-2471.12	-4035.43	-4854.51	-5172.57	-5163.09	-3379.04	-5200.27	.00880
b) Current Crossing $z = 0.06$ m	A									
c) B_y at										
$z = 0$ m	T	0	.024299	.038972	.046614	.049528	.049356	.0322007	.049756	.00880
$z = 0.5$ m	T									
$z = 0.10$ m	T									
$z = 0.15$ m	T									
d) Power	W	0	260.723	642.700	917.348	1036.89	1031.16	440.803	1047.05	.00880
e) Total stored energy	J	701.671	394.459	223.814	128.552	74.9847	44.5599	4.63044	701.670	0
f) Stored energy from induced field	J	0	1.4810	3.7220	5.2870	5.9490	5.8957	2.49993	5.9983	.00880
g) F_x	N	0	204.262	275.855	274.819	242.796	201.177	52.6427	281.226	.00480
F_y	N	0	-18.7112	-49.136	-70.8596	-80.3416	-79.9981	-34.236	-81.179	.00880
F_z	N									

Table 4

RESULTS TABLE FOR PROBLEM 1B

ANSYS STIF77 2-D 8-NODE ISOPARAMETRIC ELEMENT

	Quantity	Units	Value at Time 0.000 s	0.002 s	0.004 s	0.006 s	0.008 s	0.010 s	0.020 s	Peak Value	Time of Peak Value(s)
a)	Current Crossing z = 0 m	A	0	-2370.54	-3933.62	-4768.6	-5110.51	-5127.30	-3436.51	-5151.14	.0090
b)	Current Crossing z = 0.06 m	A									
c)	B_y at										
	z = 0 m	T	0	.024152	.038881	.046853	.049759	.049782	.0331847	.050076	.0090
	z = 0.5 m	T									
	z = 0.10 m	T									
	z = 0.15 m	T									
d)	Power	W	0	238.651	605.006	875.879	1001.15	1005.87	450.718	1015.90	.0090
e)	Total stored energy	J	701.671	394.447	223.806	128.579	75.0595	44.6810	4.79379	701.671	0
f)	Stored energy from induced field	J	0	1.4690	3.7140	5.3140	6.0238	6.0168	2.66328	6.0937	.0090
g)	F_x	N	0	197.419	272.100	274.346	244.895	204.938	56.4321	279.137	.0050
	F_y	N	0	-17.4826	-47.3117	-69.2653	-79.4338	-79.893	-35.8415	-80.6855	.0090
	F_z	N									

4.0 Workshop Problem 2

COMPARISON OF RESULTS, INFINITE CYLINDER IN UNIFORM FIELD

(Problem 2)

The results reported here are a compilation of data presented at the Electromagnetic Workshop at Rutherford Appleton Laboratory in March 1986 and at the Workshop at Argonne National Laboratory in June 1986. A total of six solutions to problem No. 2 are presented and compared directly in tables. Because of the large amounts of data available, only representative points were compared. For results at any other point, reference can be made to individual contributions. These can be found either in this document or in the proceedings of the RAL Workshop.

Some of the results available were not included in the comparison because they were available in a form which did not allow direct comparison. For example, the field values from PROFI were presented as r and θ components rather than x and y components. In addition, not all field and phase angle data were available at all required points. In such cases, the results were not included.

Table 1 presents a comparison of results for the x component of the field and the associated phase angles.

Table 2 is a similar comparison for the y component of the field and associated phase angles. In both cases, some of the phase angles are off by 180 degrees.

Table 3 presents the global values calculated.

Table 1. Comparison of results for the x component of the field.

	Bx (Tesla)			θx (Deg.)			
r	0	20	45	0	20	45	PROG.
.0	.0	.0	.0	-48.0	-48.0	-48.0	A
	.0	.0	.0	-166.0	-166.0	-166.0	B
	-----	-----	-----	-----	-----	-----	C
	.0	.0	.0	.0	.0	.0	D
	-----	-----	-----	-----	-----	-----	E
	.0	.0	.0	.0	.0	.0	F
.05842	.0052	-----	.0111	.0	-----	0.0	A
	.0013	-----	.0076	3.0	2.6	2.7	B
	-----	-----	-----	-----	-----	-----	C
	.0	.0068	.0106	.0	-158.6	-158.6	D
	.0009	.0026	.0101	-22.8	-15.0	-11.5	E
	.0	.0059	.0091	.0	175.2	175.2	F
.06858	.0205	-----	.0782	-11.0	-----	-11.0	A
	.0211	.0501	.0772	-10.2	-11.4	-11.4	B
	-----	-----	-----	-----	-----	-----	C
	.0	.0485	.0752	.0	-175.7	-175.7	D
	.0010	.0198	.0740	-10.4	-11.5	-10.4	E
	.0	.0504	.0783	.0	-170.2	-170.2	F
.1	.0119	-----	.0516	-14.0	-----	-14.0	A
	.0139	.0341	.0444	-14.4	-14.3	-14.3	B
	-----	-----	-----	-----	-----	-----	C
	.0	.0273	.0425	.0	-166.8	-166.8	D
	.0043	.0268	.0440	13.7	13.8	13.7	E
	.0	.0274	.0426	.0	-166.8	-166.8	F
.2	.0028	-----	.0141	-14.0	-----	-14.0	A
	.0033	.0078	.0109	-14.3	-14.3	-14.3	B
	-----	-----	-----	-----	-----	-----	C
	.0	.0068	.0106	.0	-166.8	-166.8	D
	.0013	.0081	.0096	13.7	13.7	13.7	E
	.0	.0068	.0106	.0	-166.8	-166.8	F

A - PE2D, Chris Emson, Rutherford Laboratory.
B - PE2D, Robert Lari, Argonne National Laboratory.
C - PROFI, U. Hamm, Technische Hochschule Darmstadt.
D - No Name, Toshiya Morisue, Tokushima University.
E - EDDYNDT, Nathan Ida, The University of Akron.
F - Analytical Solution, Oskar Biro, Technical University, Budapest

Table 2. Comparison of results for the y component of the field.

r	By (Tesla)			θ_y (Deg.)			
	0	20	45	0	20	45	PROG.
.0	.0233	.0233	.0233	-86.0	-86.0	-48.0	A
	.0222	.0222	.0222	-86.2	-86.2	-86.2	B
	-----	-----	-----	-----	-----	-----	C
	.0212	.0212	.0212	-95.0	-95.0	-95.0	D
	-----	-----	-----	-----	-----	-----	E
	.0211	.0211	.0211	-95.0	-95.0	-95.0	F
.05842	.0363	-----	.0261	-137.0	-----	-115.0	A
	.0293	.0359	.0270	-123.9	-138.1	-118.4	B
	-----	-----	-----	-----	-----	-----	C
	.0222	.0210	.0187	-35.8	-41.5	-64.2	D
	.0295	.0220	.0195	-33.8	-36.6	-64.2	E
	.0028	.0027	.0023	-53.8	-57.3	71.2	F
.06858	.1736	-----	.0904	176.0	-----	-175.0	A
	.1648	.1531	.0953	177.8	177.1	-176.4	B
	-----	-----	-----	-----	-----	-----	C
	.1630	.1457	.0890	-3.1	-4.0	9.4	D
	.1740	.1606	.0920	-14.2	-3.3	-15.4	E
	.1667	.1485	.0896	2.1	1.2	-4.6	F
.1	.1464	-----	.0968	175.0	-----	-179.0	A
	.1478	.1312	.1035	175.3	176.6	179.5	B
	-----	-----	-----	-----	-----	-----	C
	.1418	.1319	.0999	2.9	3.2	.0	D
	.1440	.1333	.1000	2.7	2.1	1.8	E
	.1418	.1319	.1000	3.9	3.2	.0	F
.2	.1136	-----	.1000	178.0	-----	-180.0	A
	.1138	.1101	.1032	178.2	178.7	179.5	B
	-----	-----	-----	-----	-----	-----	C
	.1104	.1079	.1000	1.3	1.0	.0	D
	.1131	.1036	.1000	1.8	.9	1.8	E
	.1104	.1080	.1000	1.3	1.0	.0	F

A - PE2D, Chris Emson, Rutherford Laboratory.
B - PE2D, Robert Lari, Argonne National Laboratory.
C - PROFI, U. Hamm, Technische Hochschule, Darmstadt.
D - No Name, Toshiya Morisue, Tokushima University.
E - EDDYNDT, Nathan Ida, The University of Akron.
F - Analytical Solution, Oskar Biro, Technical University, Budapest.

Table 3. Comparison of global quantities.

	Time Average	Amplitude	Phase (Deg.)	PROG.
Total Eddy	.0	11385.0	164.4	A
Current in	.0	11239.0	166.5	B
the Whole	-------	-------	-----	C
cylinder.	-------	10325.0		D
[A]	-------	10511.0	-----	E
	.0	10569.0	12.4	F
Power Loss	2688.0	2413.0	-30.1	A
(1/4 Cylin-	2613.0	2346.0	-29.6	B
der)	20578.0	-------	-----	C
	2177.0	1949.0	27.0	D
[Watt/m]	-------	1912.4	-----	E
	2288.0	2043.0	27.6	F
Stored	1.74	1.54	7.1	A
Energy	1.69	1.49	7.5	B
(1/4 Cylin-	.04	--------	-----	C
der)	1.92	1.20	-27.7	D
.05715<r<	--------	1.25	-----	E
.06985 [Joule/m]	1.60	1.41	-8.8	F
Stored	.276	.271	-176.6	A
Energy	.270	.260	-175.8	B
(1/4 Cylin-	2.130	---------	-----	C
der)	.229	.229	169.9	D
r<.05715	---------	.230	-----	E
[Joule/m]	.228	.228	180.0	F
Stored	362.9	362.2	-1.0	A
Energy	265.0	264.0	-1.3	B
(1/4 Cylin-	2365.0	--------	-----	C
der)	273.5	273.8	.6	D
r>.06985	-------	286.2	-----	E
[Joule/m]	273.6	273.1	.5	F
Stored	-------	--------	-----	A
Energy of	12.3	10.9	-1.2	B
Induced	-------	--------	-----	C
Field	.0	2.6	117.0	D
[Joule/m]	-------	2.8	-----	E
	-------	--------	-----	F

Table 3. (Continued)

Force on 1/4 Cylinder [N/m] Fx	-386.0 -375.0 ------- -314.0 ------- -333.0	407.0 396.0 -------- 348.0 -343.7 352.0	171.5 172.0 ----- -175.0 ----- -173.6	A B C D E F
Force on 1/4 Cylinder [N/m] Fy	-196.0 -190.0 ------- -157.0 ------- -167.0	375.0 363.0 ------- 164.0 155.7 166.0	163.2 163.6 ----- -158.0 ----- -155.8	A B C D E F

A - PE2D, Chris Emson, Rutherford Laboratory.
B - PE2D, Robert Lari, Argonne National Laboratory.
C - PROFI, Technische Hochschule, Darmstadt.
D - No Name, Toshiya Morisue, Tokushima University.
E - EDDYNDT, Nathan Ida, The University of Akron.
F - Analytical Solution, Oskar Biro, Technical University, Budapest.

International Electromagnetic Workshop
Problem 2 : Infinitely Long Cylinder in a Sinusoidal Field

T. Morisue, University of Tokushima, Japan

Introduction

In this report, Problem 2 is solved using the magnetic vector potential and integral equation method. The computing process consists of two phases: in Phase 1 the boundary values of the vector potential and its normal derivative are calculated, and in Phase 2 the magnetic field and eddy current at the specified points are computed using the finite difference method (in the cylinder) and the integral equation method (both inside and outside the cylinder). The results coincide well with the analytical solution.

The Field Equations

in the cylinder: $\quad \mathrm{div}\,(\,\mathrm{grad}\,Az\,) - j\omega\mu\sigma Az = 0$

inside the cylinder: $\quad \mathrm{div}\,(\,\mathrm{grad}\,Az\,) = 0$

outside the cylinder: $\quad \mathrm{div}\,(\,\mathrm{grad}\,Az\,) + \mu Jzo = 0$

The Interface Conditions

$$Az1 = Az2, \quad Az2 = Az3$$

$$\underline{n}.\mathrm{grad}\,Az1 = \underline{n}.\mathrm{grad}\,Az2, \quad \underline{n}.\mathrm{grad}\,Az2 = \underline{n}.\mathrm{grad}\,Az3$$

where 1 = inside, 2 = in, 3 = outside the cylinder, and $\underline{n}$ = a unit vector normal to the interface.

The Boundary Condition

$$Az3(\underline{r}) = O(1/r) \quad \text{at infinity} \qquad (O = \text{order of})$$

Note: Az3 is the induced vector potential.

The Boundary Integral Equations

for conductor:
$$1/2\,Az(\underline{r}) = \int(\underline{n}.\mathrm{grad}\,Az(\underline{r}'))j/4\,H(k|\underline{r} - \underline{r}'|)ds' - \int Az(\underline{r}')(\underline{n}.\mathrm{grad}(j/4\,H(k|\underline{r} - \underline{r}'|))ds'$$

for nonconductor:
$$1/2\,Az(\underline{r}) = \int(\underline{n}.\mathrm{grad}\,Az(\underline{r}'))1/2\pi\,\log(1/|\underline{r} - \underline{r}'|)ds' - \int Az(\underline{r}')(\underline{n}.\mathrm{grad}(1/2\pi\,\log(1/|\underline{r} - \underline{r}'|)ds' + \iint \mu Jzo(\underline{r}'')\,1/2\pi\,\log(1/|\underline{r} - \underline{r}''|)dv''$$

where $j = \sqrt{-1}$, $k = (-1 + j)\sqrt{\omega\mu\sigma/2}$, $H(w)$ is the first kind Hankel function and the integral form representation of it is as follows.

$$H(w) = -2j/\pi\int_0^\infty \exp(jw.\cosh(t))\,dt$$

Note: For this problem,

$$\iint \mu Jzo(\underline{r}") \, 1/2\pi \log(1/|\underline{r} - \underline{r}"|) \, dv" = 0 \qquad \text{on the inner interface,}$$

$$= -Bo.R\cos\theta \qquad \text{on the outer interface}$$

where Bo = external uniform magnetic field, R = outer radius of the cylinder.

Description of the Boundary Elements

The inner and outer surfaces of the cylinder are divided into 40 identical elements, respectively, as shown in Fig.1. The vector potential and its normal derivative are assumed to be of constant value on each element.

From the interface conditions and the fourfold symmetry, total number of variables is 40.

Calculation of the Vector Potential in the Cylinder

After the calculation of the boundary values of the vector potential, the values in the cylinder can be calculated using the following equation as a Dirichlet type boundary-value-problem.

$$\partial^2 Az/\partial r^2 + 1/r\, \partial Az/\partial r + 1/r^2\, \partial^2 Az/\partial\theta^2 + k^2 Az = 0$$

The computation is carried out using the finite difference method and the iterative method. The finite difference mesh shown in Fig.2 is used.

Calculation of the Vector Potential inside and outside the Cylinder

The values of the vector potential both inside and outside the cylinder are calculated using the integral equations given above. (The coefficient of $Az(\underline{r})$ should be changed from 1/2 to 1.)

Calculation of the Magnetic Flux Density

The values of the magnetic flux density are calculated from the values of the vector potential using a central difference of the first derivative.

Analytical Solution

Problem 2 has an analytical solution which is expressed as follows.

in the cylinder: $Az(r, \theta) = (aJ1(kr) + bN1(kr))\cos\theta$

inside the cylinder: $Az(r, \theta) = cr\cos\theta$

outside the cylinder: $Az(r, \theta) = Bo(-r + d/r)\cos\theta$

where a = 2BoR(N1(kR1) - kR1.N1'(kR1))/D, b = -2BoR(J1(kR1) - kR1.J1'(kR1))/D

c = 2Bo.kR(J1'(kR1)(N1(kR1) - kR1.N1'(kR1)) - N1'(kR1)(J1(kR1) - kR1.
J1'(kR1)))/D

d = R²(1 + 2(J1(kR)(N1(kR1) - kR1.N1'(kR1)) - N1(kR)(J1(kR1) - kR1.
J1'(kR1)))/D)

D = (J1(kR1) - kR1.J1'(kR1)).(N1(kR) + kR.N1'(kR))
- (N1(kR1) - kR1.N1'(kR1)).(J1(kR) + kR.J1'(kR))

J1(w) = the first order Bessel function, N1(w) = the first order Neumann function, J1'(w) = dJ1(w)/dw, N1'(w) = dN1(w)/dw. R1 = inner radius of the cylinder. The computed result is as follows. ($R = .06985$, $R1 = .05715$, $Bo = 0.1$, $f = 60$, $\mu = 4\pi$ E-07, $\rho = 3.94$E-08.)

$a = -0.1240 - j0.03237$, $b = 0.03243 - j0.1240$

$c = 0.002024 + j0.02094$, $d = 4.141\text{E-}03 + j9.702\text{E-}04$

Calculation of the Stored Energy

Stored energy in the volume $R1 < r < R$:

$$\int_{R1}^{R}\int_{0}^{2\pi}(Bx(r,\theta,t)^2 + By(r,\theta,t)^2)\,r\,dr\,d\theta\;/2\mu$$

Stored energy in the volume $0 < r < R1$:

$$\int_{0}^{2\pi} Az(R1,\theta,t)(Bx(R1,\theta,t)\sin\theta - By(R1,\theta,t)\cos\theta)R1\,d\theta\;/2\mu$$

Stored energy in the volume $R < r < Rb$ ($Rb = 0.42$) :

$$\int_{0}^{2\pi} Az(Rb,\theta,t)(Bx(Rb,\theta,t)\sin\theta - By(Rb,\theta,t)\cos\theta)Rb\,d\theta/2\mu$$

$$-\int_{0}^{2\pi} Az(R,\theta,t)(Bx(R,\theta,t)\sin\theta - By(R,\theta,t)\cos\theta)R\,d\theta/2\mu$$

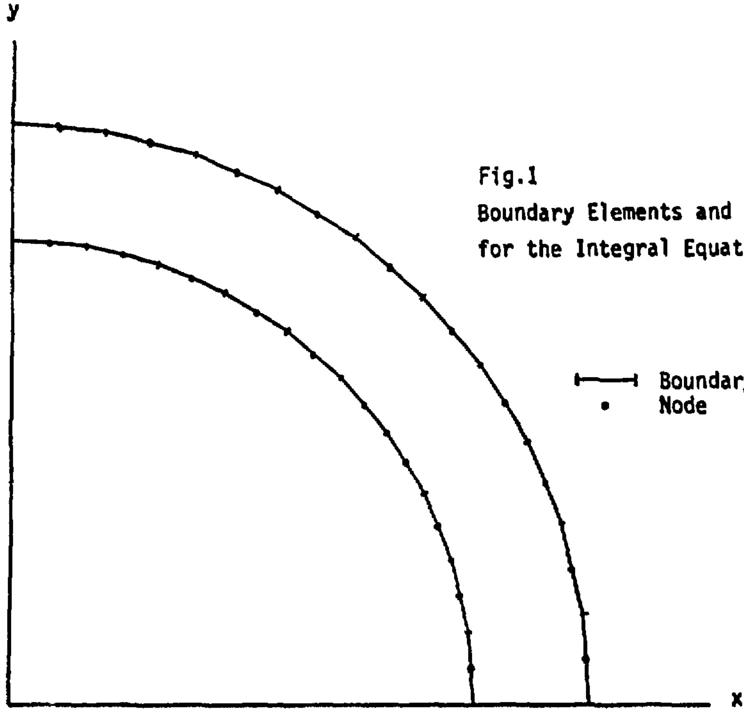

Fig.1
Boundary Elements and Nodes
for the Integral Equation Method

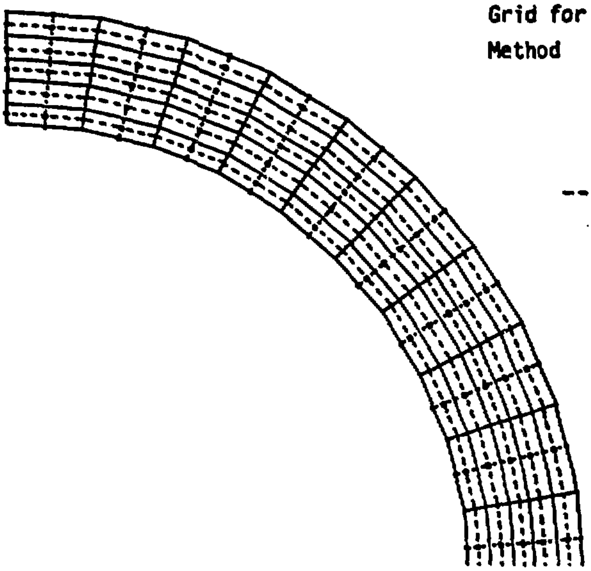

Fig.2
Grid for the Finite Difference
Method

Fig. 3 Comparison of the numerical solution with the analytical solution

(The vector potential on the inner and outer surface of the cylinder)

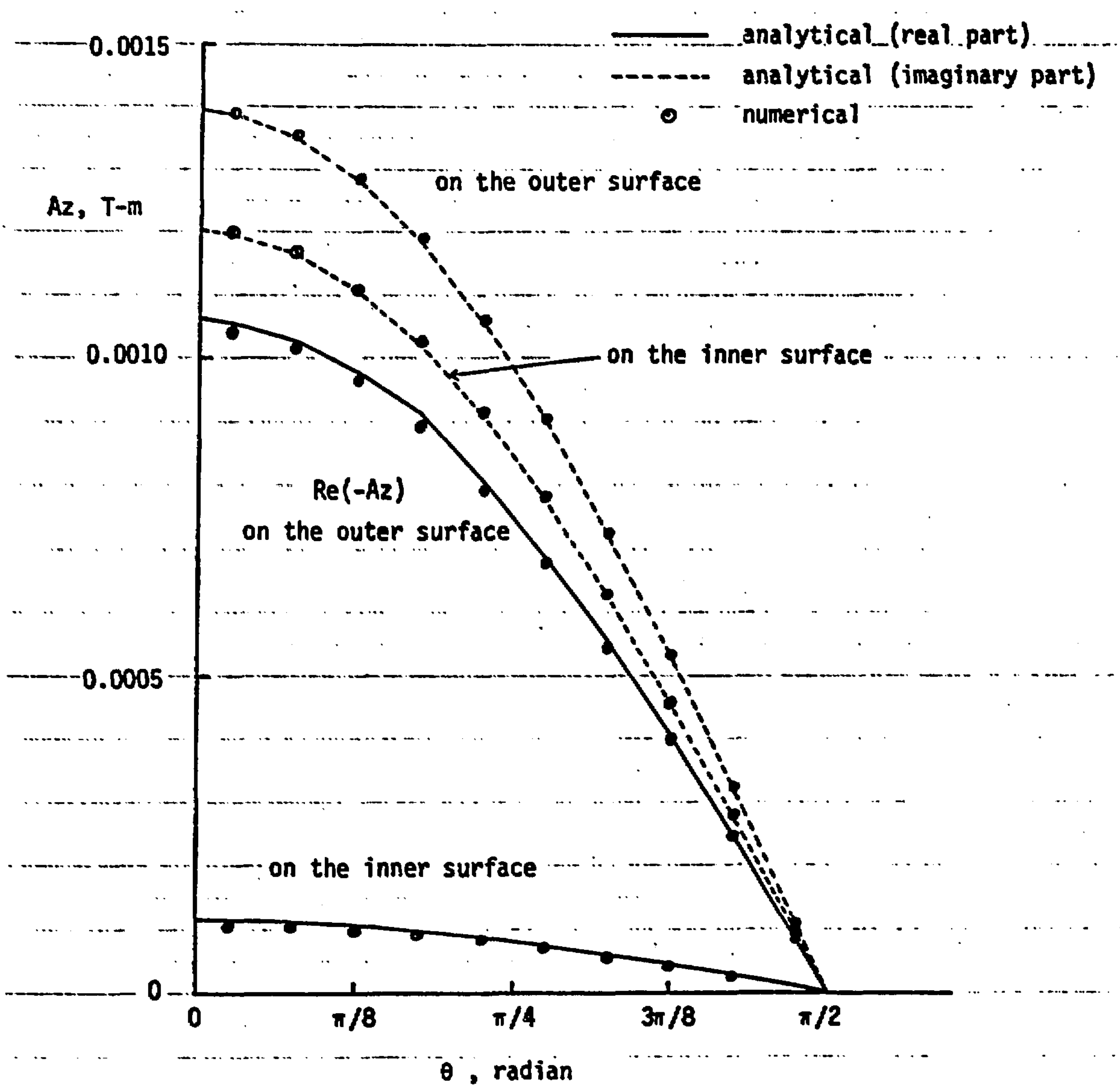

Table 2.1

Results for Problem 2
Field Calculations

Field Points at Mesh Points

R (M)	θ (DEG)	B_x (T)	ϕ_x (DEG)	B_y (T)	ϕ_y (DEG)
.00	0.0	0	-	.02120	-95.04
.01	0.0	0	-	.02120	-95.04
.02	0.0	0	-	.02120	-95.04
.03	0.0	0	-	.02120	-95.04

Field Points on Mesh Lines

R (M)	θ (DEG)	B_x (T)	ϕ_x (DEG)	B_y (T)	ϕ_y (DEG)
.04	0.	0	-	.02120	-95.04
.05	0.	0	-	.02102	-95.04
.05842	0.	0	-	.02222	-35.84
.06858	0.	0	-	.1630	-3.117
.075	0.	0	-	.1737	6.431
.10	0.	0	-	.1418	3.930
.15	0.	0	-	.1185	2.087
.20	0.	0	-	.1104	1.260
.25	0.	0	-	.1066	.8344
.30	0.	0	-	.1046	.5907
.35	0.	0	-	.1034	.4391
.40	0.	0	-	.1026	.3388
.05	45.	.0001509	- 95.04	.02120	-95.04
.05842	45.	.01058	-158.6	.01873	-64.17
.06858	45.	.07522	-175.7	.08897	-9.376
.075	45.	.07546	-166.3	.1004	- .4000
.10	45.	.04253	-166.8	.09993	- .008924
.15	45.	.01890	-166.8	.09998	- .001788
.20	45.	.01063	-166.8	.1000	- .0005586
.25	45.	.006805	-166.8	.1000	- .0002551
.30	45.	.004725	-166.8	.1000	- .00009338
.35	45.	.003472	-166.8	.1000	- .00006337
.40	45.	.002658	-166.8	.1000	- .00003502

Table 2.2

Results for Problem 2
Field Calculations

Field Points Inside of Elements (R < .07)

R (M)	θ (DEG)	B_x (T)	ϕ_x (DEG)	B_y (T)	ϕ_y (DEG)
.01	7.5	0	-	.02120	-95.04
.02	7.5	0	-	.02120	-95.04
.03	7.5	0	-	.02120	-95.04
.04	7.5	0	-	.02120	-95.04
.05	7.5	.0001155	-95.04	.02105	-95.04
.05842	7.5	.002738	-158.6	.02204	-36.60
.06858	7.5	.01947	-175.7	.1606	- 3.230
.01	14.	0	-	.02120	-95.04
.02	14.	0	-	.02120	-95.04
.03	14.	0	-	.02120	-95.04
.04	14.	0	-	.02120	-95.04
.05	14.	.00002887	- 95.01	.02155	-95.04
.05842	14.	.005012	-158.6	.02162	-38.39
.06858	14.	.03565	-175.7	.1550	- 3.506
.01	20.	0	-	.02120	-95.04
.02	20.	0	-	.02120	-95.04
.03	20.	0	-	.02120	-95.04
.04	20.	0	-	.02120	-95.04
.05	20.	.0001357	- 95.05	.02098	-95.04
.05842	20.	.006819	-158.6	.02099	-41.49
.06858	20.	.04850	-175.7	.1457	- 4.003
.01	45.	0	-	.02120	-95.04
.02	45.	0	-	.02120	-95.04
.03	45.	0	-	.02120	-95.04
.04	45.	0	-	.02120	-95.04
.05	45.	.0001509	- 95.04	.02120	-95.04
.05842	45.	.01058	-158.6	.01873	-64.17
.06858	45.	.07522	-175.7	.08897	- 9.376

Table 2.3

Results for Problem 2
Field Calculations

Field Points Inside of Elements (R > .07)

R (M)	θ (DEG)	B_x (T)	ϕ_x (DEG)	B_y (T)	ϕ_y (DEG)
.075	7.5	.01951	-167.3	.1722	5.464
.10	7.5	.01097	-166.8	.1404	3.834
.15	7.5	.004886	-166.8	.1179	2.027
.20	7.5	.002750	-166.8	.1100	1.221
.25	7.5	.001760	-166.8	.1064	.8076
.30	7.5	.001222	-166.8	.1045	.5714
.35	7.5	.0008985	-166.8	.1033	.4246
.40	7.5	.0006880	-166.8	.1025	.3275
.075	14.	.03523	-166.0	.1647	5.899
.10	14.	.01991	-166.8	.1369	3.593
.15	14.	.008863	-166.8	.1163	1.877
.20	14.	.004988	-166.8	.1092	1.125
.25	14.	.003193	-166.8	.1059	.7421
.30	14.	.002218	-166.8	.1041	.5242
.35	14.	.001630	-166.8	.1030	.3891
.40	14.	.001248	-166.8	.1023	.3000
.075	20.	.04865	-166.7	.1589	3.439
.10	20.	.02727	-166.8	.1319	3.231
.15	20.	.01214	-166.8	.1141	1.659
.20	20.	.006830	-166.8	.1079	.9865
.25	20.	.004372	-166.8	.1051	.6485
.30	20.	.003037	-166.8	.1035	.4571
.35	20.	.002231	-166.8	.1026	.3389
.40	20.	.001708	-166.8	.1020	.2610

Table 2.4

Results for Problem 2

The Infinite Cylinder

Global Results

$\omega = 2\pi f$

	Time Average	Amplitude	Phase (degree)
b) Total current (A) $I = I_0 \cos(\omega t + \phi)$		20650.	12.11
c) Power losses (W/m) $P = P_a + P_0 \cos(2\omega t + \phi)$	8707.	7795.	26.97
d) Stored energy .05715 < r < .06985 (J/m) $E = E_a + E_0 \cos(2\omega t + \phi)$	7.678	4.801	-27.73
e) Stored energy r < .05715 (J/m)	.9151	.9151	169.9
f) Stored energy r > .06985 (J/m)	1094.	1095.	.5908
g) Stored energy of induced field (J/m)	0	10.34	117.0
h) Force on one fourth of the cylinder (N/m) $F_x = F_{xa} + F_{xo} \cos(2\omega t + \phi)$	-314.1	348.1	-175.0
$F_y = F_{ya} + F_{yo} \cos(2\omega t + \phi)$	-157.5	163.9	-158.0

Recalculation of Test Problem 2 for the International Electromagnetic Workshops

Robert J. Lari
Argonne National Laboratory
May 27, 1986

Summary

Test Problem 2 was calculated using PE2D[1] and reported at the Rutherford Appleton Laboratory Workshop on March 27, 1986. It has been recalculated using a closer approximation to the specified mesh. In addition, quadratic elements were used in the specified mesh to compare with the linear element solution. Finally, a finer mesh using both linear and quadratic elements has been calculated. All of these results are reported here.

Problem Description

The desired mesh is shown in Figs. 1a and 1b with specified potentials at the seven mesh points on the circular arc of radius 42 cm to produce a uniform field of 0.1 Tesla. In the previous calculation, the mesh was extended outward from a radius of 42 cm because PE2D can only assign potentials to element sides and not nodes. Since that calculation, John Simkin of Vector Fields has shown me how to "cheat" on the program and assign a potential at a node. This is done by defining a very small quadrilateral region with only one node coincident with the desired potential node and the other three nodes not coincident with any other nodes. This is illustrated in Fig. 2a by the regions 10 through 15 and in Fig. 2b where region 13 is shown enlarged. The assigned potential of the left side of region 13 now assigns a potential to the lower left corner node. This method can be used on interior nodes as well. This mesh has 12 more elements and 18 more nodes than the specified mesh but the potentials are assigned at the specified points.

Results of the Calculation

The results of the calculation are given in five sets of tables as defined below.

Table No.	Mesh Used
2.1.1 to 2.4.1	These calculations were for the mesh described above and linear triangular finite elements.
2.1.2 to 2.4.2	These calculations were for the mesh described above and quadratic triangular finite elements.
2.1.3 to 2.4.3	These calculations were for four times the number of linear triangular finite elements in the mesh described above. This mesh is shown in Figs. 3a and 3b.
2.1.4 to 2.4.4	These calculations were for four times the number of quadratic triangular finite elements in the mesh described above. This mesh is shown in Figs. 3a and 3b.

2.1.5 to 2.4.5	This is the analytic solution as reported by A. IVANYI, I. BARDI, and O. BIRO[2], at the Rutherford Appleton Laboratory Workshop in March 1986.

An asterisk (*) in the tables means that the value calculated was very much wrong.

Comments and Conclusions

These calculations were made using version 7.0 of PE2D installed on a VAX 780 computer. The largest errors in the field calculation occur inside the conductor at r = 5.842 cm where the calculated field is about 10 times the analytic value. At a radius smaller than 5 cm the error is about +9 percent. For radii 7.5 cm and larger, the error is about four percent.

When quadratic elements are used, the error in the field calculation changes sign and is reduced slightly for $r < 5$ cm. Inside the conductor, the error becomes slightly larger and for $r > 7.5$ cm it doubles. It appears as if the error is not always reduced by going to quadratic elements.

Quadrupling the number of linear elements reduced the error for $r < 5$ by a factor of two but did not reduce the error significantly for other radii. Using quadratic elements resulted in some reduction in the error.

References:

1. Obtained from Vector Fields, Ltd., Kemp Hall Bindery, Osney Mead, Oxon OX2 OEE, United Kingdom.

2. A. Ivanyi, I, Bardi, O, Biro, "Analytical Solution to Problem 2 of the International Electromagnetic Workshop," Department of Electromagnetic Theory, Technical University of Budapest, H-1521 BUDAPEST, Hungary.

RJL:ehr

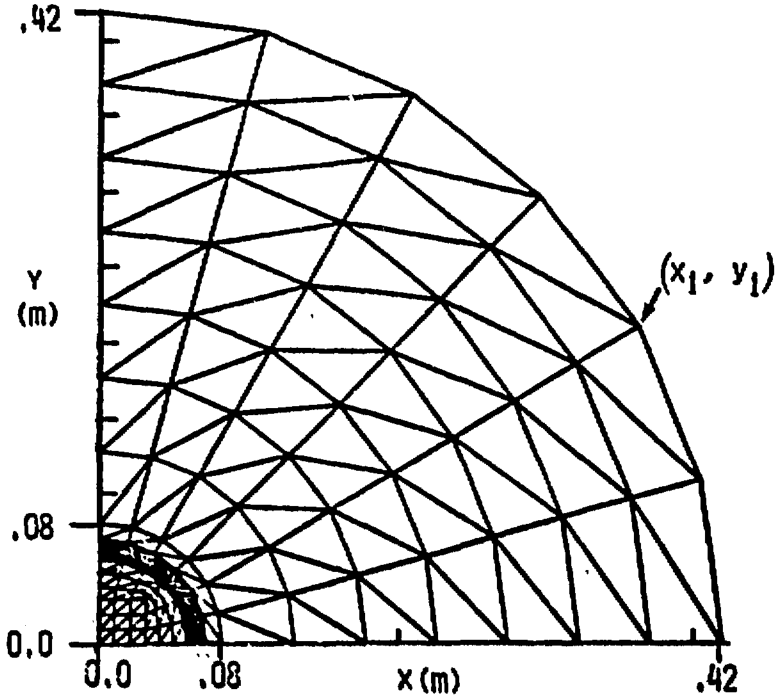

Figure 1a.

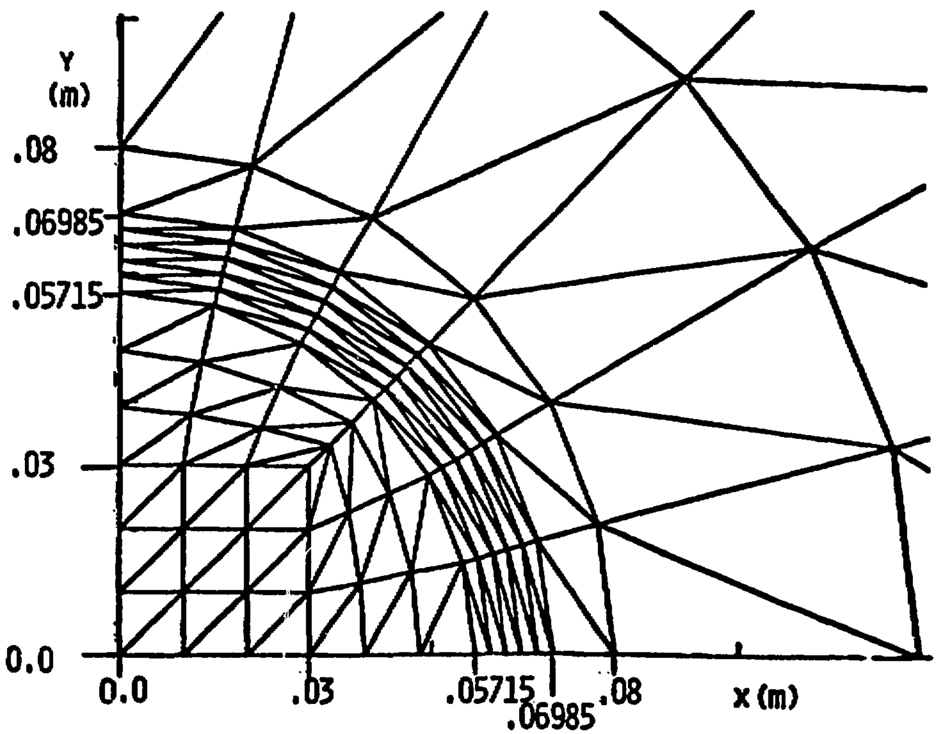

Figure 1b.

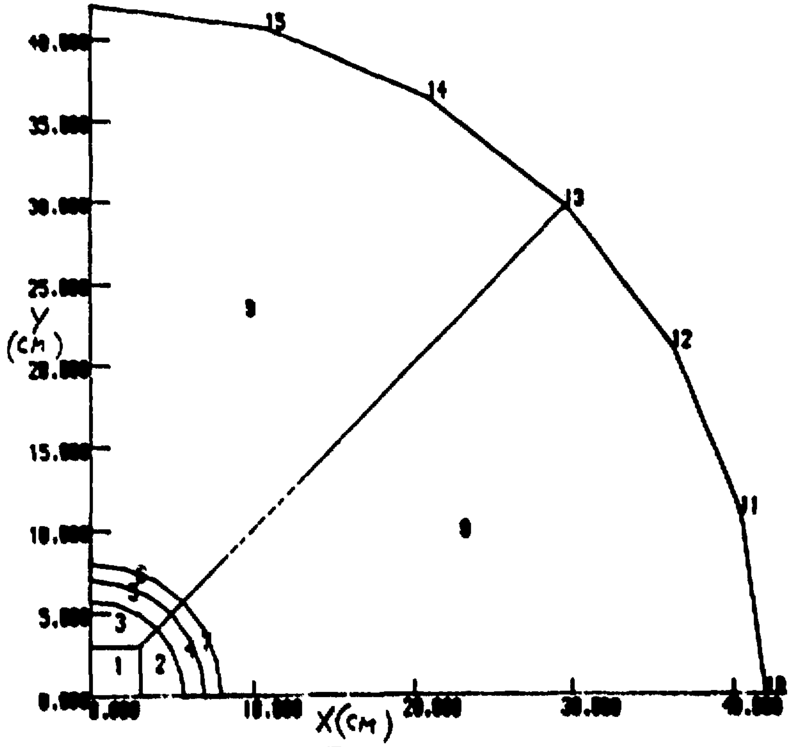

FIGURE 2a

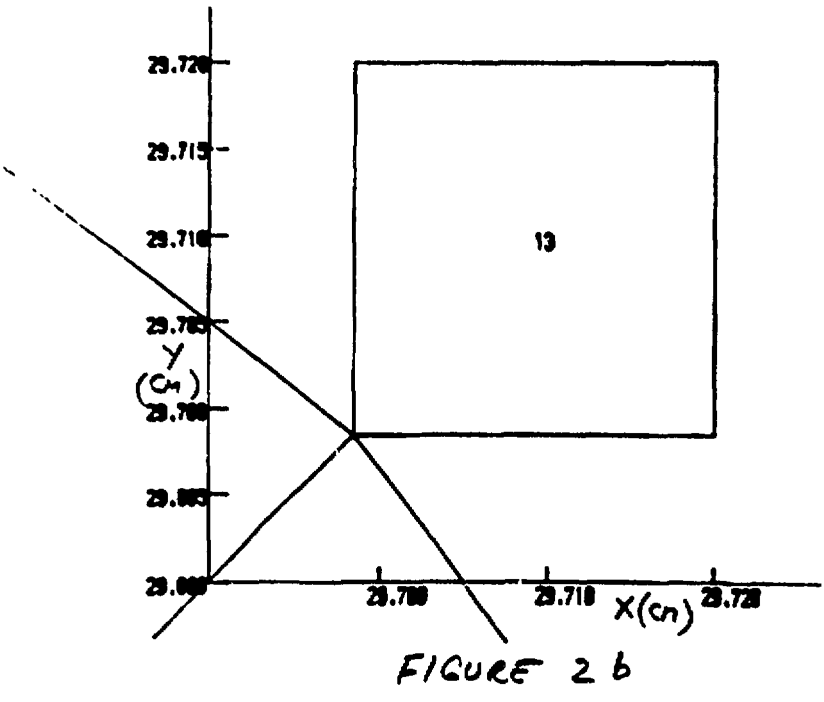

FIGURE 2b

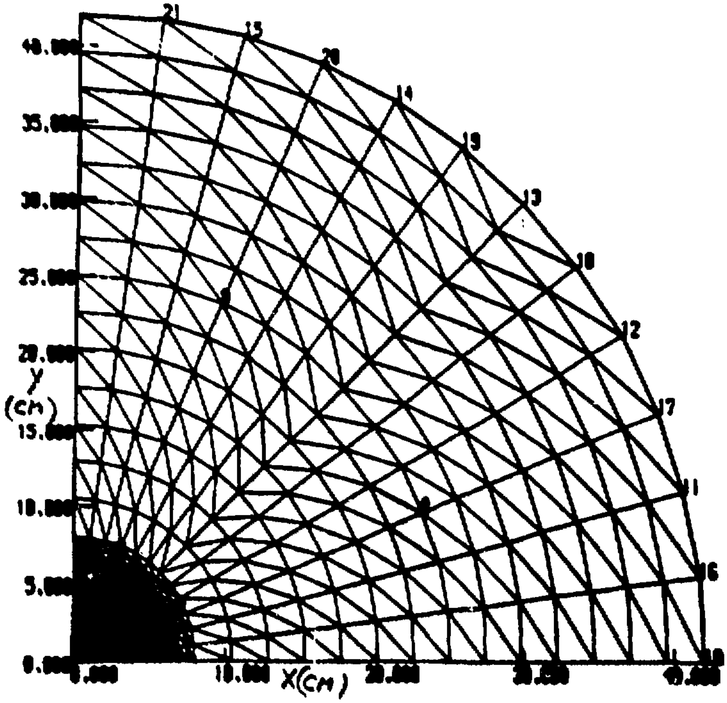

FIGURE 3a

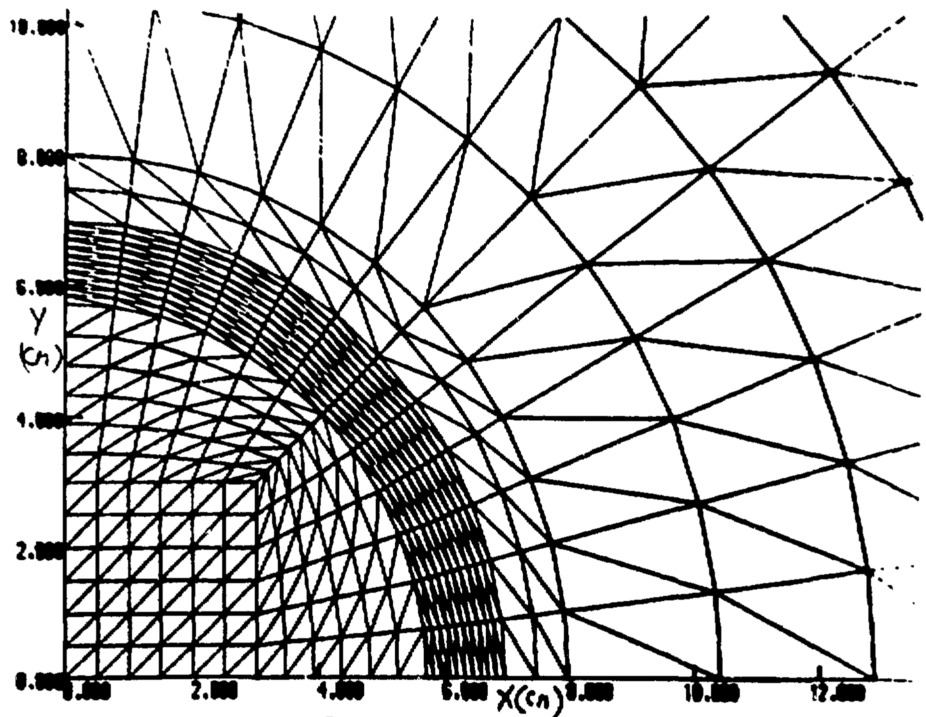

FIGURE 3b

TABLE 2.1.1

Problem 2 Using the Mesh Described Above and Linear Triangular Elements. Field Calculations

__Field Points at Mesh Points__

R (M)	θ (DEG)	B_x (T)	ϕ_x (DEG)	B_y (T)	ϕ_y (DEG)
.00	0.0	.0000	-166.5	.0222	-86.2
.01	0.0	.0000	-169.8	.0229	-86.3
.02	0.0	.0001	-175.5	.0229	-86.4
.03	0.0	.0002	-179.4	.0230	-86.8

__Field Points on Mesh Lines__

R (M)	θ (DEG)	B_x (T)	ϕ_x (DEG)	B_y (T)	ϕ_y (DEG)
.04	0.	.0006	178.1	.0229	-87.7
.05	0.	.0010	175.6	.0230	-93.5
.05842	0.	.0013	3.0	.0293	-123.9
.06858	0.	.0211	-10.2	.1648	177.8
.075	0.	.0205	-13.4	.1690	174.9
.10	0.	.0139	-14.4	.1478	175.3
.15	0.	.0062	-14.3	.1238	177.2
.20	0.	.0033	-14.3	.1138	178.2
.25	0.	.0021	-14.3	.1096	178.7
.30	0.	.0014	-14.3	.1073	179.0
.35	0.	.0010	-14.3	.1060	179.2
.40	0.	*	-14.3	*	179.3
.05	45.	.0007	-174.1	.0231	84.1
.05842	45.	.0134	2.7	.0270	-118.4
.06858	45.	.0772	-11.4	.0953	-176.8
.075	45.	.0684	-13.6	.1026	-179.9
.10	45.	.0444	-14.3	.1035	179.5
.15	45.	.0202	-14.3	.1043	179.4
.20	45.	.0109	-14.3	.1032	179.5
.25	45.	.0069	-14.3	.1029	179.6
.30	45.	.0048	-14.3	.1027	179.6
.35	45.	.0035	-14.3	.1026	179.6
.40	45.	*	*	*	178.0

__Field Points Inside of Elements (R < .07)__

R (M)	θ (DEG)	B_x (T)	ϕ_x (DEG)	B_y (T)	ϕ_y (DEG)
.01	7.5	.0000	-168.7	.0229	-86.3
.02	7.5	.0001	-173.9	.0229	-86.4
.03	7.5	.0002	-177.6	.0230	-86.7
.04	7.5	.0005	-179.8	.0230	-87.2
.05	7.5	.0004	168.1	.0231	-93.4
.05842	7.5	.0004	4.0	.0364	-139.4
.06858	7.5	.0313	-11.5	.1672	176.5
.01	14.	.0000	-167.8	.0229	-86.3
.02	14.	.0001	-172.6	.0229	-86.4
.03	14.	.0002	-176.0	.0230	-86.6
.04	14.	.0004	-177.9	.0230	-86.9
.05	14.	.0003	174.5	.0231	-91.6
.05842	14.	.0053	3.2	.0336	-134.8
.06858	14.	.0388	-11.2	.1594	177.4
.01	20.	.0000	-167.0	.0229	-86.2
.02	20.	.0001	-171.5	.0229	-86.3
.03	20.	.0002	-174.7	.0230	-86.4
.04	20.	.0004	-176.2	.0230	-86.6
.05	20.	.0002	4.5	.0231	-90.6
.05842	20.	.0076	2.6	.0359	-138.1
.06858	20.	.0501	-11.4	.1531	177.1
.01	45.	.0000	-163.4	.0229	-86.2
.02	45.	.0001	-163.9	.0229	-86.1
.03	45.	.0002	-166.5	.0231	-85.8
.04	45.	.0004	-171.8	.0230	85.3
.05	45.	.0007	-174.1	.0231	84.1
.05842	45.	.0134	2.7	.0270	-118.4
.06858	45.	.0772	-11.4	.0953	-176.4

Table 2.3.1

Results for Problem 2
Field Calculations

Field Points Inside of Elements (R > .07)

R (M)	θ (DEG)	B_x (T)	ϕ_x (DEG)	B_y (T)	ϕ_y (DEG)
.075	7.5	.0298	-13.5	.1631	175.0
.10	7.5	.0220	-14.3	.1421	175.7
.15	7.5	.0096	-14.3	.1213	177.5
.20	7.5	.0050	-14.3	.1126	178.4
.25	7.5	.0031	-14.3	.1088	178.8
.30	7.5	.0021	-14.3	.1069	179.1
.35	7.5	.0015	-14.3	.1057	179.2
.40	7.5	*	*	*	179.8
.075	14.	.0360	-13.6	.1603	175.2
.10	14.	.0244	-14.3	.1411	175.8
.15	14.	.0109	-14.3	.1208	177.5
.20	14.	.0059	-14.3	.1122	178.4
.25	14.	.0037	-14.3	.1086	178.9
.30	14.	.0025	-14.3	.1067	179.1
.35	14.	.0018	-14.3	.1055	179.2
.40	14.	*	*	*	179.9
.075	20.	.0474	-13.5	.1486	175.8
.10	20.	.0341	-14.3	.1312	176.6
.15	20.	.0148	-14.3	.1165	177.9
.20	20.	.0078	-14.3	.1101	178.7
.25	20.	.0049	-14.3	.1073	179.0
.30	20.	.0033	-14.3	.1058	179.2
.35	20.	.0024	-14.3	.1049	179.3
.40	20.	*	*	*	179.9

Table 2.4.1

Results for Problem 2
The Infinite Cylinder

Global Results

$\omega = 2\pi f$

	Time Average	Amplitude	Phase (degree)
b) Total current (A) $I = I_o \cos(\omega t + \phi)$	0	11239	166.5
c) Power losses (W/m) $P = P_a + P_o \cos(2\omega t + \phi)$	2613	2346	-29.6
d) Stored energy .05715 < r < .06985 (J/m) $E = E_a + E_o \cos(2\omega t + \phi)$	1.69	1.49	7.5
e) Stored energy r < .05715 (J/m)	.27	.26	-175.8
f) Stored energy r > .06985 (J/m)	265	264	-1.3
g) Stored energy of induced field (J/m)	12.3	10.9	-1.2
h) Force on one fourth of the cylinder (N/m) $F_x = F_{xa} + F_{xo} \cos(2\omega t + \phi)$	-375	396	172.0
$F_y = F_{ya} + F_{yo} \cos(2\omega t + \phi)$	-190	363	163.6

TABLE 2.1.2

Problem 2 Using the Mesh Described and Quadratic Triangular Elements.
Field Calculations

Field Points at Mesh Points

R (M)	θ (DEG)	B_x (T)	ϕ_x (DEG)	B_y (T)	ϕ_y (DEG)
.00	0.0	.0000	151.1	.0197	-85.6
.01	0.0	.0000	93.8	.0197	-85.6
.02	0.0	.0000	-41.5	.0197	-85.6
.03	0.0	.0000	174.0	.0197	-85.6

Field Points on Mesh Lines

R (M)	θ (DEG)	B_x (T)	ϕ_x (DEG)	B_y (T)	ϕ_y (DEG)
.04	0.	.0000	-178.9	.0197	-85.6
.05	0.	.0000	-178.6	.0197	-86.8
.05842	0.	.0013	167.3	.0287	-129.6
.06858	0.	.0037	-22.7	.1549	176.9
.075	0.	.0028	-27.3	.1600	174.1
.10	0.	.0001	-107.8	.1344	179.9
.15	0.	.0009	166.4	.1095	177.6
.20	0.	.0003	166.4	.1017	178.4
.25	0.	.0002	168.6	.0982	178.9
.30	0.	.0008	178.0	.0971	179.1
.35	0.	.0102	179.4	.1073	179.3
.40	0.	*	179.4	*	179.4
.05	45.	.0002	-0.7	.0196	-85.4
.05842	45.	.0098	3.4	.0217	-111.4
.06858	45.	.0736	-10.7	.0830	-176.3
.075	45.	.0696	-13.6	.0918	179.7
.10	45.	.0438	-13.6	.0913	179.8
.15	45.	.0181	-13.6	.0915	179.8
.20	45.	.0101	-13.6	.0918	179.8
.25	45.	.0064	-13.6	.0918	179.8
.30	45.	.0046	-13.0	.0917	179.7
.35	45.	.0070	-6.5	.0918	179.7
.40	45.	*	-180.0	*	180.0

Table 2.2.2

Results for Problem 2
Field Calculations

Field Points Inside of Elements (R < .07)

R (M)	θ (DEG)	B_x (T)	ϕ_x (DEG)	B_y (T)	ϕ_y (DEG)
.01	7.5	.0000	61.5	.0197	-85.6
.02	7.5	.0000	-36.4	.0197	-85.6
.03	7.5	.0000	-105.0	.0197	-85.6
.04	7.5	.0000	-175.7	.0197	-85.6
.05	7.5	.0000	-177.9	.0197	-86.7
.05842	7.5	.0021	5.8	.0322	-138.9
.06858	7.5	.0208	-12.7	.1578	175.5
.01	14.	.0000	28.3	.0197	-85.6
.02	14.	.0000	-35.4	.0197	-85.6
.03	14.	.0000	-90.7	.0197	-85.6
.04	14.	.0000	-169.2	.0197	-85.6
.05	14.	.0000	-165.7	.0197	-86.6
.05842	14.	.0050	3.2	.0277	-131.3
.06858	14.	.0349	-11.3	.1478	176.9
.01	20.	.0000	7.1	.0197	-85.6
.02	20.	.0000	-34.7	.0197	-85.6
.03	20.	.0000	-88.7	.0197	-85.6
.04	20.	.0000	-165.5	.0197	-85.6
.05	20.	.0001	-0.1	.0197	-86.4
.05842	20.	.0071	3.1	.0305	-136.2
.06858	20.	.0468	-11.5	.1433	176.2
.01	45.	.0000	-22.7	.0197	-85.6
.02	45.	.0000	-34.7	.0197	-85.6
.03	45.	.0000	-18.5	.0197	-85.6
.04	45.	.0000	-7.0	.0197	-85.6
.05	45.	.0002	-0.7	.0197	-85.9
.05842	45.	.0098	3.4	.0217	-111.4
.06858	45.	.0736	-10.7	.0830	-176.3

Table 2.3.2

Results for Problem 2
Field Calculations

<u>Field Points Inside of Elements (R > .07)</u>

R (M)	θ (DEG)	B_x (T)	ϕ_x (DEG)	B_y (T)	ϕ_y (DEG)
.075	7.5	.0206	-14.0	.1534	174.4
.10	7.5	.0163	-13.7	.1296	175.8
.15	7.5	.0058	-13.6	.1077	177.8
.20	7.5	.0030	-13.6	.1008	178.5
.25	7.5	.0018	-13.8	.0976	179.0
.30	7.5	.0008	-19.8	.0966	179.2
.35	7.5	.0040	-177.8	.1060	179.9
.40	7.5	*	180.0	*	179.9
.075	14.	.0325	-13.8	.1515	174.5
.10	14.	.0206	-13.7	.1291	175.9
.15	14.	.0082	-13.6	.1073	177.8
.20	14.	.0046	-13.6	.1005	178.6
.25	14.	.0030	-13.4	.0974	179.0
.30	14.	.0028	-10.0	.0960	179.2
.35	14.	.0104	-2.4	.1004	179.4
.40	14.	*	-179.9	*	180.0
.075	20.	.0446	-13.7	.1396	175.2
.10	20.	.0304	-13.6	.1198	176.6
.15	20.	.0119	-13.6	.1040	178.2
.20	20.	.0065	-13.6	.0987	178.8
.25	20.	.0042	-13.4	.0963	179.1
.30	20.	.0038	-10.2	.0952	179.3
.35	20.	.0138	-2.5	.0993	179.4
.40	20.	*	-180.0	*	180.0

Table 2.4.2

Results for Problem 2
The Infinite Cylinder

Global Results

$\omega = 2\Pi f$

	Time Average	Amplitude	Phase (degree)
b) Total current (A) $I = I_o \cos(\omega t + \phi)$	0	9664	167.2
c) Power losses (W/m) $P = P_a + P_o \cos(2\omega t + \phi)$	1933	1729	-28.4
d) Stored energy .05715 < r < .06985 (J/m) $E = E_a + E_o \cos(2\omega t + \phi)$	1.37	1.21	7.5
e) Stored energy r < .05715 (J/m)	.20	.19	-171.8
f) Stored energy r > .06985 (J/m)	232	232	-1.1
g) Stored energy of induced field (J/m)	9.2	8.1	-1.1
h) Force on one fourth of the cylinder (N/m) $F_x = F_{xa} + F_{xo} \cos(2\omega t + \phi)$	-287	302	172.6
$F_y = F_{ya} + F_{yo} \cos(2\omega t + \phi)$	-143	274	164.7

TABLE 2.1.3

Problem 2 Using Four Times As Many Linear Elements
Field Calculations

Field Points at Mesh Points

R (M)	φ (DEG)	B_x (T)	$φ_x$ (DEG)	B_y (T)	$φ_y$ (DEG)
.00	0.0	.0000	-155.5	.0220	-85.5
.01	0.0	.0000	-169.5	.0220	-85.6
.02	0.0	.0000	-172.6	.0220	-85.6
.03	0.0	.0000	-175.6	.0220	-85.7

Field Points on Mesh Lines

R (M)	φ (DEG)	B_x (T)	$φ_x$ (DEG)	B_y (T)	$φ_y$ (DEG)
.04	0.	.0001	179.5	.0220	-85.9
.05	0.	.0004	178.4	.0219	-86.8
.05842	0.	.0003	28.8	.0282	-125.7
.06858	0.	.0110	-9.6	.1701	177.6
.075	0.	.0110	-14.0	.1801	173.8
.10	0.	.0062	-13.7	.1464	175.6
.15	0.	.0027	-13.7	.1218	177.5
.20	0.	.0015	-13.7	.1132	178.4
.25	0.	.0009	-13.7	.1093	178.8
.30	0.	.0007	-13.7	.1072	179.1
.35	0.	.0005	-13.7	.1059	179.2
.40	0.	.0003	-13.7	.0957	179.3
.05	45.	.0002	-174.3	.0220	-84.8
.05842	45.	.0102	4.5	.0245	-111.2
.06858	45.	.0814	-11.0	.0943	-176.7
.075	45.	.0757	-13.7	.1046	179.4
.10	45.	.0432	-13.7	.1039	179.5
.15	45.	.0190	-13.7	.1032	179.6
.20	45.	.0106	-13.7	.1028	179.6
.25	45.	.0068	-13.7	.1026	179.6
.30	45.	.0047	-13.7	.1025	179.6
.35	45.	.0035	-13.7	.1025	179.7
.40	45.	*	-13.7	*	180.0

Table 2.2.3

Results for Problem 2
Field Calculations

Field Points Inside of Elements (R < .07)

R (M)	φ (DEG)	B_x (T)	$φ_x$ (DEG)	B_y (T)	$φ_y$ (DEG)
.01	7.5	.0000	-167.8	.0220	-85.6
.02	7.5	.0000	-171.5	.0220	-85.6
.03	7.5	.0000	-174.9	.0220	-85.7
.04	7.5	.0001	-177.9	.0220	-85.8
.05	7.5	.0002	179.9	.0220	-86.0
.05842	7.5	.0019	6.7	.0289	-126.5
.06858	7.5	.0214	-10.6	.1691	177.3
.01	14.	.0000	-166.7	.0220	-85.6
.02	14.	.0000	-170.9	.0220	-85.6
.03	14.	.0000	-174.0	.0220	-85.6
.04	14.	.0001	-176.2	.0220	-85.7
.05	14.	.0002	-177.6	.0220	-85.7
.05842	14.	.0043	4.2	.0290	-126.8
.06858	14.	.0381	-10.7	.1631	177.4
.01	20.	.0000	-165.7	.0220	-85.6
.02	20.	.0000	-169.7	.0220	-85.6
.03	20.	.0000	-173.1	.0220	-85.6
.04	20.	.0001	-174.9	.0220	-85.7
.05	20.	.0002	-175.2	.0220	-85.6
.05842	20.	.0064	3.9	.0288	-126.3
.06858	20.	.0520	-10.8	.1541	177.8
.01	45.	.0000	-162.6	.0220	-85.5
.02	45.	.0000	-162.7	.0220	-85.5
.03	45.	.0000	-163.0	.0220	-85.5
.04	45.	.0001	-168.4	.0220	-85.3
.05	45.	.0002	-174.3	.0220	-84.8
.05842	45.	.0102	4.5	.0245	-111.2
.06858	45.	.0814	-11.0	.0943	-176.7

Table 2.3.3

Results for Problem 2
Field Calculations

Field Points Inside of Elements (R > .07)

R (M)	θ (DEG)	B_x (T)	ϕ_x (DEG)	B_y (T)	ϕ_y (DEG)
.075	7.5	.0206	-13.7	.1770	174.0
.10	7.5	.0119	-13.7	.1448	175.7
.15	7.5	.0052	-13.7	.1211	177.6
.20	7.5	.0029	-13.7	.1128	178.4
.25	7.5	.0018	-13.7	.1090	178.8
.30	7.5	.0013	-13.7	.1070	179.1
.35	7.5	.0009	-13.7	.1058	179.2
.40	7.5	.0007	-13.7	.0987	179.3
.075	14.	.0367	-13.7	.1700	174.3
.10	14.	.0213	-13.7	.1408	176.0
.15	14.	.0093	-13.7	.1193	177.7
.20	14.	.0052	-13.7	.1118	178.5
.25	14.	.0033	-13.7	.1084	178.9
.30	14.	.0023	-13.7	.1066	179.1
.35	14.	.0017	-13.7	.1055	179.3
.40	14.	*	-13.7	*	179.6
.075	20.	.0498	-13.7	.1606	174.8
.10	20.	.0291	-13.7	.1352	176.4
.15	20.	.0127	-13.7	.1169	178.0
.20	20.	.0070	-13.7	.1105	178.7
.25	20.	.0045	-13.7	.1076	179.0
.30	20.	.0031	-13.7	.1060	179.2
.35	20.	.0023	-13.7	.1050	179.3
.40	20.	*	-13.7	*	179.8

Table 2.4.3

Results for Problem 2
The Infinite Cylinder

Global Results

$\omega = 2\pi f$

	Time Average	Amplitude	Phase (degrees)
b) Total current (A) $I = I_o \cos(\omega t + \phi)$	0	10933	167.1
c) Power losses (W/m) $P = P_a + P_o \cos(2\omega t + \phi)$	2454	2194	-28.6
d) Stored energy .05715 < r < .06985 (J/m) $E = E_a + E_o \cos(2\omega t + \phi)$	1.67	1.48	8.0
e) Stored energy r < .05715 (J/m)	.25	.25	-171.9
f) Stored energy r > .06985 (J/m)	277	276	-1.2
g) Stored energy of induced field (J/m)	12.8	11.4	-1.2
h) Force on one fourth of the cylinder (N/m) $F_x = F_{xa} + F_{xo} \cos(2\omega t + \phi)$	-356	376	172.7
$F_y = F_{ya} + F_{yo} \cos(2\omega t + \phi)$	-179	343	164.6

TABLE 2.1.4

Problem 2 Using Four Times As Many Quadratic Elements
Field Calculations

Field Points at Mesh Points

R (M)	θ (DEG)	B_x (T)	ϕ_x (DEG)	B_y (T)	ϕ_y (DEG)
.00	0.0	.0000	180.0	.0206	-85.4
.01	0.0	.0000	88.1	.0206	-85.4
.02	0.0	.0000	91.4	.0206	-85.4
.03	0.0	.0000	81.6	.0206	-85.4

Field Points on Mesh Lines

R (M)	θ (DEG)	B_x (T)	ϕ_x (DEG)	B_y (T)	ϕ_y (DEG)
.04	0.	.0000	-109.7	.0206	-85.4
.05	0.	.0000	-176.7	.0206	-85.3
.05842	0.	.0001	170.0	.0278	-127.8
.06858	0.	.0007	-23.6	.1630	177.5
.075	0.	.0001	-167.7	.1697	174.0
.10	0.	.0003	166.6	.1384	175.7
.15	0.	.0002	166.9	.1153	177.6
.20	0.	.0001	167.1	.1074	178.4
.25	0.	.0000	167.4	.1038	178.9
.30	0.	.0000	168.6	.1018	179.1
.35	0.	.0004	178.8	.1010	179.3
.40	0.	*	179.4	.1108	179.4
.05	45.	.0000	45.4	.0206	-85.4
.05842	45.	.0094	4.5	.0226	-109.9
.06858	45.	.0769	-10.2	.0874	-175.8
.075	45.	.0737	-13.5	.0972	179.7
.10	45.	.0422	-13.5	.0970	179.8
.15	45.	.0185	-13.5	.0972	179.7
.20	45.	.0104	-13.5	.0973	179.7
.25	45.	.0066	-13.5	;0973	179.7
.30	45.	.0046	-13.5	.0973	179.7
.35	45.	.0034	-13.2	.0973	179.7
.40	45.	*	*	*	180.0

Table 2.2.4

Results for Problem 2
Field Calculations

Field Points Inside of Elements (R < .07)

R (M)	θ (DEG)	B_x (T)	ϕ_x (DEG)	B_y (T)	ϕ_y (DEG)
.01	7.5	.0000	82.0	.0206	-85.4
.02	7.5	.0000	146.0	.0206	-85.4
.03	7.5	.0000	-101.0	.0206	-85.4
.04	7.5	.0000	-35.1	.0206	-85.4
.05	7.5	.0000	-168.6	.0206	-85.4
.05842	7.5	.0026	4.3	.0276	-127.2
.06858	7.5	.0200	-10.4	.1604	177.6
.01	14.	.0000	-86.6	.0206	-85.4
.02	14.	.0000	-128.6	.0206	-85.4
.03	14.	.0000	-107.6	.0206	-85.4
.04	14.	.0000	-52.0	.0206	-85.4
.05	14.	.0000	-168.6	.0206	-85.4
.05842	14.	.0047	4.3	.0276	-127.2
.06858	14.	.0362	-10.4	.1548	177.7
.01	20.	.0000	-88.2	.0206	-85.4
.02	20.	.0000	-114.5	.0206	-85.4
.03	20.	.0000	-114.4	.0206	-85.4
.04	20.	.0000	-81.4	.0206	-85.4
.05	20.	.0000	-162.7	.0206	-85.4
.05842	20.	.0065	4.3	.0273	-126.5
.06858	20.	.0496	-10.5	.1464	178.0
.01	45.	.0000	-108.0	.0206	-85.4
.02	45.	.0000	-125.1	.0206	-85.4
.03	45.	.0000	-144.3	.0206	-85.4
.04	45.	.0000	-152.7	.0206	-85.4
.05	45.	.0000	45.4	.0206	-85.4
.05842	45.	.0094	4.5	.0226	-109.9
.06858	45.	.0769	-10.2	.0874	-175.8

Table 2.3.4

Results for Problem 2
Field Calculations

<u>Field Points Inside of Elements (R > .07)</u>

R (M)	θ (DEG)	B_x (T)	ϕ_x (DEG)	B_y (T)	ϕ_y (DEG)
.075	7.5	.0188	-13.6	.1673	174.1
.10	7.5	.0106	-13.5	.1371	175.8
.15	7.5	.0047	-13.5	.1147	177.7
.20	7.5	.0026	-13.5	.1071	178.5
.25	7.5	.0017	-13.5	.1035	178.9
.30	7.5	.0012	-13.5	.1016	179.1
.35	7.5	.0012	-9.9	.1007	179.3
.40	7.5	*	-1.0	.1109	179.4
.075	14.	.0342	-13.5	.1609	174.4
.10	14.	.0196	-13.5	.1334	176.1
.15	14.	.0085	-13.5	.1131	177.8
.20	14.	.0048	-13.5	.1062	178.6
.25	14.	.0031	-13.5	.1030	179.0
.30	14.	.0021	-13.5	.1012	179.2
.35	14.	.0019	-11.1	.1004	179.3
.40	14.	*	*	*	179.8
.075	20.	.0467	-13.5	.1521	174.9
.10	20.	.0270	-13.5	.1282	176.5
.15	20.	.0117	-13.5	.1109	178.1
.20	20.	.0065	-13.5	.1050	178.7
.25	20.	.0042	-13.5	.1022	179.1
.30	20.	.0029	-13.5	.1007	179.3
.35	20.	.0025	-11.5	.0999	179.4
.40	20.	*	*	*	179.9

Table 2.4.4

Results for Problem 2
The Infinite Cylinder

Global Results

$\omega = 2\pi f$

	Time Average	Amplitude	Phase (degree)
b) Total current (A) $I = I_o \cos(\omega t + \phi)$	0	10270	167.2
c) Power losses (W/m) $P = P_a + P_o \cos(2\omega t + \phi)$	2166	1935	-28.3
d) Stored energy .05715 < r < .06985 (J/m) $E = E_a + E_o \cos(2\omega t + \phi)$	1.52	1.39	7.9
e) Stored energy r < .05715 (J/m)	.22	.22	-170.8
f) Stored energy r > .06985 (J/m)	261	260	-1.1
g) Stored energy of induced field (J/m)	11.3	10.1	-1.1
h) Force on one fourth of the cylinder (N/m) $F_x = F_{xa} + F_{xo} \cos(2\omega t + \phi)$	-287	302	172.6
$F_y = F_{ya} + F_{yo} \cos(2\omega t + \phi)$	-143	274	164.7

TABLE 2.1.5

Problem 2 Analytic Solution[2]
Field Calculations

Field Points at Mesh Points

R (M)	θ (DEG)	B_x (T)	ϕ_x (DEG)	B_y (T)	ϕ_y (DEG)
.00	0.0	.0000	0.0	.0211	-95.01
.01	0.0	.0000	0.0	.0211	-95.01
.02	0.0	.0000	0.0	.0211	-95.01
.03	0.0	.0000	0.0	.0211	-95.01

Field Points on Mesh Lines

R (M)	θ (DEG)	B_x (T)	ϕ_x (DEG)	B_y (T)	ϕ_y (DEG)
.04	0.	.0000	0.0	.0211	-95.01
.05	0.	.0000	0.0	.0211	-95.01
.05842	0.	.0000	0.0	.0028	-53.81
.06858	0.	.0000	0.0	.1667	2.12
.075	0.	.0000	0.0	.1745	5.68
.10	0.	.0000	0.0	.1418	3.93
.15	0.	.0000	0.0	.1185	2.09
.20	0.	.0000	0.0	.1104	1.26
.25	0.	.0000	0.0	.1066	0.83
.30	0.	.0000	0.0	.1046	0.59
.35	0.	.0000	0.0	.1034	0.44
.40	0.	.0000	0.0	.1026	0.34
.05	45.	.0000	0.0	.0211	-95.01
.05842	45.	.0091	175.18	.0023	-71.17
.06858	45.	.0783	-170.12	.0896	-4.59
.075	45.	.0757	-166.8	.1000	0.00
.10	45.	.0426	-166.8	.1000	0.00
.15	45.	.0189	-166.8	.1000	0.00
.20	45.	.0106	-166.8	.1000	0.00
.25	45.	.0068	-166.8	.1000	0.00
.30	45.	.0047	-166.8	.1000	0.00
.35	45.	.0035	-166.8	.1000	0.00
.40	45.	.0027	-166.8	.1000	0.00

Table 2.2.5

Results for Problem 2
Field Calculations

Field Points Inside of Elements (R < .07)

R (M)	θ (DEG)	B_x (T)	ϕ_x (DEG)	B_y (T)	ϕ_y (DEG)
.01	7.5	.0000	0.00	.0211	-95.01
.02	7.5	.0000	0.00	.0211	-95.01
.03	7.5	.0000	0.00	.0211	-95.01
.04	7.5	.0000	0.00	.0211	-95.01
.05	7.5	.0000	0.00	.0211	-95.01
.05842	7.5	.0024	175.18	.0028	-54.29
.06858	7.5	.0203	-170.20	.1640	2.00
.01	14.	.0000	0.00	.0211	-95.01
.02	14.	.0000	0.00	.0211	-95.01
.03	14.	.0000	0.00	.0211	-95.01
.04	14.	.0000	0.00	.0211	-95.01
.05	14.	.0000	0.00	.0211	-95.01
.05842	14.	.0043	175.18	.0027	-55.50
.06858	14.	.0368	-170.20	.1575	1.67
.01	20.	.0000	0.00	.0211	-95.01
.02	20.	.0000	0.00	.0211	-95.01
.03	20.	.0000	0.00	.0211	-95.01
.04	20.	.0000	0.00	.0211	-95.01
.05	20.	.0000	0.00	.0211	-95.01
.05842	20.	.0059	175.18	.0027	-57.27
.06858	20.	.0504	-170.20	.1485	1.17
.01	45.	.0000	0.00	.0211	-95.01
.02	45.	.0000	0.00	.0211	-95.01
.03	45.	.0000	0.00	.0211	-95.01
.04	45.	.0000	0.00	.0211	-95.01
.05	45.	.0000	0.00	.0211	-95.01
.05842	45.	.0091	175.18	.0023	-71.17
.06858	45.	.0783	-170.20	.0896	-4.59

Table 2.3.5

Results for Problem 2
Field Calculations

Field Points Inside of Elements (R > .07)

R (M)	θ (DEG)	B_x (T)	ϕ_x (DEG)	B_y (T)	ϕ_y (DEG)
.075	7.5	.0196	-166.8	.1720	5.56
.10	7.5	.0110	-166.8	.1403	3.83
.15	7.5	.0049	-166.8	.1179	2.03
.20	7.5	.0028	-166.8	.1100	1.22
.25	7.5	.0018	-166.8	.1064	0.81
.30	7.5	.0012	-166.8	.1045	0.57
.35	7.5	.0009	-166.8	.1033	0.42
.40	7.5	.0007	-166.8	.1025	0.33
.075	14.	.0355	-166.8	.1657	5.28
.10	14.	.0200	-166.8	.1369	3.59
.15	14.	.0089	-166.8	.1162	1.88
.20	14.	.0050	-166.8	.1092	1.13
.25	14.	.0032	-166.8	.1059	0.74
.30	14.	.0022	-166.8	.1041	0.52
.35	14.	.0016	-166.8	.1030	0.39
.40	14.	.0012	-166.8	.1023	0.30
.075	20.	.0486	-166.8	.1570	4.83
.10	20.	.0274	-166.8	.1319	3.23
.15	20.	.0122	-166.8	.1142	1.66
.20	20.	.0068	-166.8	.1080	0.99
.25	20.	.0044	-166.8	.1051	0.65
.30	20.	.0030	-166.8	.1035	0.46
.35	20.	.0022	-166.8	.1026	0.34
.40	20.	.0017	-166.8	.1020	0.26

Table 2.4.5

Results for Problem 2
The Infinite Cylinder

Global Results

$\omega = 2\pi f$

	Time Average	Amplitude	Phase (degree)
b) Total current (A) $I = I_o \cos(\omega t + \phi)$	0	10569.3	12.43
c) Power losses (W/m) $P = P_a + P_o \cos(2\omega t + \phi)$	2287.9	—	—
d) Stored energy .05715 < r < .06985 (J/m) $E = E_a + E_o \cos(2\omega t + \phi)$	1.5966	—	—
e) Stored energy r < .05715 (J/m)	.2278	—	—
f) Stored energy r > .06985 (J/m)	273.64	—	—
g) Stored energy of induced field (J/m)	—	—	—
h) Force on one fourth of the cylinder (N/m) $F_x = F_{xa} + F_{xo} \cos(2\omega t + \phi)$	-333.43	351.60	-173.60
$F_y = F_{ya} + F_{yo} \cos(2\omega t + \phi)$	-166.71	165.71	-155.82

INFINITELY LONG CYLINDER IN A SINUSOIDAL FIELD
(Problem 2)

Nathan Ida

Electrical Engineering Department
The University of Akron
Akron, OHIO 44325

GENERAL

The results presented here were obtained with a 2-D (and axisymmetric) eddy current program called EDDYNDT. The program uses the magnetic vector potential formulation and was specifically designed for the calculation of coil impedances in NDT applications. For normal applications, flux densities, forces, eddy current densities and stored and dissipated energies are not calculated. The program required minor modifications to calculate these quantities form the magnetic vector potential.

In its present form, program EDDYNDT cannot handle flux normal boundary conditions. To avoid this, half the cylinder was modeled as in Fig. 1, as oposed to the quarter cylinder in the mesh recommended in the problem outline. This increased the number of elements and nodes but did not change their density or location.

Both

Figure 2 presents a solution without the cylinder and Figure 3 presents the solution with the cylinder. are presented

The fields presented are calculated at the center of each element. For this reason, the values presented are interpolated between neighboring elements. This creates a problem, particularly at discontinuities where the errors are largest.

RESULTS

Field Points at Mesh Points

R (m)	ANGLE (deg)	Bx (T)	θ_x (deg)	By (T)	θ_y (deg)
0.00	0.0	-----	-----	-----	-----
0.01	0.0	.0	-----	.0275	-91.0
0.02	0.0	.0008	-----	.0276	-91.0
0.03	0.0	.0008	-----	.0276	-91.0

Field Points on Mesh Lines

R (m)	ANGLE (deg)	Bx (T)	θ_x (deg)	By (T)	θ_y (deg)
0.04	0.0	.0008	-46.4	.0276	-91.0
0.05	0.0	.0008	-46.4	.0275	-90.8
0.05842	0.0	.0009	-22.8	.0295	-33.8
0.06858	0.0	.0010	-10.4	.1740	-14.2
0.075	0.0	.0038	13.7	.1795	2.8
0.10	0.0	.0043	13.7	.1440	2.7
0.15	0.0	.0024	13.6	.1231	2.3
0.20	0.0	.0013	13.6	.1131	1.8
0.25	0.0	.0009	13.6	.1094	1.4
0.30	0.0	.0008	13.6	.1048	1.1
0.35	0.0	.0009	13.6	.1028	.9
0.40	0.0	.0007	13.6	.1007	.2
0.05	45.0	.0002	-93.6	.0233	-95.5
0.05842	45.0	.0101	-11.5	.0195	-64.2
0.06858	45.0	.0740	-10.4	.0920	-15.4
0.075	45.0	.0741	13.7	.1014	4.6
0.10	45.0	.0440	13.7	.1000	1.8
0.15	45.0	.0186	13.7	.0999	.4
0.20	45.0	.0096	13.7	.1000	.3
0.25	45.0	.0066	13.7	.1000	.2
0.30	45.0	.0041	13.7	.1000	.2
0.35	45.0	.0030	13.7	.1000	.2
0.40	45.0	.0025	13.7	.1000	.2

R (m)	ANGLE (deg)	Bx (T)	θx (deg)	By (T)	θy (deg)
Field Points Inside of Elements (R<0.07)					
0.01	20.0	.0010	------	.0212	-95.1
0.02	20.0	.0009	------	.0212	-95.1
0.03	20.0	.0010	------	.0212	-95.1
0.04	20.0	.0016	------	.0212	-95.1
0.05	20.0	.0022	-95.1	.0210	-95.1
0.05842	20.0	.0026	-15.0	.0220	-36.6
0.06858	20.0	.0198	-11.5	.1606	-3.3
0.01	45.0	.0018	------	.0223	-95.1
0.02	45.0	.0022	------	.0233	-95.1
0.03	45.0	.0041	------	.0224	-95.1
0.04	45.0	.0062	------	.0224	-95.1
0.05	45.0	.0088	-95.1	.0218	-95.1
0.05842	45.0	.0101	-11.5	.0195	-64.2
0.06858	45.0	.0740	-10.4	.0920	-15.4
Field Points Inside of Elements (R>0.07)					
0.075	20.0	.0446	13.7	.1623	3.5
0.10	20.0	.0268	13.8	.1333	2.1
0.15	20.0	.0133	13.7	.1138	1.7
0.20	20.0	.0081	13.7	.1036	.9
0.25	20.0	.0044	13.7	.1024	.6
0.30	20.0	.0038	13.7	.1008	.5
0.35	20.0	.0025	13.7	.1008	.4
0.40	20.0	.0023	13.7	.1007	.3

Global Results

	Time Average	Amplitude	Phase
Total Current (A)	-----	21022.0	-----
Power Losses (W/m)	-----	7649.0	-----
Storred Energy 0.05715<R<0.06858	-----	4.988	-----
Stored Energy R<0.05715	-----	.9166	-----
Stored Energy R>0.06985	-----	1144.6	-----
Stored Energy of Induced Field	-----	11.4	-----
Force on one fourth of Cylinder			
Fx	-----	-343.7	-----
Fy	-----	155.7	-----

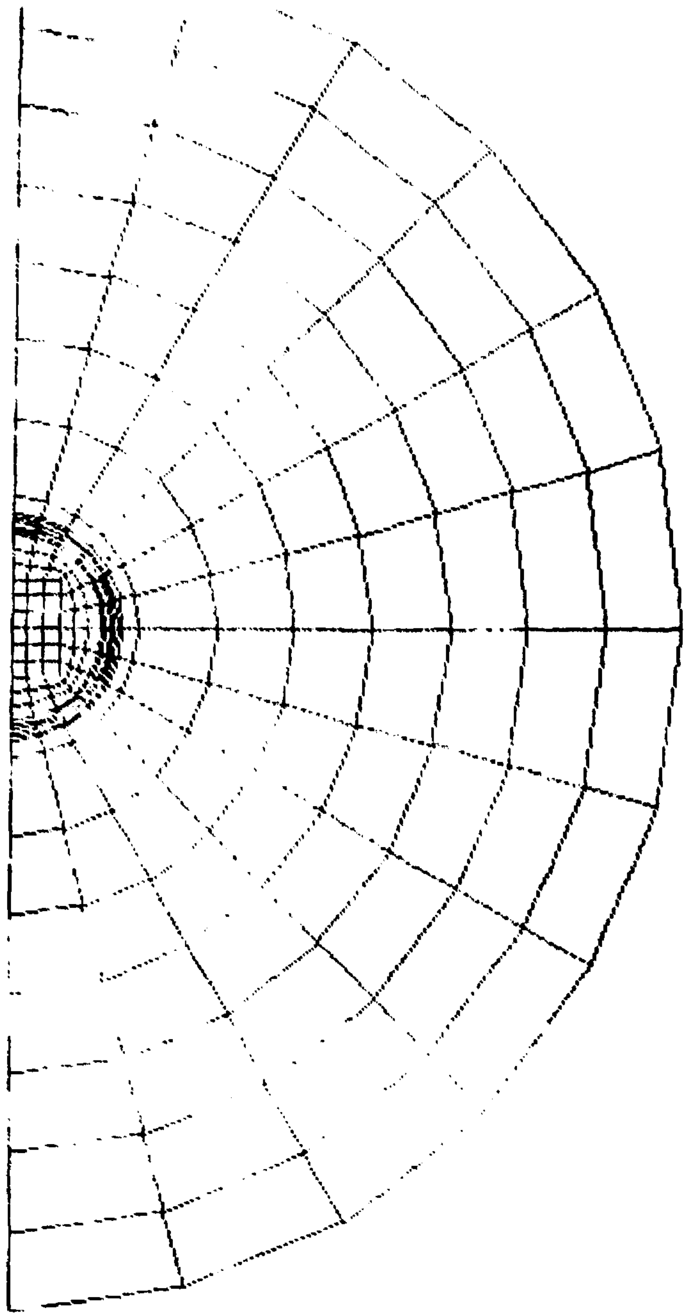

FIG. 1

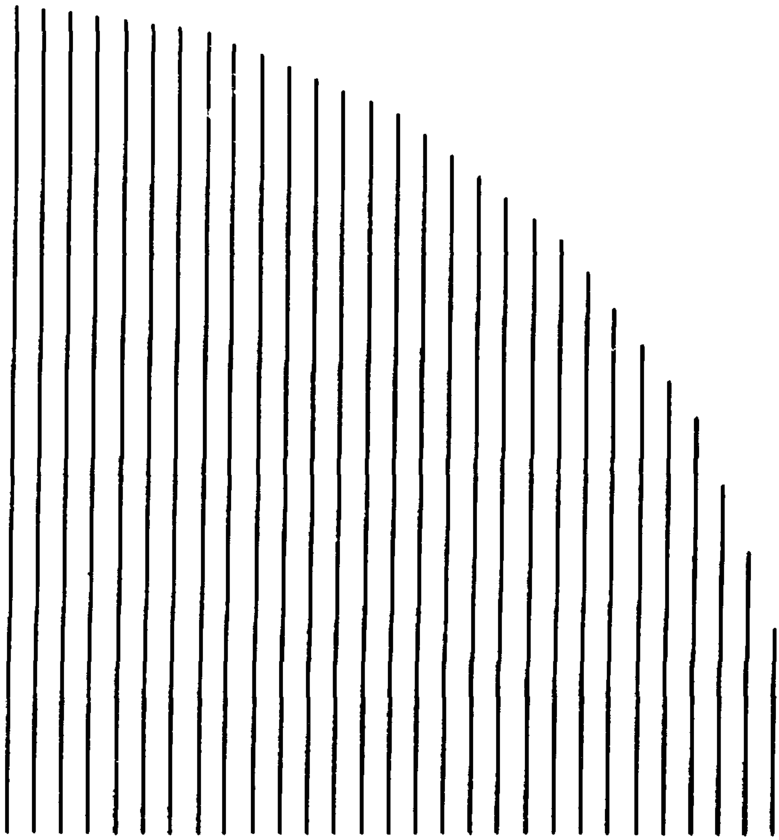

FIG. 2

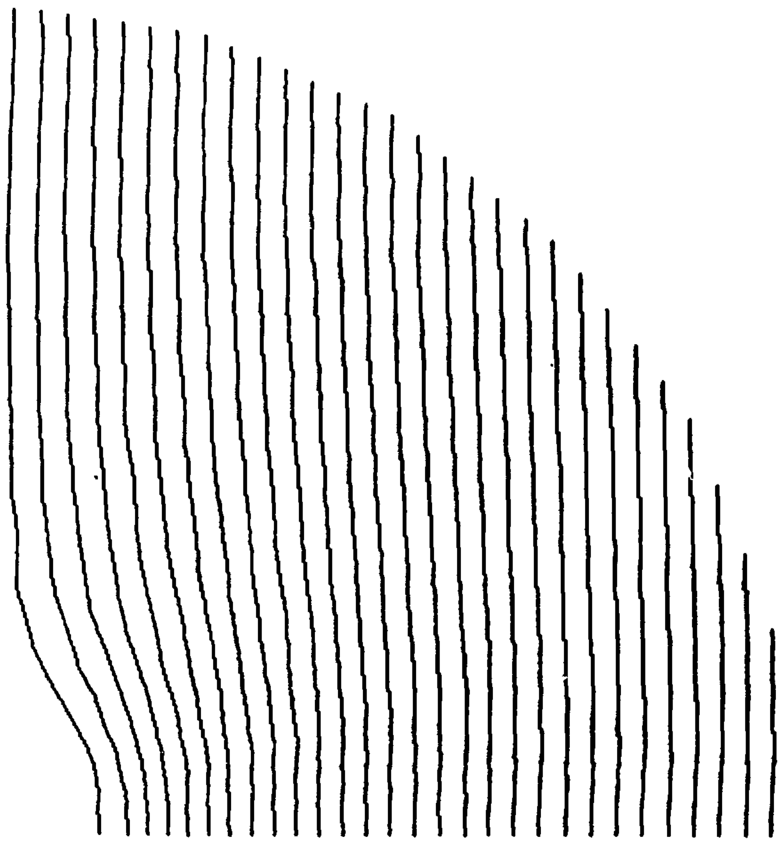

FIG. 3

O.E.
PE2D v7.0
(RAL)

Table 2a

Results for Problem 2

Infinite Cylinder

Angle (degrees)

Radial Distance (m)

r \ θ	0	7.5°	14°	20°	45°
0	0				0
0.01	0				0
0.02	0				0
0.03	0.2				0.1
0.04	0.6				0.3
0.05	1.7				0.6
0.05842	5.2				11.1
0.06858	20.5				78.2
0.075	18.3				73.2
0.1	11.9				51.6
0.15	5.2				23.6
0.2	2.8				14.1
0.25	1.7				8.3
0.3	1.0				5.2
0.35	0.5				3.6
0.4	0.1				2.4

Table 2b

Results for Problem 2

Infinite Cylinder

Angle (degrees)

Radial Distance (m)

r \ θ	0	7.5°	14°	20°	45°
0	-48				-48
0.01	-31				-66
0.02	-12				-66
0.03	-5				-52
0.04	-2				-27
0.05	-1				-20
0.05842	0				0
0.06858	-11				-11
0.075	-14				-14
0.1	-14				-14
0.15	-14				-14
0.2	-14				-14
0.25	-14				-14
0.3	-14				-14
0.35	-14				-14
0.4	-14				-14

Table 2c
Results for Problem 2
Infinite Cylinder

Radial Distance (m)

r \ θ	0	7.5°	14°	20°	45°
0	23.3				23.3
0.01	23.3				23.3
0.02	23.3				23.3
0.03	23.3				23.3
0.04	23.4				23.3
0.05	23.5				23.3
0.05842	36.3				26.1
0.06858	173.6				90.4
0.075	170.8				96.9
0.1	146.4				96.8
0.15	123.2				99.3
0.2	113.6				100.0
0.25	109.6				100.5
0.3	107.6				100.8
0.35	106.6				101.1
0.4	106.2				101.2

Angle (degrees)

Magnitude of B_y (~~Tesla~~ mT)

Table 2d
Results for Problem 2
Infinite Cylinder

Angle (degrees)

r \ θ	0	7.5°	14°	20°	45°
0	-86				-86
0.01	-86				-86
0.02	-86				-87
0.03	-86				-87
0.04	-85				-88
0.05	-90				-89
0.05842	-177				-115
0.06858	176				-175
0.075	174				-179
0.1	175				-179
0.15	177				-180
0.2	178				-180
0.25	179				-180
0.3	179				-180
0.35	179				-180
0.4	179				-180

Radial Distance (m)

Phase of B_φ (degrees)

Table 2e
Results for Problem 2
Infinite Cylinder

PE2D (RAL) / ANALYTIC	Time Average	Amplitude	Phase (degrees)
Total Eddy Current (A) $I = I_0 \cos t (\omega t + \phi)$ (for ~~whole~~ 1/4 cylinder cross section)	0 / 0	11385.3 / 10569.3	166.41 (180° − 13.59) / 12.43
Power loss (ω/m) $\int J^2 \rho \, ds$ (~~whole~~ 1/4 cylinder)	2688.19 / 2287.9	2412.67 / 2042.7	−30.06 / 27.63
Stored energy (J/m) $0.05715 < r < 0.06985$ $\int \frac{1}{2} BH \, ds$ (~~whole~~ 1/4 cylinder)	1.73559 / 1.5966	1.53816 / 1.4129	7.07 / −8.8
Stored Energy (J/m) $r < 0.05715$ (~~whole~~ 1/4 cylinder)	0.2755 / 0.2278	0.2706 / 0.2278	−176.6 / 169.99
Stored energy (J/m) $r > 0.06985$ (~~whole~~ 1/4 cylinder)	362.91 / 273.64	362.20 / 273.06	−1.01 / 0.53
Stored energy of Induced field (J/m) (~~whole~~ 1/4 cylinder)	0 / 0	3.17990 / 2.7692	−120.06 / 117.63
Force on quarter of cylinder (N/m) $F_x = \int J_z B_y \, ds$	−385.89 / −373.43	407.03 / 351.60	171.5 / −173.60
$F_y = \int J_z B_x \, ds$	−196.01 / −166.71	175.28 / 165.71	163.2 / −155.82

SPHERE IN UNIFORM MAGNETIC FIELD
(Problem 6)

Nathan Ida

Electrical Engineering Department
The University of Akron
Akron, OHIO 44325

GENERAL

The results presented here were obtained with a 3-D eddy current program called EDDY3D. The program uses the magnetic vector potential formulation and was specifically designed for the calculation of coil impedances in NDT applications. For normal applications, flux densities and eddy current densities are not calculated explicitly but the stored and dissipated energies are calculated. The program required minor modifications to calculate forces, eddy currents and flux densities.

In its present form the 3-D program cannot handle flux normal boundary conditions. To avoid this, half the cylinder was modeled as in Fig. 1, as oposed to the quarter cylinder in the mesh recommended in the problem outline. This increased the number of elements and nodes but did not change their density or location.

The program uses eight node elements. The mesh has a total of 992 elements and 1242 nodes (3726 variables). The solution time is approximately 2 hours on an IBM 3033 computer.

The results presented here are partial and preliminary. This particular problem has an analytical solution. Those results presented were compared with approximate analytical calculations. The data not presented is omitted because the program needs to be modified to get it in the form necessary. For this reason, the results are presented in a somewhat different format than required. This data and a complete analytical solution will be presented in the future.

The field as well as the eddy current densities are calculated as total values rather than as components. In addition, these are found as average values at the center of each element and are interpolated to get the values at the required points.

RESULTS

a. Total Eddy Current (A)

b. Magnetic Field (T)

x (m)	y (m)	z (m)	Bt magnitude	Bt phase
0	0	0		
0.01	0.0	0.0		
0.01	0.01	0.01		
0.03	0.025	0.02		
0.03031	0.03031	0.03031		
0.03	0.031	0.032		
0.065	0.0	0.0	1.2678	2.12
0.1	0.0	0.0	.9096	.5
0.1	0.11	0.12	1.0107	.0

c. Current Density (A/m)

x (m)	y (m)	z (m)	Jt magnitude	Jt phase
0.0525	0.0	0.0	.2457E+09	-88.0
0.03031	0.03031	0.03031	.1740E+09	-88.0
0.01345	0.0233	0.0466	.1586E+09	-64.0

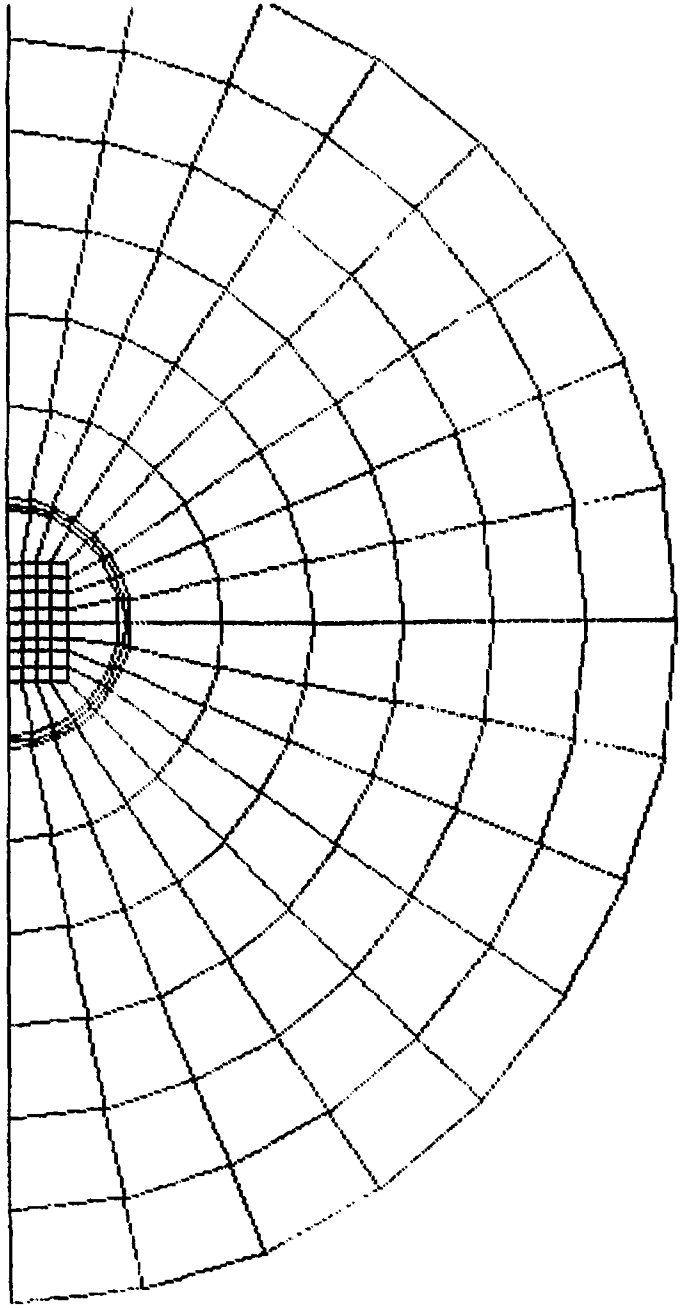

FIG. 1

3-D EDDY CURRENT CALCULATION USING THE MAGNETIC VECTOR POTENTIAL

Toshiya Morisue
University of Tokushima, Japan

Introduction

To formulate the 3-D eddy current problem as a boundary value problem using the magnetic vector potential, the gauge, interface and boundary conditions of the vector potential should first of all be defined clearly. Without them the boundary value problem could not be solved uniquely and accurately.

This contribution presents a new method for calculating 3-D eddy current problems, rigorously defining the interface and boundary conditions of the vector potential. The new field equations do not include the gauge condition explicitly and take a form of the diffusion equation. The gauge condition does appear in the interface and boundary conditions. This method yields a unique solution to the eddy current problem.

A New Formulation for the Magnetic Vector Method

Field Equations : in Conductor

$$\mathrm{curl}\,(\nu\,\mathrm{curl}\,\underline{A}) + \sigma\,(\partial\underline{A}/\partial t + \mathrm{grad}\,\phi) - \nu\,\mathrm{grad}\,(\mathrm{div}\,\underline{A} + \mu\sigma\phi)$$
$$= 0$$

$$\mathrm{div}\,(\sigma(\partial\underline{A}/\partial t + \mathrm{grad}\,\phi)) - \sigma\,\partial/\partial t\,(\mathrm{div}\,\underline{A} + \mu\sigma\,\phi) = 0 \qquad (\nu = 1/\mu)$$

in Nonconductor (Space) $\quad \mathrm{div}\,(\mathrm{grad}\,\underline{A}) + \mu_0\underline{J_0} = 0$

Interface Conditions :

$$\left.\begin{array}{l} \underline{n}\times\underline{A1} = \underline{n}\times\underline{A2} \\ \underline{n}\times(\nu\,\mathrm{curl}\,\underline{A1}) = \underline{n}\times(\nu_0\,\mathrm{curl}\,\underline{A2}) \end{array}\right\}\ \underline{B},\ \underline{H}\text{ - Interface Conditions}$$

$$\left.\begin{array}{l} \underline{n}.\underline{A1} = \underline{n}.\underline{A2} \\ \underline{n}.\mathrm{grad}\,(\underline{n}.\underline{A1}) + \mu\sigma\,\phi = \underline{n}.\mathrm{grad}\,(\underline{n}.\underline{A2}) \end{array}\right\}\ \text{Gauge Interface Conditions}$$

where 1 = Conductor, 2 = Nonconductor, and $\underline{n}$ = a unit vector normal to the Interface.

Boundary Conditions :

$\underline{A2}(\underline{r}) = O(1/r^2)$ at infinity (O = order of)

$\underline{n}.\mathrm{grad}\,\phi = -\underline{n}.\partial\underline{A}/\partial t$ on the Interface

Note: The Lorentz gauge condition ($\mathrm{div}\,\underline{A} + \mu\sigma\phi = 0$) is automatically satisfied in the above formulation.

Under a Constant Permeability and a Constant Conductivity

<u>The Conventional Formulation</u>

Field Equation :

in Conductor $\quad \mathrm{div}\ (\ \mathrm{grad}\ \underline{A}\ ) - \mu\sigma\ \partial\underline{A}/\partial t = 0$

$\qquad\qquad \mathrm{div}\ (\ \mathrm{grad}\ \phi\ ) - \mu\sigma\ \partial\phi/\partial t = 0$

in Nonconductor $\quad \mathrm{div}\ (\ \mathrm{grad}\ \underline{A}\ ) + \mu o \underline{Jo} = 0$

Gauge Condition : $\quad \mathrm{div}\ \underline{A} + \mu\sigma\ \phi = 0$ (Lorentz gauge)

Interface Conditions :

$$\underline{n} \times \underline{A1} = \underline{n} \times \underline{A2}$$

$$\underline{n} \times (\ \nu\ \mathrm{curl}\ \underline{A1}\ ) = \underline{n} \times (\ \nu o\ \mathrm{curl}\ \underline{A2}\ )$$

Boundary Conditions :

$\underline{A2}(\underline{r}) = O(1/r^2)$ at infinity

$\underline{n}.\mathrm{grad}\ \phi = -\underline{n}.\ \partial\underline{A1}/\partial t$ on the interface

<u>The New Formulation</u>

Field Equation : the same as the conventional formulation

Gauge Condition : not necessary

Interface Conditions :

$$\underline{n} \times \underline{A1} = \underline{n} \times \underline{A2}$$

$$\underline{n} \times (\ \nu\ \mathrm{curl}\ \underline{A1}\ ) = \underline{n} \times (\ \nu o\ \mathrm{curl}\ \underline{A2}\ )$$

$$\underline{n}.\underline{A1} = \underline{n}.\underline{A2}$$

$$\underline{n}.\mathrm{grad}\ (\underline{n}.\underline{A1}) + \mu\sigma\ \phi = \underline{n}.\mathrm{grad}\ (\underline{n}.\underline{A2})$$

Boundary Conditions : the same as the conventional formulation

Coefficient Matrix of the Discretized Boundary Integral Equations:

$(\underline{q} = \partial \underline{A}/\partial n)$

Ax	Ay	Az	ϕ	q1x	q1y	q1z	$\frac{\partial\phi}{\partial n}$	q2x	q2y	q2z	
F1				G1							Boundary Integral Equations on the Conductor-side Interface
	F1				G1						
		F1				G1					
			F1				G1				
dd	dd	dd		d	d	d		d	d	d	Interface Conditions of the Magnetic Field Intensity
dd	dd	dd		d	d	d		d	d	d	
			d	d	d	d		d	d	d	Gauge Interface Condition
d	d	d					d				Boundary Condition of the electric scalar potential
F2								G2			Boundary Integral Equations on the Space-side Interface
	F2								G2		
		F2								G2	

F,G : dense matrix
d : diagonal matrix
dd : bidiagonal matrix

RESULTS

The new formulation was applied to a test problem, an infinite length cylindrical conductor having a constant permeability and a constant conductivity, excited by an infinite length rectangular solenoid, which has an analytical solution against which the numerical results could be compared.

The problem geometry is shown in Fig. 2.

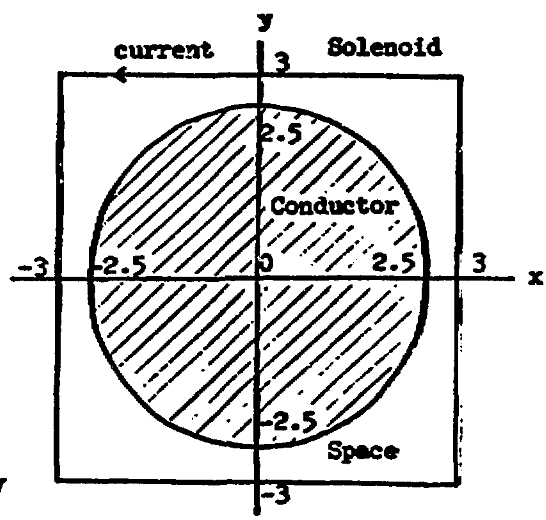

Fig. 2 The problem geometry

<u>Analytical Solution</u>

The eddy current distribution in the conductor is given as follows.

$J_\theta(r) = -j\omega\mu\sigma/(\mu_0 k).L1(kr)/L0(kr_0)$

where $r^2 = x^2 + y^2$, r_0 : radius of the cylinder,

Ln(s) : the first kind, the n-th order Bessel function (s:complex number)

Remark. Solenoid current I (ampere/meter) is assumed to be $\mu_0 I = 1$.

Numerical Solution

In this problem, the magnetic vector potential has two components:

$\underline{A}(x,y,z) = (Ax(x,y), Ay(x,y), 0)$

The fundamental solution or the Green's function of the 2-D field is

$(j/4)H1(kr)$

where H1(s) : the first kind Hankel function whose integral-form representation is as follows.

$$H1(s) = -2j/\pi \int_0^\infty \exp(js.\cosh(t))\,dt$$

The interface (the surface of the cylinder) is devided into 40 same-size boundary-elements.

The computed result of the eddy current is shown in Fig.3. The computed result of the magnetic vector potential is shown in Fig.4. (There is a four-fold symmetry in Ax(x,y).) The computed result of the electric scalar potential is shown in Fig.5. (There is a eight-fold anti-symmetry in $\phi(x,y)$.)

From the results we can conclude that the new formulation is valid.

REFERENCE

1 T.Morisue: "A new formulation of the magnetic vector potential method for three dimensional magnetostatic field problems", IEEE Trans. on Magnetics, Vol. MAG-21, No.6, Nov. 1985, pp. 2192-2195.

Fig. 3 Eddy Current Distribution along the radial direction

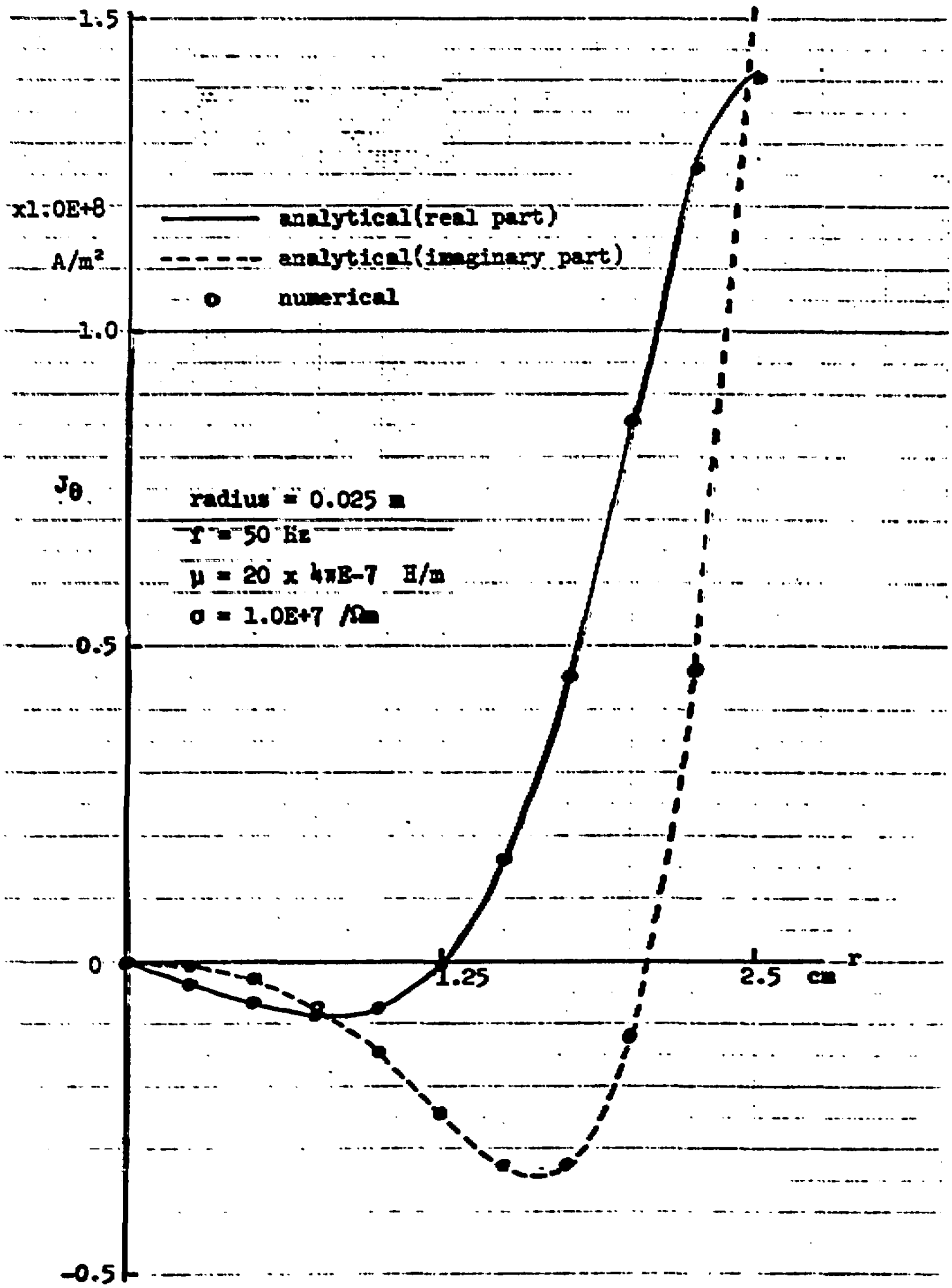

Fig. 4 Magnetic Vector Potential (Λx) along the interface

(Ay(x,y) = -Ax(y,x))

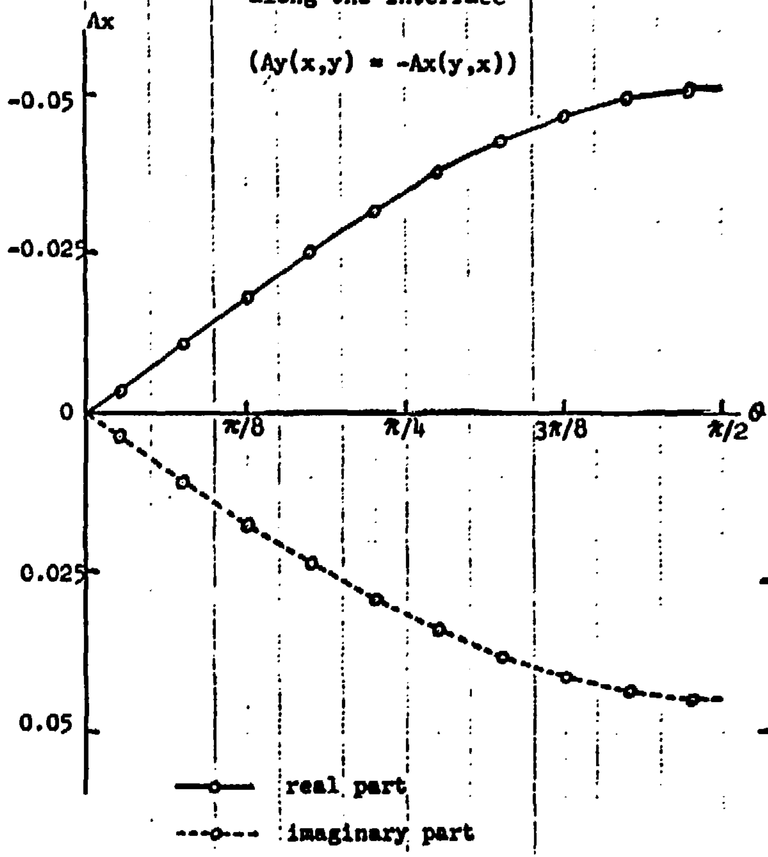

Fig. 5 Electric Scalar Potential along the interface

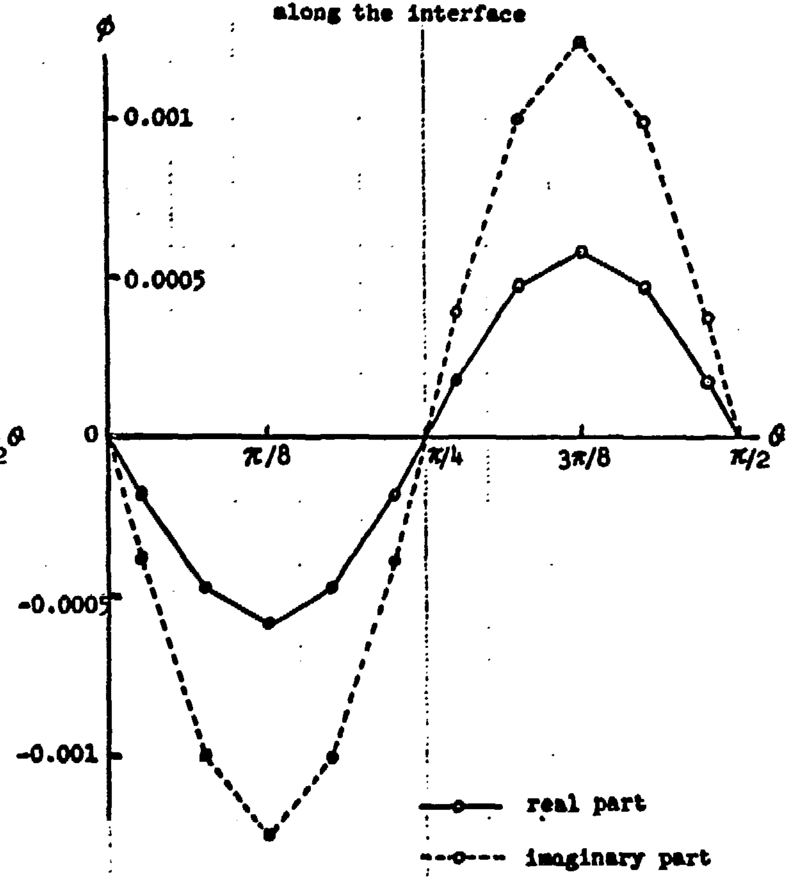

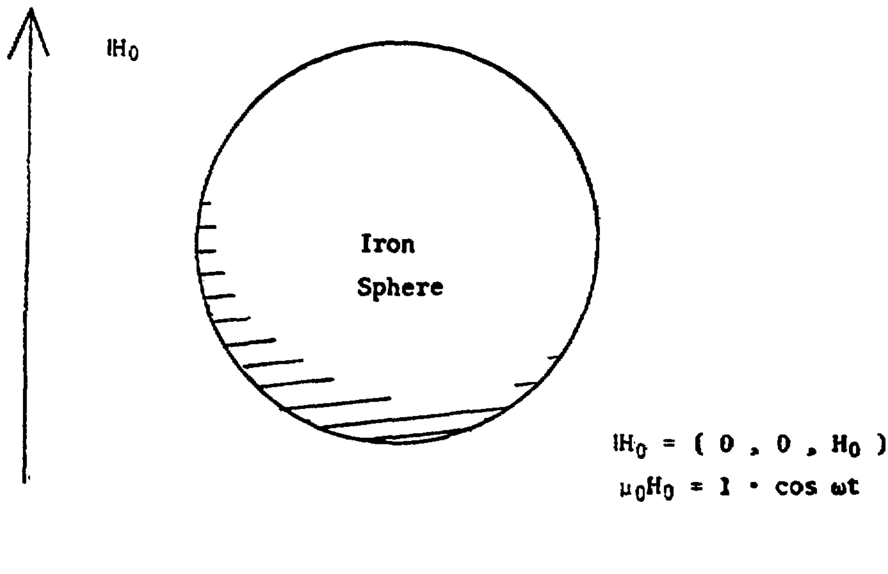
IH0
Iron
Sphere
IH0 = (0 , 0 , H0)
μ0H0 = 1 · cos ωt

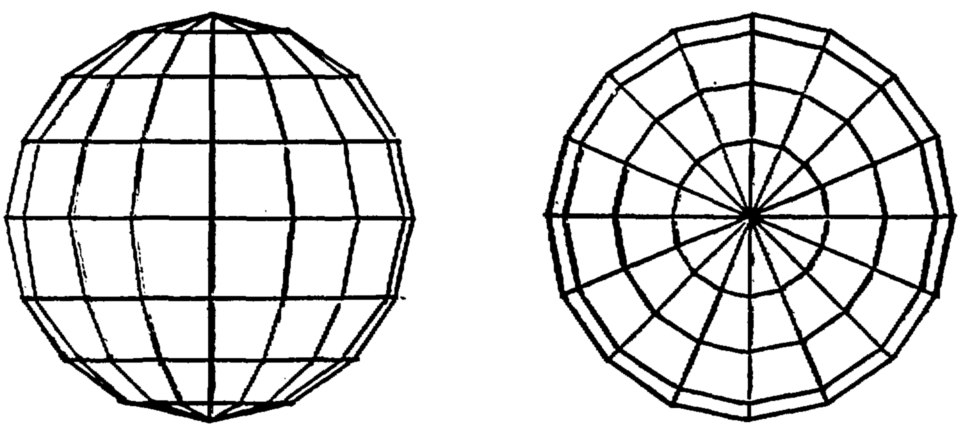

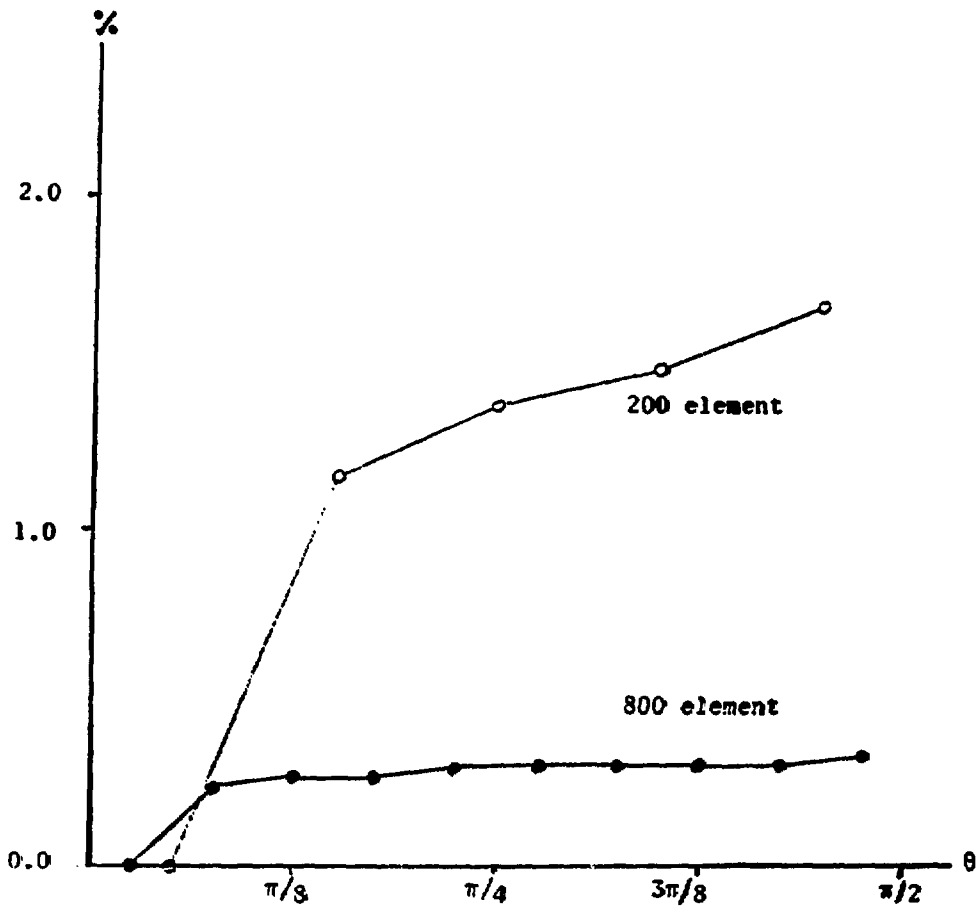

%
2.0
1.0
0.0
200 element
800 element
π/8
π/4
3π/8
π/2
θ

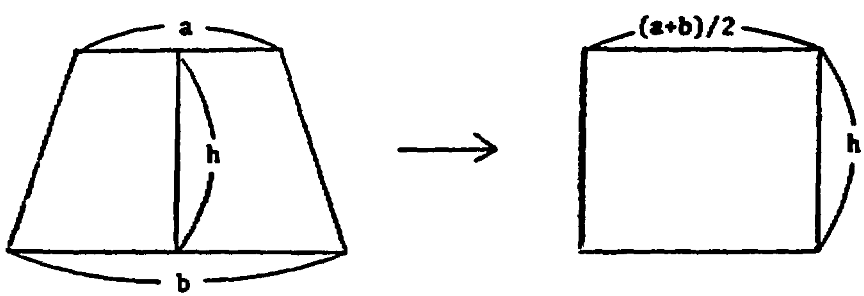

a
h
b
(a+b)/2
h

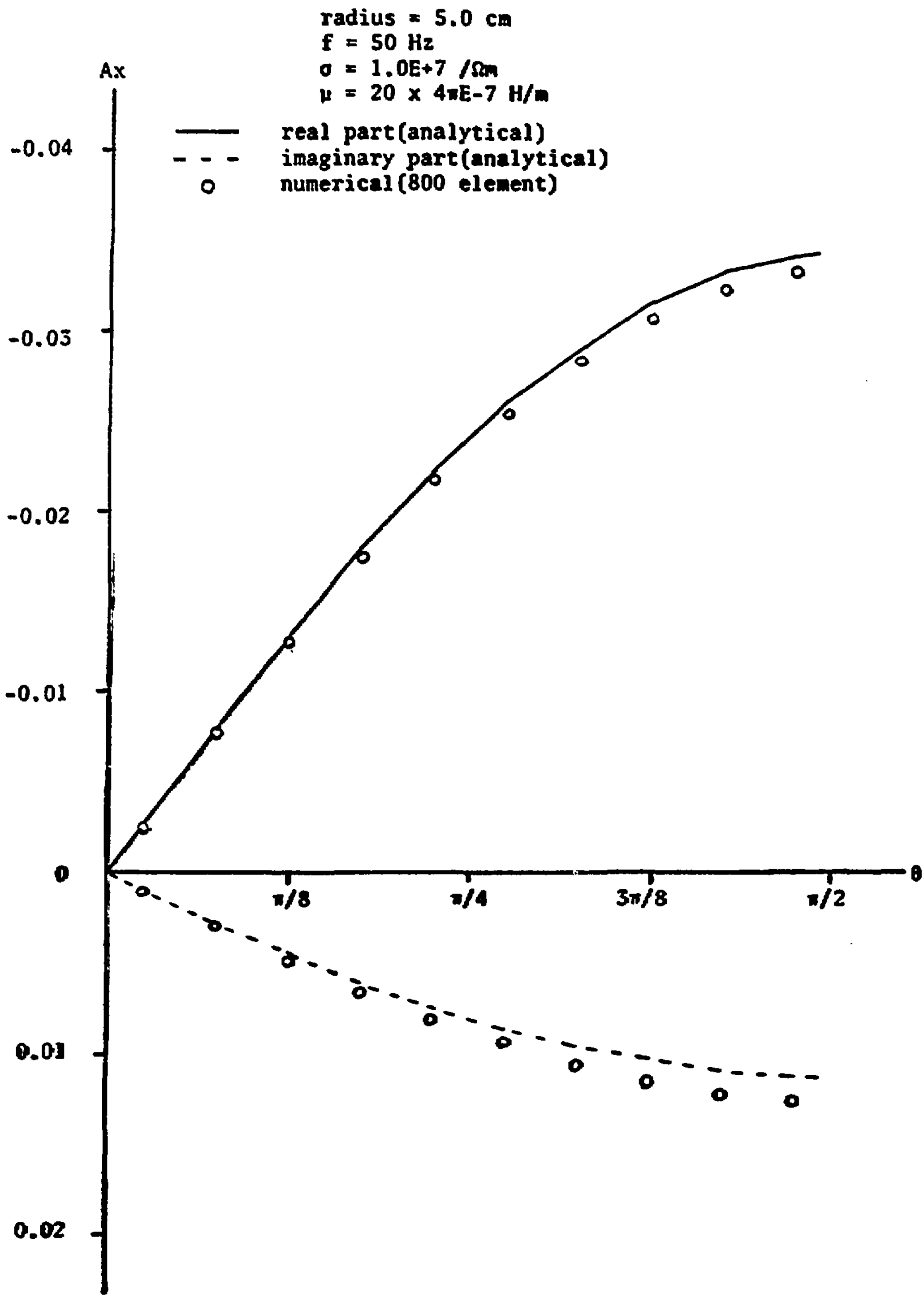

radius = 5.0 cm
f = 50 Hz
σ = 1.0E+7 /Ωm
μ = 20 x 4πE-7 H/m
Ax
real part(analytical)
imaginary part(analytical)
numerical(800 element)
-0.04
-0.03
-0.02
-0.01
0
0.01
0.02
π/8
π/4
3π/8
π/2
θ

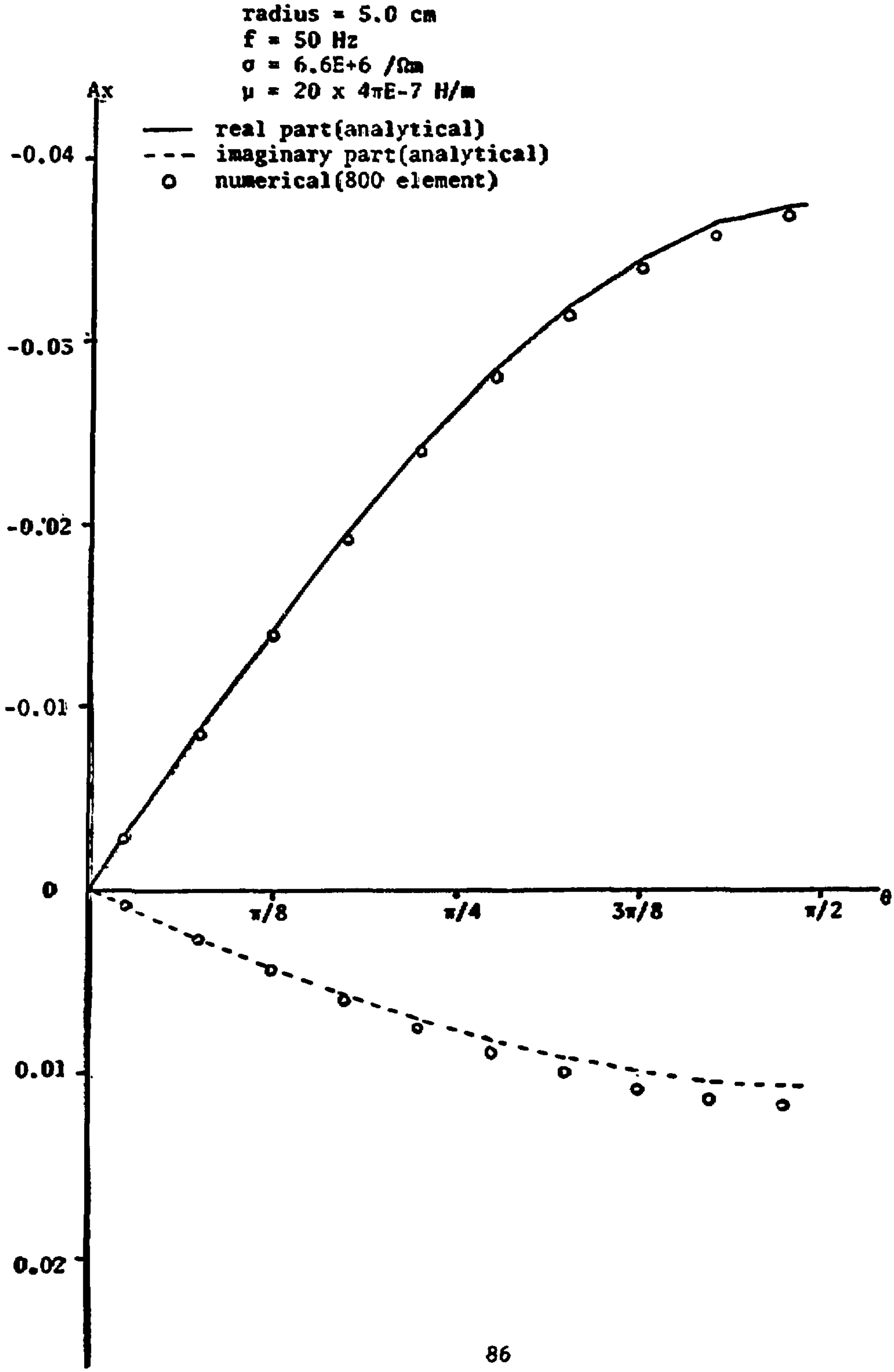
radius = 5.0 cm
f = 50 Hz
σ = 6.6E+6 /Ωm
μ = 20 x 4πE-7 H/m
Ax
real part(analytical)
imaginary part(analytical)
numerical(800 element)
-0.04
-0.03
-0.02
-0.01
0
0.01
0.02
π/8
π/4
3π/8
π/2
θ

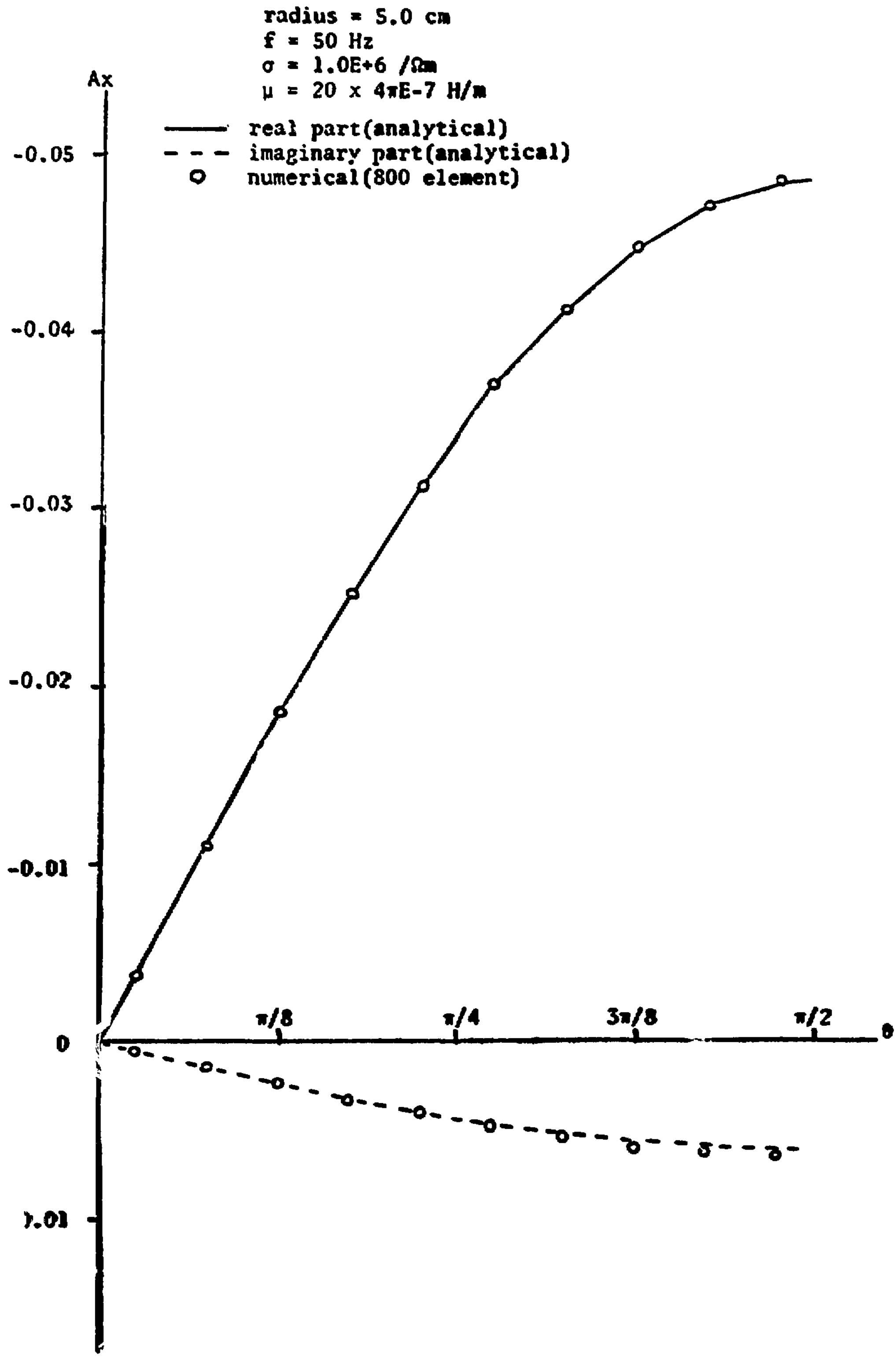

radius = 5.0 cm
f = 50 Hz
σ = 1.0E+6 /Ωm
μ = 20 x 4πE-7 H/m
real part(analytical)
imaginary part(analytical)
numerical(800 element)
Ax
-0.05
-0.04
-0.03
-0.02
-0.01
0
π/8
π/4
3π/8
π/2
θ

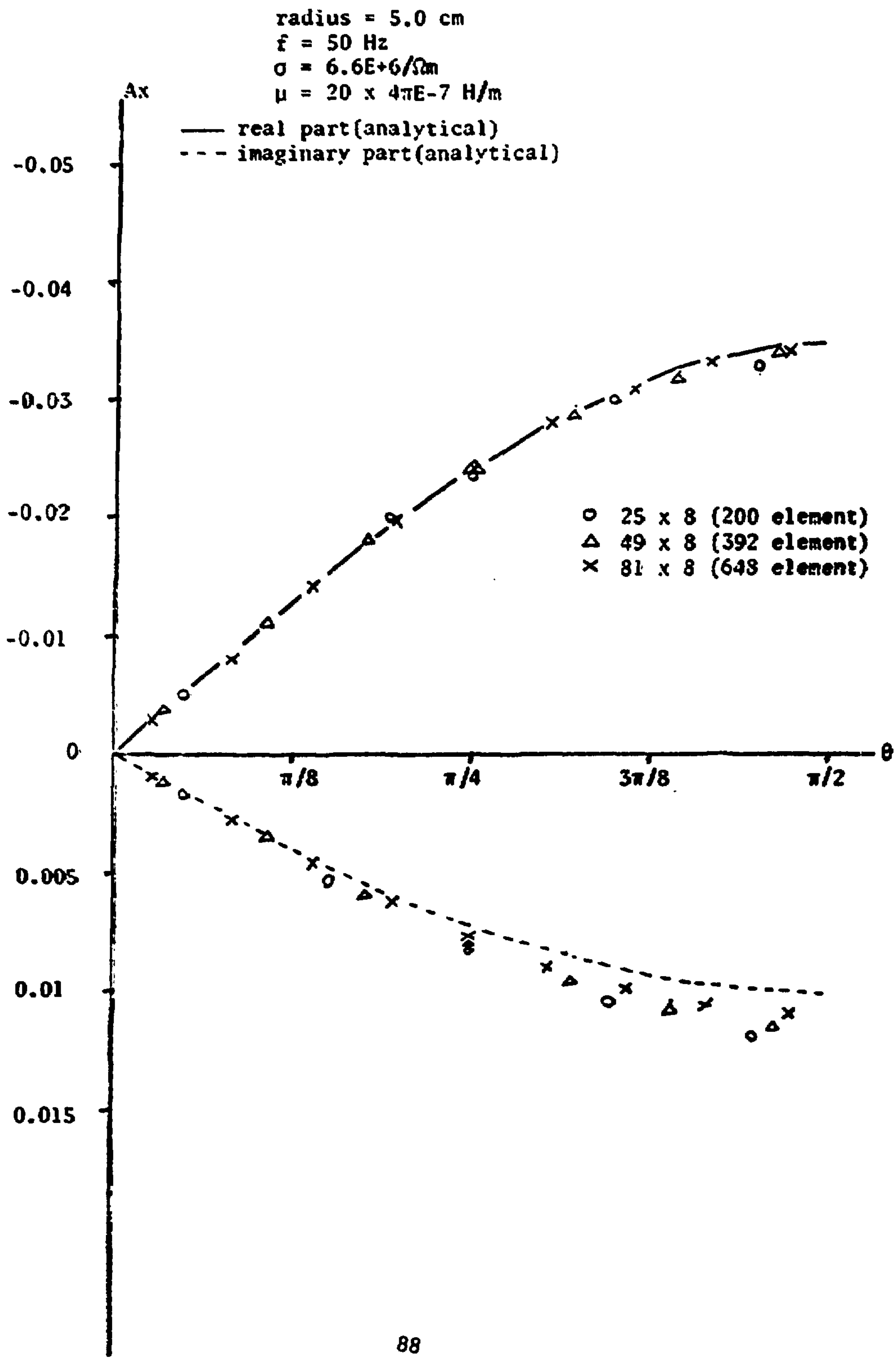
radius = 5.0 cm
f = 50 Hz
σ = 6.6E+6/Ωm
μ = 20 x 4πE-7 H/m
Ax
real part(analytical)
imaginary part(analytical)
-0.05
-0.04
-0.03
-0.02
-0.01
0
0.005
0.01
0.015
π/8
π/4
3π/8
π/2
θ
25 x 8 (200 element)
49 x 8 (392 element)
81 x 8 (648 element)

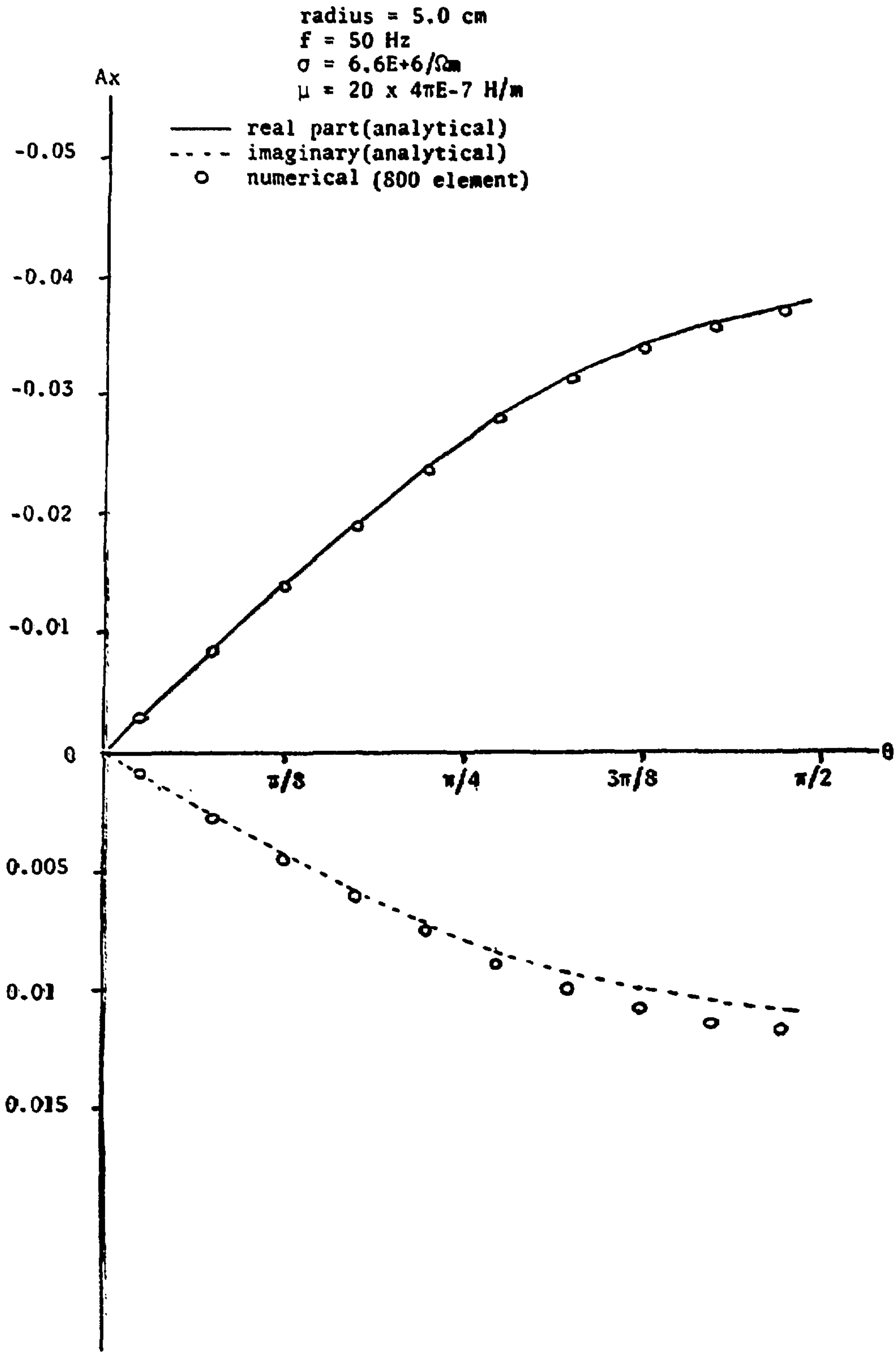
radius = 5.0 cm
f = 50 Hz
σ = 6.6E+6/Ωm
μ = 20 x 4πE-7 H/m
Ax
real part(analytical)
imaginary(analytical)
numerical (800 element)
-0.05
-0.04
-0.03
-0.02
-0.01
0
0.005
0.01
0.015
π/8
π/4
3π/8
π/2
θ

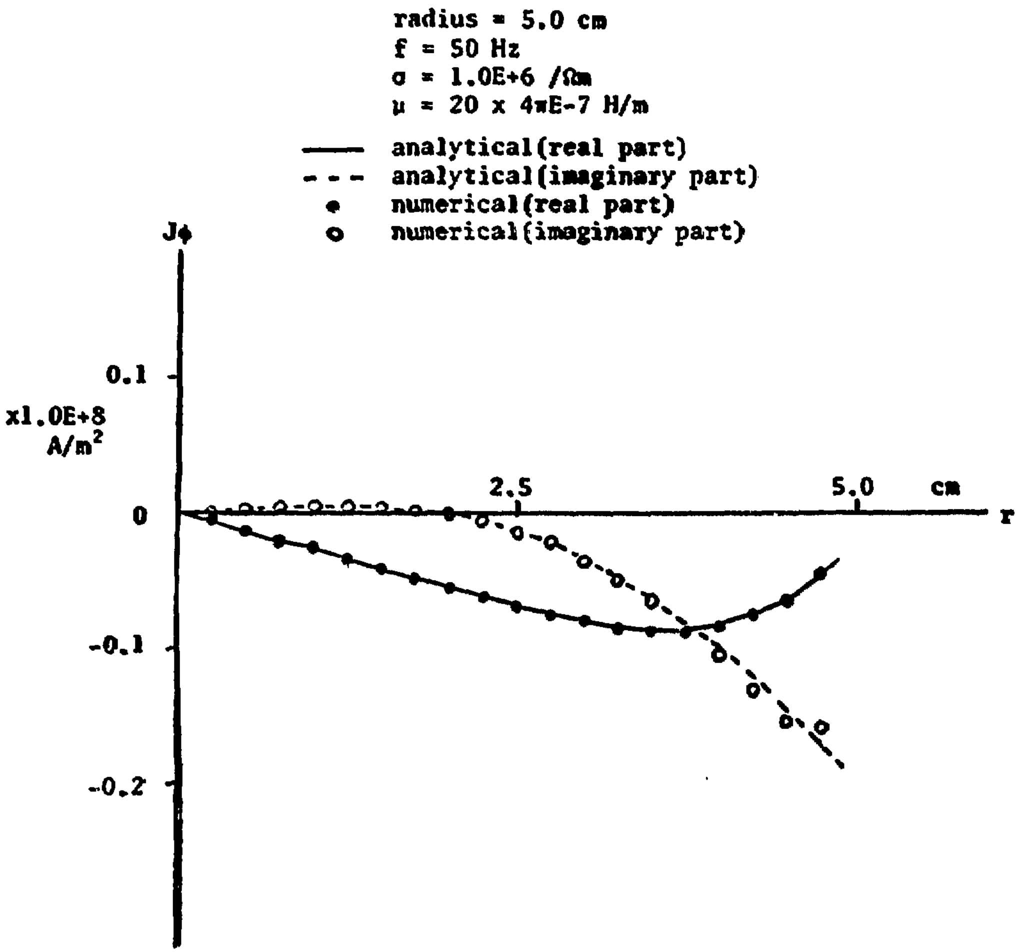
radius = 5.0 cm
f = 50 Hz
σ = 1.0E+6 /Ωm
μ = 20 x 4πE-7 H/m
analytical(real part)
analytical(imaginary part)
numerical(real part)
numerical(imaginary part)
Jϕ
0.1
x1.0E+8
A/m²
0
-0.1
-0.2
2.5
5.0
cm
r

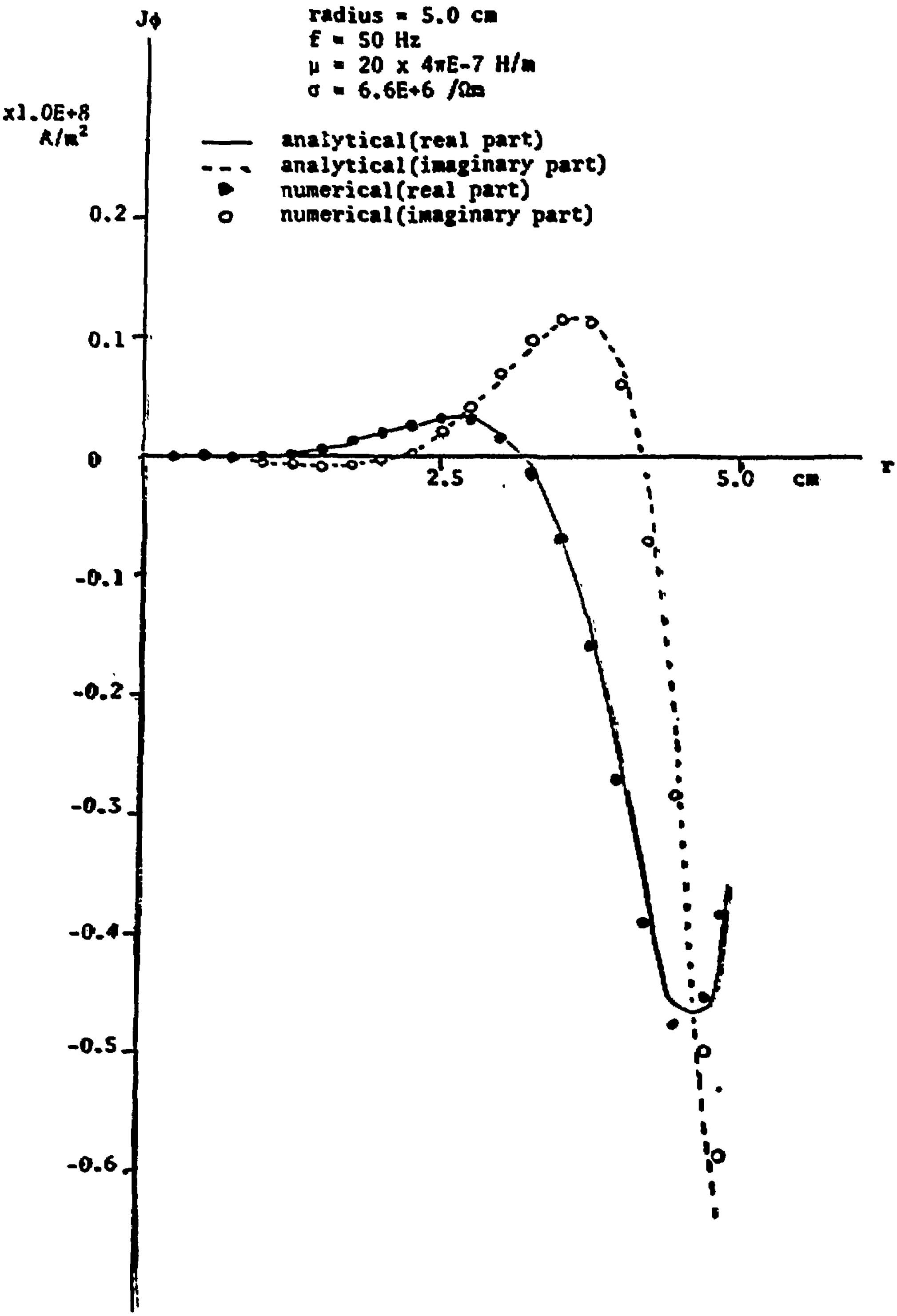

Jϕ
radius = 5.0 cm
f = 50 Hz
μ = 20 x 4πE-7 H/m
σ = 6.6E+6 /Ωm
x1.0E+8
A/m²
analytical(real part)
analytical(imaginary part)
numerical(real part)
numerical(imaginary part)
0.2
0.1
0
-0.1
-0.2
-0.3
-0.4
-0.5
-0.6
2.5
5.0
cm
r

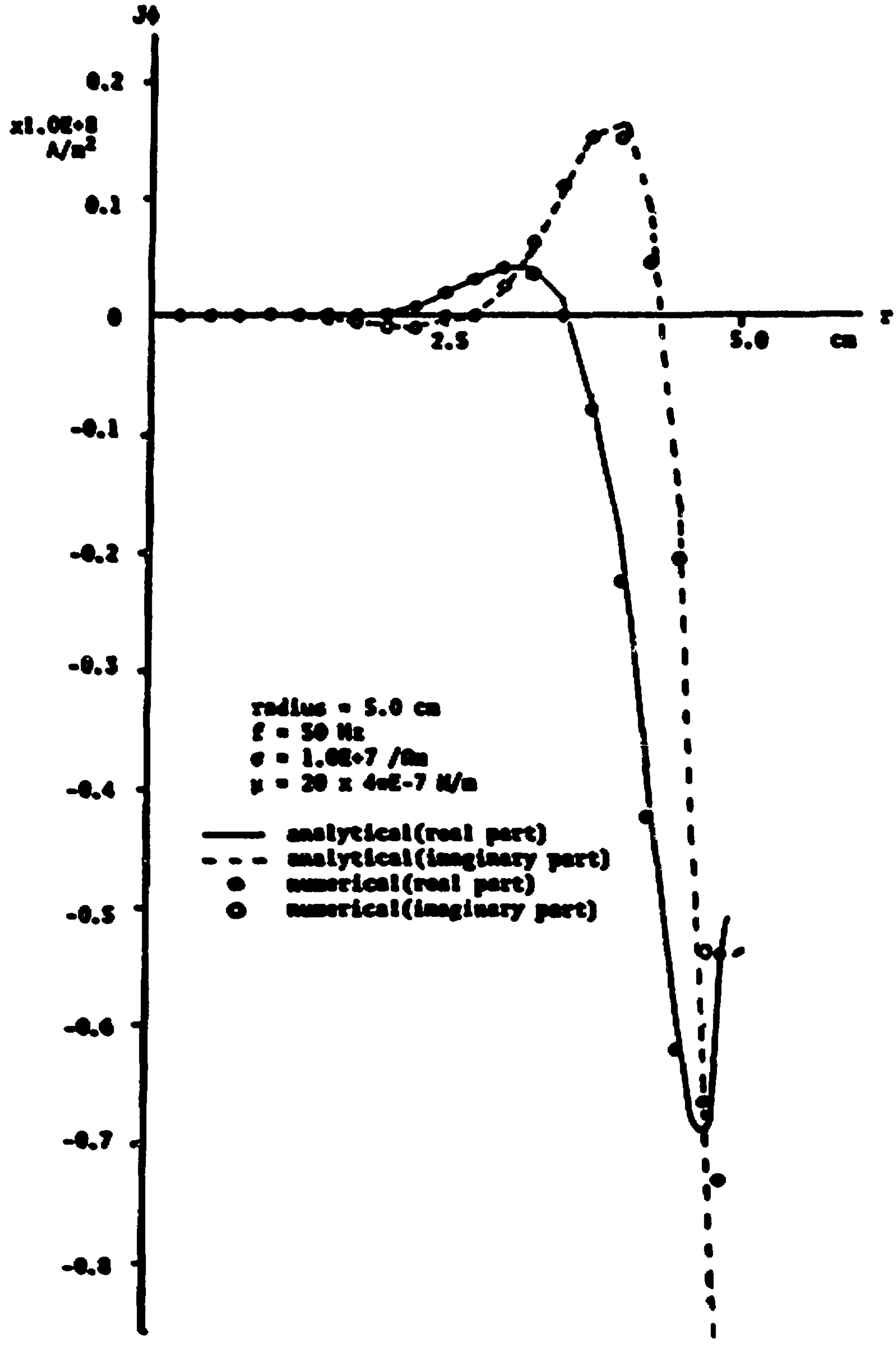

Jφ
0.2
x1.0E+8
A/m²
0.1
0
-0.1
-0.2
-0.3
-0.4
-0.5
-0.6
-0.7
-0.8
2.5
5.0
cm
r
radius = 5.0 cm
f = 50 Hz
σ = 1.0E+7 /Ωm
μ = 20 x 4πE-7 H/m
analytical(real part)
analytical(imaginary part)
numerical(real part)
numerical(imaginary part)

6.0 Appendices

6.1 Workshop Attendees and Affiliations

Kent Davey	Georgia Institute of Technology
Cris Emson	Rutherford Appleton Laboratory
Vijay K. Garg	Westinghouse R&D Center
Nathan Ida	The University of Akron
Suk H. Kim	Argonne National Laboratory
Robert J. Lari	Argonne National Laboratory
Eliane S. Lessner	Fermilab
Amitabh Mishra	Swanson Analysis Systems Inc.
Toshiya Morisue	University of Tokushima
Dale F. Ostergaard	Swanson Analysis Systems Inc.
Alan Otter	TRIUMF
Serzio Pissanetzvy	Texas Accelerator Center
Yiping Shen	The University of Akron
Larry R. Turner	Argonne National Laboratory
Soo Young Lee	Argonne National Laboratory

INTERNATIONAL ELECTROMAGNETICS WORKSHOP

ARGONNE NATIONAL LABORATORY
Building 360, Room L-119
23-24 June 1986

Monday 23 June

8:30	Registration and Coffee	
9:00	Welcome	C.C. Baker, Director, Fusion Power Program R.F. Mattas, Head, Blanket Technology Program
9:20	The International Workshops	L.R. Turner
9:40	Report on the First Workshop at Rutherford Appleton Laboratory, UK	C. Emson, RAL
10:00	Problem 2 Presentations and Discussion	
11:30	Lunch Cafeteria Room D	
1:30	Problem 1 Presentations and Discussion	
3:00	Break	
3:15	Preparation of Problem Summaries by Presenters	
3:15	Tour of FELIX and ALEX	
4:00	Short Presentations	
5:30	Adjourn	
7:00	No-host Dinner	

Tuesday 24 June

9:00	Other Problems: Summary, Presentations, and Discussions
10:00	Problem 2 Summary and Discussion
11:00	Problem 1 Summary and Discussion
12:00	Lunch Cafeteria Room F
1:00	Discussion: Procedure for Future Workshops, Changes in Problems, Additional Problems
3:00	Short Presentations
4:30	Adjourn

DISTRIBUUTION LIST FOR ANL/FPP/TM-210

Internal:

C. Baker	S. Kim	D. Smith	ANL Contract File
J. Battles	R. Lari	L. Turner	ANL Libraries (8)
K. Evans	R. Mattas	R. Weeks	ANL Patent Dept.
T. Hua	W. Praeg	FPP Files (25)	TIS Files (5)

External:

DOE-TIC, for distribution per UC-20 (106)
M. Abdou, University of California, Los Angeles
Y. Akahoshi, University of Tokyo, JAPAN
N. Atkinson, Bath University, UNITED KINGDOM
D. Baker, Los Alamos National Laboratory
M. Balchin, University of Bath, UNITED KINGDOM
W. Baran, Krupp Widia GMBH, FRG
S. Baron, Brookhaven National Laboratory
M. Begg, Oxford Magnet Technology, UNITED KINGDOM
C. Biddlecombe, Vector Fields, Ltd., UNITED KINGDOM
O. Biro, Budapesti Muszaki Egyetem, HUNGARY
J. V. Bladel, University of Ghent, BELGIUM
E. Bobrov, Massachusetts Institute of Technology
R. Bond, Culham Laboratory, UNITED KINGDOM
A. Bossavit, Electricite de France, FRANCE
J. Brauer, A. O. Smith Data Systems
C. Bryant, Imperial College, UNITED KINGDOM
N. Burais, Ecole Centrale de Lyon, FRANCE
Z. Cendes, Carnegie Mellon University
M. Chari, General Electric Co.
D. Cohn, Massachusetts Institute of Technology
C. Collie, Rutherford Appleton Lab., UNITED KINGDOM
J. Crocker, EG&G Idaho, Inc
K. Davey, Georgia Institute of Technology
E. Deeley, Kings College, UNITED KINGDOM
N. El-Khatib, Imperial College London, UNITED KINGDOM
C. R. I. Emson, Rutherford Appleton Lab. A, UNITED KINGDOM
E. Freeman, Imperial College, UNITED KINGDOM
M. Fujii, Kawasaki Heavy Industires, Ltd., JAPAN
K. Fujiwara, Okayama University, JAPAN
V. Garg, Westinghouse R&D Center
J. Gerstenberger, T. H. Darmstadt, GERMANY
J. Grewall, Loughborough University, UNITED KINGDOM
U. Hamm, T. H. Darmstadt, GERMANY
R. Hancox, Culham Laboratory, UNITED KINGDOM
G. Harding, Culham Laboratory, UNITED KINGDOM
A. Hatayama, Toshiba Corporation, JAPAN
E. Heighway, Los Alamos National Laboratory
C. Henning, Lawrence Livermore National Laboratory
W. Herrmannsfeldt, Standford Linear Accel. Center
T. Honma, Hokkaido University, JAPAN

N. Ida, The University of Akron
K. Jungst, KfK, Karlsruhe, FRG
A. Kameari, Mitsubishi Atomic Power Ind., Inc., JAPAN
H. Kanayama, FUJIFACOM Corporation, JAPAN
T. Kawamoto, CRIEPI, JAPAN
M. Kazimi, Massachusetts Institute of Technology
P. Komarek, Institute fur Technische Physik, FRG
S.-Y. Lee, Korea Advanced Inst. for Science & Technology, KOREA
P. Leonard, Bath University, UNITED KINGDOM
E. Lessner, Fermilab
W. Lord, Colorado State University
G. Logan, Lawrence Livermore National Laboratory
D. Lowther, McGill University, CANADA
K. Majorkowsak-Knap, Warsaw Technical University, Poland
C. Mandel, Imperial College London, UNITED KINGDOM
H. Mansir, ENSIEG, FRANCE
F. Matsuoka, Mitsubishi Heavy Industries, Inc., JAPAN
G. Miley, University of Illinois-Urbana
A. Minato, CRIEPI, JAPAN
A. Mishra, Swanson Analysis Systems Inc.
K. Miya, University of Tokyo, JAPAN
R. Moir, Lawrence Livermore National Laboratory
P. Molfino, Universita di Genova, ITALY
G. Molinari, Universita di Genova, ITALY
D. Montgomery, Massachusetts Institute of Technology
F. Moon, Cornell University
T. Morisue, University of Tokushima, JAPAN
W. Mueller, T H Darmstadt, GERMANY
W. Muller, Inst. fur Elekt. Energiewandlung, FRG
T. Nakata, Okayama University, JAPAN
A. Nicolas, Ecole Centrale de Lyon, FRANCE
M. Nishikawa, Mitsubishi Atomic Power Ind., Inc., JAPAN
T. Nomura, CRL, Mitsubishi Electric Corporation, JAPAN
D. Ostergaard, Swanson Analysis Systems, Inc.
A. Otter, TRIUMF, CANADA
T. Phemister, CA Parsons, UNITED KINGDOM
R. Pillsbury, Massachusetts Institute of Technology
S. Pissanetzky, Texas Accelerator Center
T. Preston, Stafford Laboratory, UNITED KINGDOM
P. Reardon, Brookhaven National Laboratory
F. Ribe, University of Washington
K. Richter, Technical University of Graz, AUSTRIA
D. Rodger, Bath University, UNITED KINGDOM
D. Rowe, Rowe and Associates
G. Rubinacci, University of Salerno, ITALY
J.-C. Sabonnadiere, Laboratoire d'Electrotechnique, FRANCE
M. Schaefer, T. H. Darmstadt, GERMANY
J. Schmidt, Princeton Plasma Physics Laboratory
J. Scott, Oak Ridge National Laboratory
Y. Shen, The University of Akron
P. Silvester, McGill University, CANADA
J. Simkin, Vector Fields, UNITED KINGDOM
W. Stacey, Jr., Georgia Institute of Technology
K. Symon, Synchrotron Radiation Center

T. Takagi, Hitachi, Ltd., JAPAN
F. Takahashi, Tohoku University, JAPAN
R. Thome, Massachusetts Institute of Technology
C. Trowbridge, Rutherford Appleton Laboratory, UNITED KINGDOM
H. Tsuboi, Okayama University, JAPAN
T. Tsutsumi, Mitsubishi Research Institute, JAPAN
T. Uchida, Nagoya University, JAPAN
M. Uesaka, Ishikawajima-Harima Heavy Ind., JAPAN
J. Verite, Electricite de France, FRANCE
A. Viviani, Universita di Genova, ITALY
J. Waddington, ECRD, Capenhurst, UNITED KINGDOM
J. Weiss, Westinghouse Electric Corp.
D. Weissenburger, Princeton University
H. Yamashita, Hiroshima University, JAPAN
I. Yanagisawa, Mitsubishi Atomic Power Ind., JAPAN
Z. Yoshida, University of Tokyo, JAPAN
S.-A. Zhou, Royal Inst. of Technology, Stockholm, SWEDEN
Bibliothek, Max-Planck-Institute fur Plasmaphysik, WEST GERMANY
C.E.A. Library, Fontenay-aux-Roses, FRANCE
Librarian, Culham Laboratory, ENGLAND
Library Laboratorio Gas Ionizati, ITALY
Thermonuclear Library, Japan Atomic Energy Research Institute, JAPAN